

**Thiostrepton in Phospholipid Micelles: Development of Scalable Production
Method and *In Vivo* Evaluation**

BY

KARINA ESPARZA

B PHARM, University of Sao Paulo, Brazil, 2013

THESIS

Submitted in partial fulfillment of the requirements
for the degree of Doctor of Philosophy in Biopharmaceutical Sciences
in the Graduate College of the
University of Illinois at Chicago, 2019

Chicago, Illinois

Defense Committee:

Hayat Onyuksel (Chair and Advisor)
Steven Dudek, College of Medicine
Michael Federle
Hyun-Young Jeong
Hyunwoo Lee

This thesis is dedicated to my husband Elliott and my son Kevin, my endless source of love, strength, and joy. Also, to my parents Isaura and Demóstenes for their unconditional love and support in my academic pursuits.

ACKNOWLEDGMENTS

I am profoundly grateful to God for giving me the opportunity, wisdom, and resources to complete this doctoral thesis. I am also thankful to my advisor, Dr. Hayat Onyuksel, for believing in my potential and offering her constant guidance, knowledge, and encouragement to become a better scientist and achieve my highest research goals. I thank all my collaborators for providing me with resources, expertise, and suggestions to the various studies in this project: Dr. Hyunwoo Lee and Dr. Jerry Khee Keong Woo for their contribution in the microbiological studies; Dr. Steven Dudek, Dr. Huashan Wang, and Dr. Lucille Meliton for their support with the *in-vivo* staphylococcal pneumonia studies; Dr. Albert Larsen and Brendan Heffron for their assistance with the quantitative analytical methods; and Dr. Richard Minshall, Dr. Suellen D’Arc dos Santos Oliveira, and Maricela Castellon for their support with the *in-vivo* polymicrobial sepsis experiments. I am also thankful to my committee members Dr. Michael Federle and Dr. Huyn-Young Jeong for their time and suggestions that contributed to the progression of this project. I thank the faculty, staff, and students of the Department of Pharmaceutical Sciences for providing me with a nurturing environment that allowed me to achieve all the milestones of the program. I am also very thankful to fellow graduate students and friends Dr. Camila Crnkovic, Nilanjana Sadhu, and Dr. Dulari Jayawardena for their ongoing support and camaraderie. Finally, I am especially grateful to my best friend and husband, Elliott Esparza, without whom I could have not completed this thesis.

KE

CONTRIBUTION OF AUTHORS

The development of the co-solvent freeze-drying method has been previously published at the International Journal of Pharmaceutics (Esparza and Onyuksel 2019). The original text has been modified here to fit the thesis format and improve flow with the overall project. I contributed with the conceptualization of the method, design, and execution of experiments, data interpretation, and elaboration of the manuscript. My advisor, Dr. Hayat Onyuksel, contributed with the conceptualization of the method, experimental design, data interpretation, and revision of the manuscript.

TABLE OF CONTENTS

<u>CHAPTER</u>	<u>PAGE</u>
I. INTRODUCTION.....	1
A. Sterically stabilized micelles (SSM).....	1
1. Chemistry and properties of SSM	1
2. Potential use of SSM for passive targeting in infections.....	4
3. Use of SSM for the delivery of antibiotic drugs.....	5
B. Thiostrepton (TST)	7
1. Chemistry and biological properties of TST	7
2. Limitations of the therapeutic application of TST.....	13
C. Drug encapsulation in SSM.....	16
1. Limitations of large-scale production of SSM nanomedicines	16
2. Basic principles of lyophilization/freeze-drying	17
3. Drug encapsulation by Fournier's method.....	23
D. Staphylococcal pneumonia	25
1. Methicillin-resistant <i>Staphylococcus aureus</i> (MRSA)	25
2. Pathogenesis of staphylococcal pneumonia	27
3. Current therapies against staphylococcal pneumonia.....	33
4. Murine models of staphylococcal pneumonia	36
E. Sepsis.....	38
1. Pathogenesis of sepsis	38
2. Current therapies for sepsis	42
3. Cecum ligation and puncture (CLP) sepsis mouse model.....	43
F. Limitations of therapies against staphylococcal infections and sepsis	44
G. Hypothesis and specific aims	46
H. Significance of the project	48
II. MATERIALS AND METHODS	51
A. Materials	51
B. Animals	52
C. Methods	52
1. Preparation and characterization of TST-SSM nanomedicine	52
1.1. Determination of TST aqueous solubility by the modified shake-flask method	53
1.2. Preparation of TST-SSM nanomedicine	53
1.2.1. Thin-film hydration method.....	53
1.2.2. Co-solvent freeze-drying method	54
1.3. Characterization of TST-SSM nanomedicine.....	57
1.3.1. Particle size distribution by dynamic light scattering (DLS)	57
1.3.1.1. Viscosity of TBA: water co-solvent system	58
1.3.1.2. Refractive index of TBA: water co-solvent system.....	59
1.3.2. TST quantification by HPLC	59
1.3.3. Internal morphology of lyophilized cake	59
1.3.4. Reconstitution time of the lyophilized cake.....	60
1.3.5. Turbidity of reconstituted TST-SSM	60

TABLE OF CONTENTS (Continued)

<u>CHAPTER</u>	<u>PAGE</u>
1.3.6. Determination of the number of encapsulated drug molecules per micelle	60
1.3.7. Residual tert-butanol concentration.....	61
1.3.8. Osmolality	62
1.3.9. Moisture Analysis.....	62
1.3.10. Minimum inhibitory concentration (MIC).....	63
1.4. Short-term stability of reconstituted TST-SSM nanomedicine	64
1.5. Long-term stability of freeze-dried TST-SSM nanomedicine	65
2. In-vitro efficacy of TST-SSM against gram-positive bacteria.....	67
2.1. Minimum inhibitory concentration (MIC) of TST-SSM nanomedicine	67
2.2. TST accumulation in MRSA USA 300	67
2.2.1. TST quantification by LC-MS/MS	68
2.3. Stability of TST-SSM nanomedicine in spent media of MRSA USA 300 ...	70
3. <i>In vivo</i> efficacy of TST-SSM nanomedicine.....	72
3.1. Filtration of TST-SSM nanomedicine.....	72
3.2. Staphylococcal pneumonia.....	72
3.2.2. Preparation of MRSA USA300 inoculum.....	73
3.2.3. Induction of MRSA pneumonia in mice	74
3.2.4. Bacterial burden in lungs.....	76
3.2.5. TST concentration in lungs	76
3.3. Polymicrobial sepsis	77
3.3.1. Preparation of drug treatments	77
3.3.2. Induction of sepsis in mice by the cecal ligation and puncture (CLP) method	77
3.3.3. Cytokine profile in plasma	80
3.3.4. Nitric oxide derivatives (NOx) in plasma	80
3.3.5. Blood chemistry.....	81
3.3.6. Bacterial burden	81
4. Statistical analysis.....	81
III. RESULTS	82
A. Development of TST-SSM nanomedicine	82
1. TST solubility in aqueous media	82
2. Maximum loading capacity of TST in SSM by the thin-film hydration method ..	83
3. Preparation of TST-SSM nanomedicine by the co-solvent freeze-drying method	85
3.1. Effect of TBA on DSPE-PEG ₂₀₀₀ micelle formation	86
3.2. Effect of TBA proportion on drug loading.....	91
3.3. Effect of reconstitution method on drug loading.....	93
3.4. Effect of PBS salts on reconstitution time and drug loading	94
3.5. Effect of phospholipid concentration on reconstitution time and drug loading	96
3.6. Effect of fill and reconstitution volumes on drug loading	97
3.7. Residual TBA in the TST-SSM lyophilized cake	98

TABLE OF CONTENTS (Continued)

<u>CHAPTER</u>	<u>PAGE</u>
3.8. Osmolality of reconstituted TST-SSM nanomedicine	99
3.9. Internal lyophilized cake morphology and reconstitution time	100
4. Stability of TST-SSM nanomedicine	102
4.1. Short-term stability of reconstituted TST-SSM nanomedicine	102
4.2. Long-term stability of freeze-dried TST-SSM nanomedicine	106
B. <i>In vitro</i> activity of TST-SSM nanomedicine	112
1. Antimicrobial activity of TST-SSM nanomedicine against several Gram-positive bacteria	112
2. Accumulation of TST-SSM in MRSA USA300	114
3. Stability of TST-SSM in spent media of MRSA USA300	115
C. <i>In vivo</i> efficacy of TST-SSM nanomedicine	116
1. Filtration of reconstituted TST-SSM nanomedicine	116
2. Staphylococcal pneumonia	120
2.1. Bacterial burden	120
2.2. Drug concentration	122
3. Polymicrobial sepsis	124
3.1. Survival study	124
3.2. Cytokine profile in plasma	125
3.3. Nitric oxide derivatives (NOx) in plasma	127
3.4. Biomarkers of hepatic and renal injury	128
3.5. Bacterial burden	130
IV. DISCUSSION	131
A. Development of TST-SSM nanomedicine	131
1. Drug encapsulation by the thin-film hydration method	131
2. Drug encapsulation by the co-solvent freeze-drying method	133
3. Stability of TST-SSM nanomedicine	140
B. <i>In vitro</i> activity of TST-SSM nanomedicine	142
C. <i>In vivo</i> efficacy of TST-SSM nanomedicine	144
1. Filtration of reconstituted TST-SSM nanomedicine for animals studies	144
2. Staphylococcal pneumonia	145
3. Polymicrobial sepsis	147
4. Other activities	149
V. CONCLUSIONS	151
VI. FUTURE DIRECTIONS	155
REFERENCES	158
APPENDICES	175
Appendix A: Animal protocols approval letters	175
Appendix B: Copyright clearance proofs	179
VITA	190

LIST OF TABLES

<u>TABLE</u>	<u>PAGE</u>
TABLE I: BIOLOGICAL PROPERTIES OF THIOSTREPTON (TST).	11
TABLE II: REPORTED MINIMUM INHIBITORY CONCENTRATION (MIC) OF TST AGAINST GRAM-POSITIVE BACTERIA.	12
TABLE III: COMPOSITION OF TESTED TST-SSM FORMULATIONS.....	56
TABLE IV: LONG-TERM STABILITY OF TST-SSM NANOMEDICINE.	66
TABLE V: STANDARD SOLUTIONS OF TST FOR QUANTIFICATION BY LC-MS/MS.	69
TABLE VI: TREATMENT GROUPS FOR SEPSIS STUDY.....	79
TABLE VII: TST SOLUBILITY IN AQUEOUS MEDIA.....	82
TABLE VIII: REFRACTIVE INDEX, DENSITY, AND VISCOSITY OF DIFFERENT PROPORTIONS OF TBA IN WATER AT 25°C.	87
TABLE IX: RESIDUAL TERT-BUTANOL (TBA) IN OPTIMIZED TST-SSM LYOPHILIZED CAKES.....	99
TABLE X: OSMOLALITY OF TST-SSM RECONSTITUTED IN ONE-THIRD OF FILL VOLUME.	99
TABLE XI: MINIMUM INHIBITORY CONCENTRATION (MIC) OF RECONSTITUTED TST-SSM STORED AT 4°C OR 25°C.	106
TABLE XII: MOISTURE IN TST-SSM LYOPHILIZED CAKES AFTER STORAGE AT 5°C, 30°C/60% RH OR 40°C/75% RH FOR 7 MONTHS.....	107
TABLE XIII: MINIMUM INHIBITORY CONCENTRATION (MIC) OF TST-SSM AFTER STORAGE OF LYOPHILIZED CAKE AT 5°C, 30°C/60% RH OR 40°C/75% RH.....	112

LIST OF TABLES (Continued)

<u>TABLE</u>	<u>PAGE</u>
TABLE XIV: MINIMUM INHIBITORY CONCENTRATION OF TST, TST-SSM OR POSITIVE CONTROLS AGAINST GRAM-POSITIVE PATHOGENS.	113
TABLE XV: MINIMUM INHIBITORY CONCENTRATION (MIC) OF RECONSTITUTED TST-SSM BEFORE AND AFTER FILTRATION.....	119
TABLE XVI: TST CONCENTRATION IN LUNG HOMOGENATE.	123

LIST OF FIGURES

<u>FIGURE</u>	<u>PAGE</u>
Figure 1: Scheme of sterically stabilized micelles (SSM) formation.	3
Figure 2: Mechanism of action of polymyxin B.	6
Figure 3: Polymyxin B in SSM nanocarrier.	7
Figure 4: Structure of thiostrepton (TST).	8
Figure 5: Scheme of the thin film hydration drug encapsulation method.	17
Figure 6: Scheme of freeze-dryer components.	18
Figure 7: Phase diagram of water with the triple point.	20
Figure 8: Swelling of PVP-b-PDLLA micelles with increases in TBA content.	24
Figure 9: Scheme of co-solvent freeze-drying encapsulation method.	24
Figure 10: Historical evolution of methicillin-resistant <i>Staphylococcus aureus</i> (MRSA).	27
Figure 11: Virulence factors of <i>Staphylococcus aureus</i>	29
Figure 12: Extracellular Toll-like receptors (TLR).	31
Figure 13: Intracellular Toll-like receptors (TLR).	32
Figure 14: Pathogenesis of sepsis.	41
Figure 15: Experimental procedures for drug stability in spent media.	71
Figure 16: Regression analysis of OD ₆₀₀ vs CFU of MRSA USA300.	74
Figure 17: Staphylococcal pneumonia mouse model with single-dose treatment.	75
Figure 18: Staphylococcal pneumonia mouse model with two doses of treatment.	76
Figure 19: Study design of sepsis animal experiments.	78
Figure 20: Particle size of SSM or TST-SSM prepared by the thin-film hydration method.	84

LIST OF FIGURES (Continued)

<u>FIGURE</u>	<u>PAGE</u>
Figure 21: Particle size of SSM and TST-SSM prepared by the co-solvent freeze-drying with 30% TBA: water (v/v) and reconstituted in 0.9% saline.	86
Figure 22: Particle size of DSPE-PEG2000 micelles in TBA: 0.9% saline co-solvent system.....	89
Figure 23: Average particle size of DSPE-PEG2000 micelles in TBA: 0.9% saline co-solvent system.	90
Figure 24: Particle size of SSM or TST-SSM prepared by the co-solvent freeze-drying method with 50% or 75% TBA: water (v/v) and reconstituted with 0.9% saline.....	92
Figure 25: Turbidity of TST-SSM samples using different reconstitution methods.	93
Figure 26: Visual appearance of 5mM of DSPE-PEG ₂₀₀₀ dispersed in different co-solvent systems before freeze-drying.....	95
Figure 27: Particle size and TST quantification of SSM or TST-SSM prepared by the co-solvent freeze-drying method with 50% TBA: 2X PBS (v/v) and reconstituted with deionized water.	95
Figure 28: Formation of drug aggregates due to the increase of phospholipid concentration in formulations containing 5 TST molecules per micelle.	96
Figure 29: TST-SSM samples with a fill volume of 6 mL (top) or 12 mL (bottom) and reconstituted in one-third of the volume.	98
Figure 30: Scanning electron microscopy and reconstitution time of different preparations of TST-SSM.....	101
Figure 31: Particle size of reconstituted TST-SSM stored at 4°C or 25°C.....	102

LIST OF FIGURES (Continued)

<u>FIGURE</u>	<u>PAGE</u>
Figure 32: Representative particle size analysis of reconstituted TST-SSM after short-term storage.	103
Figure 33: Drug concentration of reconstituted TST-SSM stored at 4°C or 25°C.	104
Figure 34: Representative chromatogram of TST-SSM at day 0 and day 7 of storage at 4°C or 25°C.	105
Figure 35: Reconstitution time of TST-SSM lyophilized cakes after long-term storage.	108
Figure 36: Particle size of TST-SSM after long-term storage of lyophilized cake.	108
Figure 37: Representative particle size of TST-SSM after long term storage of lyophilized cake.	109
Figure 38: Drug concentration of TST-SSM after long-term storage of lyophilized cake.	110
Figure 39: Chromatogram of TST-SSM after long-term storage of lyophilized cake at 5°C, 30°C/60% RH and 40°C/75% RH.	111
Figure 40: Accumulation of TST in MRSA USA 300 bacterial cells.	115
Figure 41: Remaining TST (%) after incubation in fresh media, MRSA USA300 spent media, or MRSA USA 300 lysate for 24h at 37°C.	116
Figure 42: Particle size of reconstituted TST-SSM before and after filtration.	117
Figure 43: Representative particle size analysis of TST-SSM (A) before and (B) after filtration.	118

LIST OF FIGURES (Continued)

<u>FIGURE</u>	<u>PAGE</u>
Figure 44: Drug concentration of reconstituted TST-SSM before and after filtration..	119
Figure 45: Bacterial burden in the lungs of mice with MRSA pneumonia.	121
Figure 46: Survival rate of mice with CLP-induced sepsis.....	125
Figure 47: Cytokine profile in plasma of mice with CLP-induced sepsis.....	126
Figure 48: Total nitrite and nitrate levels in plasma and peritoneal lavage.	127
Figure 49: Biomarkers of hepatic and renal injury.	129
Figure 50: Bacterial burden in blood and peritoneal lavage.	130
Figure 51: Activity of TST-SSM nanomedicine against high grade serous ovarian cancer mouse model.	150

LIST OF ABBREVIATIONS

ALT	Alanine aminotransferase
AST	Aspartate aminotransferase
ANOVA	Analysis of variance
BRL	Biological resources laboratory
BUN	Blood urea nitrogen
CA-MRSA	Community-acquired <i>Staphylococcus aureus</i>
CARS	Compensatory anti-inflammatory response syndrome
CASP	Colon ascendens stent peritonitis
CDC	Center for Disease Control
CFU	Colony-forming units
CLP	Cecal ligation and puncture
CMC	Critical micelle concentration
CpG	Cytosine-phosphate-guanosine
DLS	Dynamic light scattering
DMSO	Dimethyl sulfoxide
DSPE-PEG ₂₀₀₀	Distearoyl phosphatidylethanolamine-polyethylene glycol 2000
ELISA	Enzyme-linked immunosorbent assay
EPR	Enhanced permeation and retention
FOXM1	Transcription factor forkhead box M1
GC-MS	Gas chromatography-mass spectroscopy
HPLC	High-performance liquid chromatography
IgG	Immunoglobulin G

LIST OF ABBREVIATIONS (Continued)

IL	Interleukin
iNOS	Inducible nitric oxide synthase
IP	Intraperitoneal
IV	Intravenous
LC-MS/MS	Liquid chromatography with tandem mass spectroscopy
LPS	Lipopolysaccharide
MARS	Mixed antagonist response syndrome
MCP-1	Macrophage/monocyte chemoattractant protein-1
MIC	Minimum inhibitory concentration
MIP-1	Macrophage-inflammatory protein-1
MRSA	Methicillin-resistant <i>Staphylococcus aureus</i>
MSSA	Methicillin-sensitive <i>Staphylococcus aureus</i>
NO	Nitric oxide
NOS	Nitric oxide synthase
OD	Optical density
PAMP	Pathogen-associated molecular pattern
PAX8	Paired box transcription factor 8
PBP	Penicillin-binding proteins
PES	Polyethersulfone
PBS	Phosphate-buffered saline
PMN	Polymorphonuclear neutrophils
PVDF	Polyvinylidene fluoride

LIST OF ABBREVIATIONS (Continued)

PVP-b-PDLLA	Poly(N-vinyl-2-pyrrolidone)-block-poly(D,L-lactide)
PVL	Panton-Valentine leucocidin
qSOFA	Quick sequential organ failure assessment
RH	Relative humidity
RPM	Revolutions per minute
RRC	Research resources center
SC	Subcutaneous
SD	Standard deviation
SEM	Scanning electron microscopy
SIRS	Systemic inflammatory response syndrome
SpA	Staphylococcal protein A
SSM	Sterically stabilized micelles
SSP	Sterically stabilized particles
TipA	Thiostrepton-induced proteins A
TGF- β	Transforming growth factor-beta
TLR	Toll-like receptor
TNF- α	Tumor necrosis factor-alpha
<i>tsr</i>	Thiostrepton resistance gene
TST	Thiostrepton
TST-SSM	Thiostrepton encapsulated in sterically stabilized micelles
UIC	University of Illinois at Chicago
VAN	Vancomycin

LIST OF ABBREVIATIONS (Continued)

VISA	Vancomycin intermediate-resistant <i>Staphylococcus aureus</i>
VRE	Vancomycin-resistant Enterococcus
VRSA	Vancomycin-resistant <i>Staphylococcus aureus</i>

SUMMARY

Sterically stabilized micelle (SSM) is a simple and useful drug delivery system to transport hydrophobic drugs and amphiphilic peptides in the body. This system is composed of 1,2-distearoyl-sn-glycero-3-phosphoethanolamine-N-methoxy-poly(ethylene glycol 2000) (DSPE-PEG₂₀₀₀), a PEGylated phospholipid with documented safety, present in the FDA-approved product Doxil®. DSPE-PEG₂₀₀₀ self-assembles into a core-shell structure when placed in aqueous media above the critical micellar concentration (CMC = 1 μ M) with hydrophobic tails clustered in the center and hydrated PEG moieties facing the aqueous environment. The hydrophobic core carries hydrophobic molecules improving their apparent aqueous solubility and physical stability, while the PEG corona can accommodate amphiphilic peptides and protect drugs from aggregation or enzymatic degradation. As a result, therapeutic molecules can be safely transported in the blood circulation and reach target sites in their active form.

Besides improving drug solubility and stability in aqueous media, SSM also increases drug circulation time and accumulation at the target site *in vivo*. The hydrated PEG corona forms a protective shield that prevents micelle interaction with opsonins, thus avoiding particle elimination by the reticuloendothelial system and extending the drug half-life. In addition, SSM promotes preferential drug accumulation at diseased sites with leaky vasculatures such as in cancer and inflammation. Passive targeting is achieved due to the ideal size of SSM – approximately 15 nm in diameter – which is large enough to prevent drug extravasation to healthy tissues and renal excretion, but small enough to deliver the drug to sites with increased vascular permeability. As a

SUMMARY (Continued)

result, higher drug concentrations are achieved at the site of action for improved drug efficacy and reduced toxicity to healthy tissues. Passive targeting has been largely explored for the delivery of anticancer and anti-inflammatory drugs, but evidence suggests that this phenomenon also occurs in infected sites, providing a novel strategy to treat localized infections.

Bacterial infections induce local vascular permeability that can be potentially explored for the passive targeting of SSM nanomedicines. Pathogen-associated molecular patterns (PAMPs) activate toll-like receptors (TLR) on immune cells, triggering the release of pro-inflammatory cytokines that stimulate the production of vasodilatory mediators such as nitric oxide, bradykinin, and prostanoids. This vasodilation is intended to facilitate the migration of immune cells from the blood circulation to infected tissues and combat the infection. In addition, certain pathogens try to gain access to the blood circulation by releasing toxic proteases that cause direct degradation of extracellular matrix and endothelial cells. These vascular changes can potentially enhance the permeation and retention of therapeutic nanoparticles to infected tissues and provide a new targeted approach to aim pathogens with better efficacy and safety.

Methicillin-resistant *Staphylococcus aureus* (MRSA) is a widespread human pathogen that causes an array of diseases, ranging from minor skin conditions to life-threatening invasive infections. Despite the existence of marketed drugs to combat MRSA such as vancomycin, linezolid, or clindamycin, staphylococcal infections are becoming more difficult to treat as resistant isolates continue to emerge. As a result,

SUMMARY (Continued)

an increasing number of patients experience therapeutic failure with spreading of the infection to other sites, sepsis, and death. This global antibiotic crisis has prompted the reconsideration of old antimicrobial molecules for development, which were previously disregarded due to their unfavorable physicochemical properties or unacceptable toxicity. Using current scientific knowledge and modern technology, old drugs such as daptomycin and fidaxomicin were successfully introduced to the market decades after their discovery, and many other molecules remain to be revived.

To this end, thiostrepton (TST) is an excellent antimicrobial candidate for re-evaluation and possible clinical development. This natural compound was discovered in 1954 from *Streptomyces* species and exhibits potent bacteriostatic activity against Gram-positive microorganisms, including MRSA. TST inhibits protein synthesis by forming a complex with the bacterial ribosome in a highly conserved domain between the protein L11 and 23S rRNA. However, despite remarkable *in vitro* and *in vivo* activity, poor water solubility and delivery issues have hampered the clinical development of TST for human use. Therefore, this project seeks to explore the use of phospholipid nanocarrier (SSM) to improve TST aqueous solubility and enable its targeted parenteral application for the treatment of resistant infections with improved safety and efficacy.

For over 20 years, our research group has encapsulated several drugs in SSM with anticancer and anti-inflammatory properties but had little success developing antimicrobial nanomedicines. For example, polymyxin B – a cyclic cationic peptide with attached acyl chain – self-associated with SSM to prevent aggregation, but it lost activity as determined by *in vitro* experiments. Similarly, KSLW, a cationic amphiphilic

SUMMARY (Continued)

antimicrobial decapeptide, effectively associated with SSM but failed to demonstrate *in vitro* and *in vivo* activity in a mouse model of skin wound healing. In both cases, the loss of drug activity upon SSM association was attributed to the shielding of drug charge that is essential for interaction with bacterial cells. We believe that uncharged hydrophobic drugs like TST are better candidates for delivery in SSM than charged amphiphilic molecules. This is because the absence of the charge in physiological pH of TST reduces the potential for lasting electrostatic interaction with SSM affecting the drug biological activity. However, despite the great potential of using SSM for the delivery of water-insoluble drugs, the clinical development of such nanomedicines is hampered by difficulties with large-scale production.

DSPE-PEG₂₀₀₀ micelles are spontaneously formed in aqueous media, but special techniques are required to encapsulate hydrophobic drugs in the micelle core. The thin-film hydration is the most conventional encapsulation method, but it cannot be easily scaled-up for industrial purposes due to technical challenges to obtain the thin-film. In this method, phospholipid and drug are solubilized in organic solvents and dried in a rotary evaporator to form a homogeneous thin film in a round bottom flask. Once the film is completely dry, the material is re-suspended in aqueous media under vigorous sonication and mixing to promote micelles self-assembly and concomitant drug encapsulation. Given the limitations of round bottom flask sizes and rotary evaporator capabilities, this method is impractical for large-scale production and it would probably require several small batches to achieve useful volumes of nanomedicine, leading to long production time, high batch-to-batch variability, and inflated manufacturing costs.

SUMMARY (Continued)

To address these limitations, in this study we aimed to develop a new scalable method called co-solvent freeze-drying to produce TST-SSM nanomedicine.

Freeze-drying or lyophilization is a common technological process used in the pharmaceutical industry to remove water from liquid formulation and extend the shelf-stability of drug products. This method relies upon three basic steps: (1) freezing of liquid product, (2) primary drying or sublimation of solvent crystals under low pressure and low temperature, and (3) secondary drying to remove bound water by desorption. We speculated that freeze-drying can remove solvent from drug and phospholipid mixture to form a dried matrix with a large surface area containing all ingredients evenly dispersed, similar to the thin film obtained with the rotary evaporator. The organic solvent used in the thin-film hydration method (chloroform) can be substituted with a safer freeze-dryable solvent system composed of water and tert-butanol (TBA). Drug-loaded micelles can be formed upon reconstitution in water with gentle swirling, which is a user-friendly method for hospital settings.

The central hypothesis of this project was that TST could be developed into a useful antibiotic nanomedicine when encapsulated in DSPE-PEG₂₀₀₀ micelles using a production method that is amenable for large-scale production. Our objectives were to develop and optimize the scalable co-solvent freeze-drying method to prepare TST-SSM nanomedicine (**specific aim 1**), investigate possible mechanisms by which SSM can improve the *in vitro* efficacy of TST against MRSA USA 300 (**specific aim 2**), evaluate the *in vivo* efficacy of TST-SSM nanomedicine against murine models of MRSA USA 300 pneumonia and polymicrobial sepsis (**specific aim 3**).

SUMMARY (Continued)

For the development of TST-SSM nanomedicine, we first determined the maximum drug loading in DSPE-PEG₂₀₀₀ micelles using the conventional thin-film hydration method. We determined that up to 5 TST molecules could be encapsulated in each micelle. Having this maximum drug loading as a reference, we proceeded to develop the scalable co-solvent freeze-drying method.

The co-solvent freeze-drying method was developed as a scalable technique to encapsulate TST in SSM with high loading efficiency. In our first attempt, we dissolved TST in TBA and DSPE-PEG₂₀₀₀ in water and combined these two solutions under constant stirring for a final proportion of 50% of TBA: water (v/v). The mixture was aliquoted to glass vials and freeze-dried for 24h. The resulting lyophilized cakes were reconstituted in saline using gentle swirling and characterized for particle size distribution and drug concentration. We found that only one drug molecule could be encapsulated in each micelle without the formation of larger particles, which is below the target loading of 5 drug molecules per micelle. Given these results, we investigated possible factors responsible for the poor drug loading and use this information to optimize the co-solvent freeze-drying method.

We hypothesized that the drug was not being completely dissolved in the co-solvent system, leading to the presence of drug particles in the freeze-dried product. To test this hypothesis, we increased the hydrophobicity of the co-solvent system by elevating the TBA proportion from 50% to 75%. However, this change did not improve the drug loading in SSM and large particles were still being detected in the final product.

SUMMARY (Continued)

This suggested that possible drug particles before freeze-drying were not responsible for the poor drug loading.

A difference between the thin film hydration and the co-solvent freeze-drying encapsulation methods is the technique used to reconstitute the dried matrix. The first method applies sonication and vortexing to promote micelle formation and drug loading, while the second one uses gentle swirling as a realistic method for healthcare practitioners. We hypothesized that swirling did not provide enough energy into the system to promote efficient drug encapsulation. To test this hypothesis, we prepared TST-SSM formulations containing 1 to 5 TST molecules per micelle by the co-solvent freeze-drying method and reconstituted using three different methods: spontaneous, swirling, or sonication. We observed that only 1 drug molecule could be encapsulated in each micelle regardless of the reconstitution method. However, samples reconstituted by sonication were considerably less turbid than other methods, likely due to the breakdown of large precipitates promoted by sonication. Since the reconstitution method did not improve the drug loading, we focused our efforts to improve the cake structure and polarity by altering the cake formulation.

We incorporated PBS salts before freeze-drying to increase the hydrophilicity of the cake and accelerate the reconstitution time after adding water. However, we observed that DSPE-PEG₂₀₀₀ was prone to precipitation at 75% of TBA in the presence of buffer salts likely due to the low availability of free water molecules to interact with phospholipids. This forced us to reduce the TBA proportion to 50% to maintain both drug and phospholipid in solution in the co-solvent system. By adding PBS salts in the

SUMMARY (Continued)

formulation before freeze-drying, the reconstitution time reduced from 2.8 minutes to less than 20 seconds and we were able to load 5 TST molecules per micelle (277.8 μM of TST in 5mM of DSPE-PEG₂₀₀₀). In addition, after analyzing lyophilized cakes by scanning electron microscopy (SEM), we observed that the internal morphology of cakes containing PBS salts was visually more porous which could have facilitated the penetration of water and reconstitution of dry material.

We attempted to improve the strength of the formulation by doubling or tripling the quantity of ingredients in the formulation. However, the reconstitution time increased from less than 20 seconds to 1.2 minutes and 3.7 minutes, respectively. In addition, concentrated formulations exhibited additional large particles and even visible drug precipitation possibly due to the increase in cake density causing inefficient reconstitution. To overcome this problem, we prepared the loose lyophilized cake with only 5 mM of DSPE-PEG₂₀₀₀ with adjusted PBS salts and reconstituted the product with water in one-third of the original filling volume to concentrate the product 3 times (final concentration 833.4 μM of TST and 15mM of DSPE-PEG₂₀₀₀). Using this approach, we successfully obtained a clear formulation with a single particle population of 12.2 nm and confirmed drug concentration corresponding to optimally loaded micelles. Since the volume of the cake was higher than the volume of reconstitution media, the cake took about 1.7 minutes to reconstitute instead of <20 seconds. Finally, we evaluated if the fill volume of the optimized formulation could affect the final TST-SSM product. We tested filling volumes of 6 mL and 12 mL in 20 mL scintillation vials and reconstituted the formulation in 2 mL and 4mL, respectively. Interestingly, the formulation with 6 mL fill

SUMMARY (Continued)

volume was clear with acceptable characteristics, but the formulation containing 12 mL exhibited additional large particles on the DLS, indicating that space to properly agitate the sample during reconstitution was also critical for the formation of the final product.

We tested the stability of the optimized TST-SSM formulation regarding short-term storage of reconstituted nanomedicine and long-term storage of the freeze-dried product. The reconstituted formulation was stable for at least 1 day at 25°C or 7 days at 4°C. On the other hand, the lyophilized cake was stable for at least 7 months at $5 \pm 3^\circ\text{C}$ or at $30 \pm 2^\circ\text{C} / 65 \pm 5\% \text{ RH}$, but exhibited signs of degradation as early as 1 month after storage at $40 \pm 2^\circ\text{C} / 75 \pm 5\% \text{ RH}$. Nonetheless, reasonable storage stability at 30 °C indicated that TST-SSM could become a viable marketed product. In addition, these results suggested the great potential of the TST-SSM formulation be further developed for clinical application with an easier transition to large-scale production than formulations prepared by the thin-film hydration.

After the successful development of the optimized TST-SSM nanomedicine by the co-solvent freeze-drying method, our next goal was to test the *in vitro* efficacy of TST-SSM against Gram-positive pathogens. We compared the antimicrobial activity of TST-SSM nanomedicine versus TST dissolved in 4% dimethylsulfoxide (DMSO) against five Gram-positive microorganisms –*Staphylococcus aureus* USA 300, *S. aureus* COL, *Bacillus anthracis* Sterne, *B. cereus* 14579, and *B. thuringiensis* konkukian 97-27. We performed the microdilution assay to determine the minimal inhibitory concentration (MIC) after 24 hours of incubation at 37°C. We found that SSM encapsulation preserved the antimicrobial activity of TST and surprisingly, nanomedicine exhibited higher activity

SUMMARY (Continued)

against all microorganisms compared to the free drug. This finding is extremely encouraging since previous studies using amphiphilic antimicrobial peptides failed to show any *in vitro* antimicrobial activity upon encapsulation in SSM. We believe that the loss of activity of amphiphilic peptides was due to the hindrance of essential peptide charge by the nanocarrier. However, hydrophobic drugs such as TST surpass such impediments because they do not rely on electrostatic charge for activity.

To understand how SSM encapsulation improved the activity of TST *in vitro*, we tested whether SSM enhanced TST accumulation in the bacterial cell or protected TST from degradation in the bacterial media. First, we incubated free TST dissolved in DMSO, free TST + DSPE-PEG₂₀₀₀ dissolved in DMSO or TST-SSM nanomedicine with MRSA USA300 (OD₆₀₀ \approx 1) and periodically measured intracellular TST concentration by LC-MS/MS for 2 hours. We observed no statistical differences in intracellular drug accumulation. Next, we incubated TST dissolved in DMSO or TST-SSM nanomedicine with fresh tryptic soy broth (TSB), spent media of MRSA USA 300 culture (cell-free), or diluted MRSA USA 300 bacterial lysate and measured the drug concentration before and after 24h incubation at 37°C at 200 rpm by HPLC. We found that SSM significantly reduced the TST degradation in all media types compared to free TST. Because we observed this protection even in fresh media, we believe that SSM protected TST mostly against chemical degradation (hydrolysis) rather than any possible enzymatic degradation. Taken together, these results indicate that SSM improves the antimicrobial activity of TST by keeping the drug protected in the hydrophobic core rather than affecting drug penetration in the bacterial cell.

SUMMARY (Continued)

Our next step was to investigate the therapeutic value of TST-SSM nanomedicine in animal models. First, we sterilized the reconstituted TST-SSM product by filtration through 0.22 μ m polyethersulfone (PES) syringe filter and did not observe changes in drug concentration, particle size distribution, and antimicrobial activity. Then, in collaboration with Dr. Steven Dudek, we tested if TST-SSM could reduce the bacterial burden in lungs of animals infected with MRSA USA 300. We induced pneumonia in C56BL/6 mice by inoculating approximately 1×10^8 CFU/ mouse intratracheally, treated animals with TST-SSM intravenously via retro-orbital injection at time points 6h and 16h, and euthanized animals 24h post-infection. Unfortunately, we observed no significant difference in the bacterial burden in lungs of animals treated with the TST-SSM nanomedicine compared to empty micelles. We hypothesized that the lack of *in vivo* efficacy of TST-SSM was due to the anti-inflammatory properties of TST that counteract the antibiotic activity in lungs. TST is known to inhibit the activation of Toll-like receptors (TLR) 7-9 by blocking proteasome and endosomal acidification in mammalian cells. TLR-9 is an important mediator for bacterial clearance in lungs in murine models of pneumonia caused by MRSA USA 300. Therefore, TST-SSM likely blocks TLR-9 in the lungs and impairs with the bacterial clearance promoted by immune cells.

We investigated the application of TST-SSM as a TLR-9 inhibitor to prevent sepsis-related death in collaboration with Dr. Richard Minshall. Sepsis is a life-threatening condition caused by the irregular immunological response to infection leading to tissue damage and multiple organ failure. Reports in the literature suggest

SUMMARY (Continued)

that TLR9 inhibition suppresses excessive host inflammatory response and attenuates sepsis-induced mortality and acute kidney injury in the cecal ligation and puncture (CLP) murine model. However, to the best of our knowledge, TST has never been directly tested as a therapeutic option for the management of sepsis. We found that TST-SSM nanomedicine increased the median survival of CLP-induced septic mice from 31h to 44h. In addition, TST-SSM treatment lessened the bacterial burden in the blood and peritoneal lavage, reduced pro-inflammatory cytokines in plasma (IL-6 and TNF- α), lowered vasodilatory nitric oxide derivatives in plasma, and significantly improved the renal and hepatic biomarkers of function (creatinine and AST).

Incidentally, as a separate activity, TST-SSM nanomedicine was also tested against high-grade ovarian cancer in collaboration with Dr. Joanna Burdette's group. Previously, this group has shown that TST interfered with the oncogenic transcription factor PAX8 *in vitro*, but preliminary *in vivo* efficacy study failed because of severe precipitation and toxicity of the drug. To overcome this drug delivery issue, we tested the optimized TST-SSM nanomedicine (20 mg/kg/dose IP) and observed that the nanomedicine significantly reduced tumor burden in mice. These encouraging results illustrated the potential of TST-SSM nanomedicine in enabling the therapeutic application of hydrophobic TST and supporting the discovery of new molecular targets.

In conclusion, we successfully developed a novel nanomedicine of TST-SSM with improved aqueous solubility and stability that can be scaled-up for clinical and commercial purposes. We believe that the co-solvent freeze-drying encapsulation method can be applied to other SSM nanomedicines containing other hydrophobic

SUMMARY (Continued)

drugs and facilitate their clinical translation as well. In addition, SSM improved the *in vitro* antimicrobial activity of TST by protecting the drug from degradation in aqueous media but lacked *in vivo* antimicrobial activity in the MRSA pneumonia animal model possibly due to drug interference with the immune system. However, for the first time, we identified that TST-SSM nanomedicine has great potential as a therapeutic for the management of sepsis mostly due to its anti-inflammatory properties. Finally, the development of water-soluble TST-SSM nanomedicine also provides the investigation of additional therapeutic uses and molecular mechanisms of TST as illustrated with the ovarian cancer study.

I. INTRODUCTION

A. Sterically stabilized micelle (SSM)

(Previously published as Esparza, K., Onyuksel, H. (2019) Development of co-solvent freeze-drying method for the encapsulation of water-insoluble thiostrepton in sterically stabilized micelles, *Int. J. Pharm.* 556, 21-29).

1. Chemistry and properties of SSM

Over the past two decades, our laboratory has reported the effective use of PEGylated phospholipid micelles as targeted nanocarriers to deliver water-insoluble drugs and amphiphilic peptides (Vuković et al. 2013; Onyuksel, Jeon, and Rubinstein 2009; O. M. Y. Koo, Rubinstein, and Onyuksel 2011; Dagar et al. 2012; Gülçür et al. 2013). Sterically stabilized micelles (SSM) are composed of 1,2-distearoyl-sn-glycero-3-phosphoethanolamine-N-methoxy-poly(ethylene glycol 2000) (DSPE-PEG₂₀₀₀), a biodegradable and biocompatible ingredient present in the FDA-approved product Doxil® (Lim, Banerjee, and Onyuksel 2012). DSPE-PEG₂₀₀₀ self-assembles into a core-shell structure when placed in water above the critical micellar concentration (1.0 μM) (Ashok et al. 2004) with hydrophobic tails clustered in the center and hydrated PEG moieties facing the aqueous environment (**Figure 1**) (Vuković et al. 2013; Vukovic et al. 2011; Esparza and Onyuksel 2019). The hydrophobic core is capable of carrying water-insoluble molecules in their molecular form rather than particles, thus improving the delivery of drug molecules that are readily available to interact with their biological targets (Lim, Banerjee, and Onyuksel 2012). Examples of hydrophobic drugs formulated in SSM as nanomedicines in our laboratory are paclitaxel, camptothecin, and curcumin (Krishnadas, Rubinstein, and Onyuksel 2003; Dagar et al. 2012; O. M. Y. Koo,

Rubinstein, and Onyukse 2011; O. M. Koo, Rubinstein, and Onyukse 2005; Gülçür et al. 2013). In addition, SSM can accommodate amphiphilic peptide drugs in the interface between the hydrophobic core and the PEG corona, protecting them from aggregation and hydrolysis (Banerjee and Onyukse 2012). Peptide-SSM association occurs spontaneously through hydrophobic forces between hydrophobic residues of the peptide drug and fatty acid chains of the phospholipid. In addition, electrostatic interactions between positively-charged residues and negatively-charged phosphate head groups of the lipid also play a role in this interaction (Vuković et al. 2013). Optimal characteristics of peptide for delivery in SSM are length between 17 and 42 residues, presence of hydrophobic residues, and flexible random coil structure that can convert into an active alpha-helix inside micelles (Banerjee and Onyukse 2012). Peptides studied in our laboratory include vasoactive intestinal peptide, glucagon-like peptide-1, pancreatic polypeptide, neuropeptide Y, and secretin (Jayawardena et al. 2017; Anbazhagan et al. 2017; Lim et al. 2011; Banerjee and Onyukse 2013; Kuzmis et al. 2011; Gandhi et al. 2002).

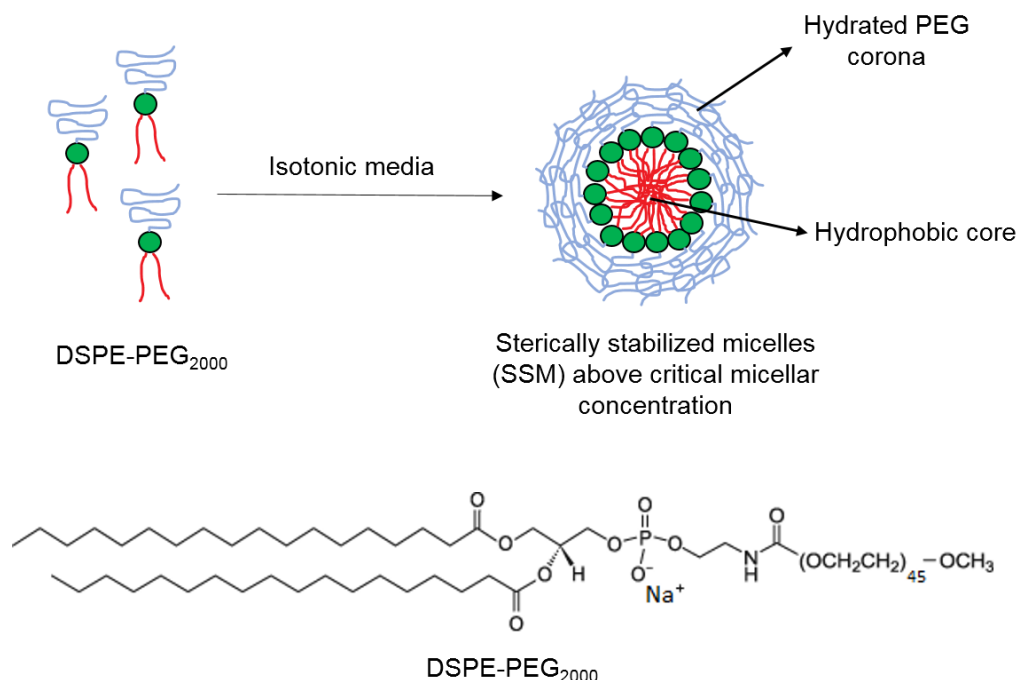


Figure 1: Scheme of sterically stabilized micelles (SSM) formation.
 Reprinted by permission from the Copyright Clearance Center: Elsevier, International Journal of Pharmaceutics, (Esparza and Onyuksel 2019), Copyright 2019.

SSM also increases circulation time and biological half-life of loaded drugs *in vivo*. For example, a pharmacokinetic study with VIP-SSM nanomedicine showed that the mean residence time of VIP increased from 0.5h to 19.5h SSM after encapsulation in SSM (Sethi et al. 2013). The hydrated PEG layer of SSM serves as a protective shield that prevents interaction with other molecules such as degrading enzymes and opsonins and circumvents particle elimination by the reticuloendothelial system. In addition, SSM promotes preferential drug accumulation at diseased sites with leaky vasculatures, such as in cancer and inflammation (Lim, Banerjee, and Onyuksel 2012). This so-called passive targeting is achieved due to the ideal size of SSM (approximately

15 nm in diameter), which is large enough to prevent drug extravasation to healthy tissues (capillary pore size ~3-4 nm) or renal excretion (cut-off size ~10 nm), but small enough to deliver the drug to sites with increased vascular permeability (capillary pore size ~200 nm) (Lim, Banerjee, and Onyuksel 2012). Therefore, passive targeting increases the drug concentration at the site of action, improving drug efficacy and significantly reducing toxicity to healthy tissues. The enhanced permeation and retention (EPR) effect has been largely explored for the delivery of anticancer and anti-inflammatory drugs, but evidence suggests that this phenomenon also occurs in infectious diseases, providing a novel strategy to treat localized infections, such as pneumonia (Maeda 2012; Azzopardi, Ferguson, and Thomas 2013).

2. Potential use of SSM for passive targeting in infections

SSM has been shown to increase the delivery of drugs to solid tumors and inflamed tissues due to the enhanced particle accumulation in sites with leaky microvasculature (O. M. Y. Koo, Rubinstein, and Onyuksel 2011; Dagar et al. 2012; Sethi et al. 2013). Since infections are often accompanied by inflammation and vascular changes, it is plausible that SSM could also be explored for the targeted delivery of antibiotics. Complex interactions occur between the host and the pathogen during the development of an infection that enhances the local vascular permeability. These vascular changes can be induced by the immune system itself to facilitate the migration of immune cells from the blood circulation to the infected tissue, or by the invading pathogen to gain access to the circulatory system and spread the infection. For example, bacterial surface components or secreted proteases can activate the host's kallikrein-kinin cascade and increase the production of bradykinin (Azzopardi, Ferguson,

and Thomas 2013; Maeda 2012). Bradykinin is a potent vasoactive nonapeptide that stimulates endothelial cells to produce vasorelaxant agents such as nitric oxide (NO), prostanoids, and endothelium-derived hyperpolarizing factor.

3. Use of SSM for the delivery of antibiotic drugs

Although SSM has been shown to effectively deliver amphiphilic peptides, previous studies from our group have observed limited success with peptide antimicrobials. For example, polymyxin B is a cationic cyclic peptide containing a fatty acid chain active against resistant Gram-negative pathogens (Trimble et al. 2016). The cationic portion of polymyxin B binds to the negatively-charged lipopolysaccharide – the major component of the outer membrane of Gram-negative bacteria – while the hydrophobic tail interacts with the lipid A moiety immersed in the membrane. As polymyxin B inserts itself in the membrane, divalent cations that cross-bridge phospholipid heads are replaced by the bulkier cationic drug, causing destabilization of the membrane, increased permeability, and leakage of intracellular components. Moreover, polymyxin B can further penetrate into the inner has and cytoplasm, affecting other cellular functions such as bacterial respiration and division, which also contributes to cell death **(Figure 2)** (Trimble et al. 2016). Unfortunately, despite its potent activity, the use of polymyxin B is clinically limited by renal and neural toxicity (Trimble et al. 2016). To improve the drug safety, our research group associated polymyxin B with SSM but found that the nanocarrier completely abrogated the *in vitro* antimicrobial activity (Brandenburg et al. 2012). The loss of activity was attributed to the shielding properties of PEG layer which hindered the electrostatic charge of polymyxin B necessary for interaction with Gram-negative membranes **(Figure 3)** (Brandenburg et

al. 2012). Similarly, a study using the antimicrobial and wound healing amphiphilic decapeptide KSLW revealed loss of activity *in vitro* and *in vivo* upon association with SSM presumably due to the disruption of essential charge interaction between the peptide and bacterial membrane (Williams et al. 2012). However, SSM still has the potential to deliver hydrophobic antibiotics that do not depend on charge for activity, such as TST.

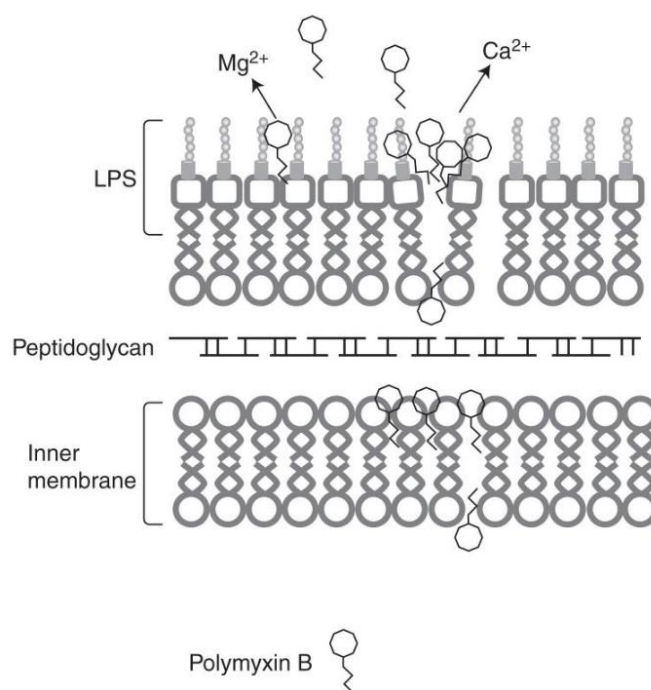


Figure 2: Mechanism of action of polymyxin B.

Reprinted by permission from the Cold Spring Harbor Laboratory Press, (Trimble et al. 2016), Copyright 2016.

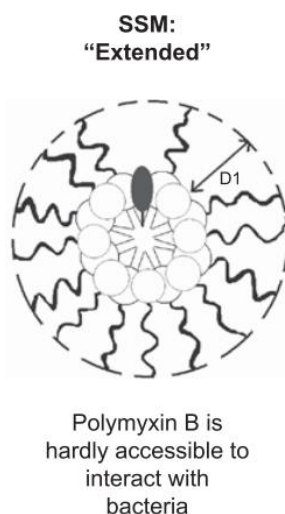


Figure 3: Polymyxin B in SSM nanocarrier.

Reprinted by permission from Taylor & Francis, Pharmaceutical Development and Technology, (Brandenburg et al. 2012), Copyright 2012.

B. Thiostrepton (TST)

(Previously published as Esparza, K., Onyuksel, H. (2019) Development of co-solvent freeze-drying method for the encapsulation of water-insoluble thiostrepton in sterically stabilized micelles, *Int. J. Pharm.* 556, 21-29).

1. Chemistry and biological properties of TST

Thiostrepton (TST) (**Figure 4**) is a thiopeptide antibiotic and an excellent candidate for re-evaluation and possible clinical development to combat resistant Gram-positive infections (Bagley et al. 2005). This natural compound was first isolated in 1954 from *Streptomyces azureus* and later from *S. hawaiiensis* and *S. laurentii* (Donovick, Joseph F, and Vandeputte 1961; Pagano et al. 1955; Cron et al. 1956; Trejo et al. 1977). The producer *Streptomyces sp.* is a Gram-positive mycelial sporulating bacteria

present predominantly in terrestrial or aquatic environments and known to synthesize attractive bioactive secondary metabolites (de Lima Procópio et al. 2012). TST is a ribosomally synthesized and post-translationally modified peptide encoded by the gene cluster *tsr* (Thomas, Mitchell, and Blanksby 2006). The 58-residue precursor peptide called TsrA is composed of two regions: a 41 amino acid N-terminal end that is eliminated during post-translational modification and a C-terminal 17 amino acid core that is processed enzymatically to the mature form of TST (Thomas, Mitchell, and Blanksby 2006; Zhang and Kelly 2015). The final form of TST exhibits a globular conformation with two large ring systems folded upon each other and a characteristic quinaldic acid group on the side ring (**Figure 4**) (Thomas, Mitchell, and Blanksby 2006). Remarkably, despite its large molecular size (1664.9 g/mol) and complex structure, TST has been successfully synthesized in the laboratory (Nicolaou 2012).

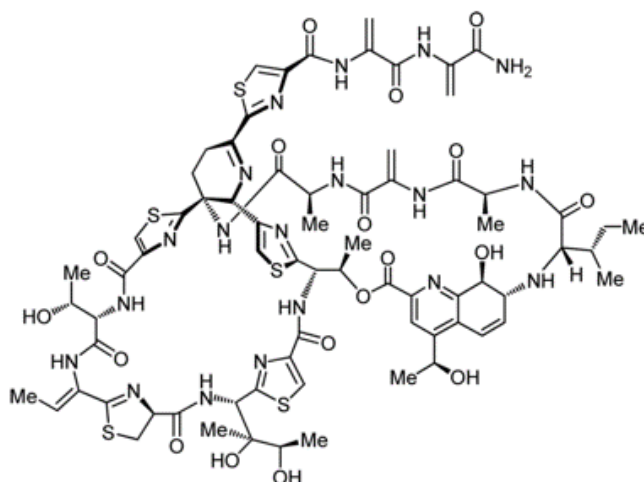


Figure 4: Structure of thioestrepton (TST).

TST possesses useful biological properties that have been explored for various therapeutic purposes (**TABLE I**). As an antibiotic, TST displays bacteriostatic activity against Gram-positive microorganisms, including resistant strains such as MRSA and vancomycin-resistant enterococcus (VRE) (**TABLE II**). The mechanism of action consists in inhibiting protein synthesis by forming a complex with the bacterial ribosome in a highly conserved domain between the protein L11 and 23S rRNA (Porse et al. 1998). Particular to tuberculosis, not only does TST inhibit protein synthesis in *Mycobacteria* but it also induces ER stress-mediated host cell autophagy to eliminate intracellular pathogen (Zheng et al. 2015). Furthermore, TST exerts antiplasmodial effect by targeting two distinct targets on the malaria parasite (Aminake et al. 2011). The first target is the ribosome of the parasite's apicoplast, a semi-autonomous organelle with prokaryotic ancestry responsible for the biosynthesis of fatty acids, isoprenoids, and heme (Mcconkey, Rogers, and Mccutchan 1997). The second target is the 20S proteasome, a multimeric protein assembly that selectively degrades unused proteins in the cell. By inhibiting the parasite's proteasome, rapid cell death occurs due to the toxic accumulation of ubiquitinated proteins (Schoof et al. 2010). TST has been explored as a potent anticancer agent with potential applications in lung, colon, breast, ovarian, and leukemia cancers (Nicolaou et al. 2005). The anticancer activity of TST has been attributed to the down-regulation of the transcription factor forkhead box M1 (FOX M1) – a regulator of cell cycle progression that is overexpressed in many malignancies – causing cell cycle arrest and death of cancer cells without affecting healthy cells (Kwok et al. 2008; M. Wang and Gartel 2011). Recently, a collaborative study with our laboratory found that TST reduces tumor burden of high grade serous

ovarian cancer by reducing paired box transcription factor 8 (PAX8) protein levels, a tumorigenic transcription factor overexpressed in ovarian cancer cells, but not in normal cells (Hardy et al. 2019). Lastly, TST possesses anti-inflammatory activity which has been successfully tested in a mouse model of psoriasis-like inflammation induced by LL-37 (Lai et al. 2015). LL-37 (cathelicidin) is a natural human antimicrobial peptide that can bind to endogenous nucleic acids and trigger inflammatory responses mediated by TLR7-9 in conditions such as psoriasis, rheumatoid arthritis, and systemic lupus erythematosus (Kahlenberg and Kaplan 2013). Topical treatment with TST suppressed the activation of TLR7-9 by preventing essential endosomal acidification and inhibiting proteasome activity (Lai et al. 2015). It is believed that TST exerts its proteasome inhibitory activity similarly to Bortezomib, disrupting the function of UNC93B1 protein required for intracellular trafficking of TLR7-9 (Hirai et al. 2011; Lai et al. 2015).

TABLE I: BIOLOGICAL PROPERTIES OF THIOSTREPTON (TST).

Activity	Disease Model	Drug vehicle (route)	Proposed mechanism	Reference
Antibiotic	Webster mice infected IP with <i>S. pyogenes</i> C203 and <i>M. pyogenes</i> var. <i>aureus</i>	Dioxane/water or N,N-dymethylacetamide (SC)	TST inhibits ribosomal protein synthesis by binding to the GTPase-associated region of the 23S rRNA/L11 protein complex (Porse et al. 1998)	(Steinberg, Jambor, and Suydam 1955)
Antituberculosis	<i>Zebrafish</i> larvae infected with <i>Mycobacterium marinum</i>	0.5% DMSO in 1X PBS (IP)	TST inhibits bacterial protein synthesis and induces ER stress-mediated autophagy in macrophages to eliminate intracellular pathogen	(Zheng et al. 2015)
Antimalaria	<i>In-vitro</i> studies only	0.5% DMSO	TST causes rapid killing of <i>P. falciparum</i> by inhibiting parasite's proteasome and delayed death by inhibiting plasmodial apicoplast	(Aminake et al. 2011)
Anticancer	MDA-MB-231 (breast cancer) and HepG2-luc (liver cancer) xenografts in athymic mice	DSPE-PEG ₂₀₀₀ particles (IV)	TST inhibits proteasome and down-regulates oncogenic FOXM1	(M. Wang and Gartel 2011)
	High grade serous ovarian cancer in athymic nude mice	SSM (IP)	TST degrades tumorigenic PAX8 protein in a proteasome-independent manner	(Hardy et al. 2019)
Anti-inflammatory	Psoriasis-like inflammation induced by application of LL-37 in C57BL/6J mice ears	Hydroxypropyl cellulose gel (topical)	TST inhibits proteasome activity and prevents trafficking and activation of TLR7-9	(Lai et al. 2015)

TABLE II: REPORTED MINIMUM INHIBITORY CONCENTRATION (MIC) OF TST AGAINST GRAM-POSITIVE BACTERIA.

Microorganism	Strain	MIC ($\mu\text{g/mL}$)	MIC (μM)	Reference
<i>Bacillus sp.</i>	ATCC 27859	0.025	0.015	(Li, Zhang, and Kelly 2011)
	SIPI-JD1001	0.016	0.010	(Liao and Liu 2011)
<i>Enterococcus faecium</i>	ATCC 12953**	0.012	0.007	(Li, Zhang, and Kelly 2011)
	ATCC 51575**	1.665	1.0	(Nicolaou et al. 2005)
<i>Staphylococcus aureus</i>	Oxford	0.02	0.012	(Chary, C., Rambhav, S., Venkateswerlu 1990)
	ATCC 33591*	0.333	0.2	(Nicolaou et al. 2005)
	ATCC 10537*	0.012	0.007	(Li, Zhang, and Kelly 2011)
	USA300 (clinical isolate)*	4.16	2.5	(Niu et al. 2017)

* Methicillin-resistant

** Vancomycin-resistant

2. Limitations of the therapeutic application of TST

Despite the broad range of applicability, the clinical development of TST is hampered by its poor water solubility and delivery issues. TST is soluble in organic solvents such as dioxane, chloroform, N,N-dimethylformamide, N,N-dimethylacetamide, benzyl alcohol, and partially soluble in methanol, ethanol, isopropanol, butanol, trichloroethylene, and propylene glycol (Donovick, Joseph F, and Vandeputte 1961). However, the drug solubility in water is extremely limited, with reported values of less than 12 μM (20 $\mu\text{g/mL}$) (Pagano et al. 1955; Zhang and Kelly 2015; Liao and Liu 2011). During initial studies of TST, Steinberg and colleagues were unable to demonstrate oral absorption of TST in mice after doses as high as 250 mg/kg (Steinberg, Jambor, and Suydam 1955). This lack of oral bioavailability could be due to two reasons: (1) insufficient dissolution of drug particles in the gastrointestinal fluids required for absorption and (2) limited permeability of drug molecules across the intestinal barrier due to its large molecular size (1.7 kDa) (Doak et al. 2014). To overcome this problem, the authors formulated TST as a fine suspension in N,N-dimethylacetamide or 5% dioxane and administered either subcutaneously or intravenously (Steinberg, Jambor, and Suydam 1955). Although this approach yielded positive pre-clinical efficacy results, the use of such organic solvents is limited in pharmaceutical products because of their inherent toxicity ("Q3C - Tables and List Guidance for Industry" 2017).

In order to make insoluble drugs suitable for intravenous administration, co-solvents and surfactants are usually employed for solubilization. Co-solvents are water-miscible organic solvents added to the primary solvent (water) to improve the drug solubility (Naguib et al. 2016). Common examples of co-solvents approved for human

use are ethanol, glycerol, low molecular weight polyethylene glycol, and propylene glycol (Nema, Washkuhn, and Brendel 1997). On the other hand, surfactants are amphiphilic molecules (i.e. contain both hydrophilic and hydrophobic groups) capable of reducing the surface tension between two phases such as hydrophobic surfaces and liquid solvent (Naguib et al. 2016). The most common surfactants used in pharmaceutical products are polysorbate 80, carboxymethyl cellulose sodium, and povidone (Nema, Washkuhn, and Brendel 1997). However, high concentrations of these excipients might not be well tolerated and cause hemolysis and/or hypersensitivity reactions (Yalkowsky, Krzyzaniak, and Ward 1998). In addition, the excipients can become too diluted during injection and might no longer be sufficient to maintain the drug in solution, resulting in precipitation. Those drug aggregates can attach to the vein wall and cause local inflammation (phlebitis) and activation of coagulation pathways, resulting in thrombus, embolus, obstruction of blood flow to essential organs, and even death (Yalkowsky, Krzyzaniak, and Ward 1998).

The toxicological effects of TST have not been thoroughly studied, but reports indicate LD₅₀ in mice of 2000 mg/kg IP, >1000 mg/kg oral, and 41 mg/kg IV ("Toxnet - Thiostrepton USP," n.d.). TST is not absorbed by the gastrointestinal tract, which contributes to high oral tolerance. On the other hand, TST is insoluble in water and likely precipitates once injected intravenously, causing toxic effects and mortality at lower doses. For this reason, the only marketed product of TST is a topical ointment combination product containing also nystatin (antifungal), neomycin sulfate (broad-spectrum aminoglycoside antibiotic), and triamcinolone acetonide (corticosteroid) for the treatment of veterinary skin infections (Just-Baringo, Albericio, and Álvarez 2014).

Additionally, a clinical trial published in 1959 demonstrated no evidence of blood chemistry, hematology, or urine changes in 25 human patients who received a total of 10 g of topical TST (1% ointment) over a one-week period for the treatment of superficial infections at the oral cavity (Kutscher et al. 1959).

Another important limitation of TST is the existence of resistance mechanisms against this drug. TST is highly active against Gram-positive bacteria and can affect *Escherichia coli* ribosomes in cell-free studies (Weisblum and Demohn 1970). However, until recently, TST was regarded as inactive against intact Gram-negative bacteria because of the lack of penetration through their outer membrane (Nicolaou et al. 2005; Delcour 2009; Donovan, Joseph F, and Vandeputte 1961). A new study found *Pseudomonas aeruginosa* and *Acinetobacter baumannii* are susceptible to TST under low-iron conditions as it can be internalized by Gram-negative bacteria through overexpressed iron transporters (pyoverdine receptor FpvA and FpvB) (M. R. M. Ranieri et al. 2019). Additionally, TST resistance can be caused by expression of the thiostrepton resistance gene (*tsr*) which encodes an RNA methyltransferase that prevents TST from binding to ribosomes by methylating the target site (Cundliffe 1978). This mechanism of resistance is the same used by TST producing microorganisms to prevent self-intoxication (Cundliffe 1978). Lastly, TST stimulates the expression of thiostrepton-induced proteins A (*tipA*) gene which regulates a stress response system against thiopeptides (Chiu et al. 1999). The *tipA* gene encodes the long protein TipAL (253 amino acids) and the short protein TipAS (144 amino acids). TipAS sequesters TST and other thiopeptides from the cytoplasm as a protection mechanism, while TipAL binds to these thiopeptides and activates *tipA* gene transcription for positive feedback

loop. The *tipA* gene is usually found in TST non-producing strains of *Streptomyces* and produces TipAS in molar excess compared to TipAL (>20:1) (Habazettl et al. 2014).

Drug stability is another challenge encountered for TST clinical application.

Pagano and colleagues found that TST maintained its *in vitro* activity after incubation in biological media such as simulated gastric and intestinal fluids, feces, urine, and plasma (Pagano et al. 1955). However, TST lost antimicrobial activity in whole blood possibly due to drug binding to blood cell components through hydrophobic interactions (Pagano et al. 1955).

Most of the physicochemical issues of TST can be addressed through encapsulation in SSM nanocarrier to improve drug solubility, safety, and stability. By formulating TST as an SSM nanomedicine, TST molecules can be transported in their molecular form in the blood and protected from aqueous environment. As a result, drug molecules are no longer subjected to aggregation and they can be safely delivered intravenously without interacting with blood components.

C. Drug encapsulation in SSM

(Previously published as Esparza, K., Onyuksel, H. (2019) Development of co-solvent freeze-drying method for the encapsulation of water-insoluble thiostrepton in sterically stabilized micelles, Int. J. Pharm. 556, 21-29).

1. Limitations of large-scale production of SSM nanomedicines

Despite multiple benefits of using SSM for the delivery of water-insoluble drugs, the conventional encapsulation method is not scalable for industrial purposes. In the thin-film hydration technique, phospholipid and drug are solubilized in organic solvents and dried in a rotary evaporator to form a homogeneous thin film in a round bottom flask

(Figure 5). Once the film is completely dry, the material is resuspended in aqueous media under vigorous sonication and mixing to promote micelles self-assembly and concomitant drug encapsulation. Given the limitations of round bottom flask sizes and rotary evaporator capabilities, this method is impractical for large-scale production and it would probably require several small batches to achieve useful volumes of nanomedicine, leading to long production time, high batch-to-batch variability, and inflated manufacturing costs. To address these limitations, we developed a scalable co-solvent freeze-drying technique to produce TST-SSM nanomedicine.

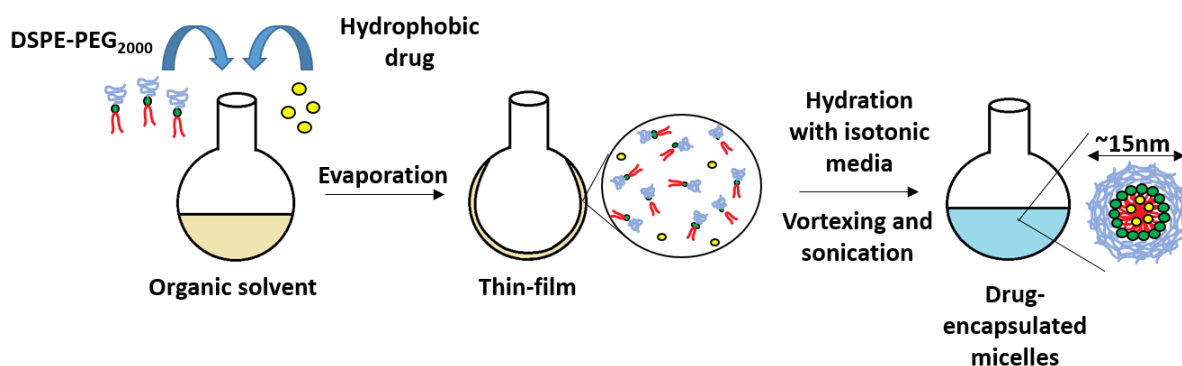


Figure 5: Scheme of the thin film hydration drug encapsulation method.

2. Basic principles of lyophilization/freeze-drying

Freeze-drying or lyophilization is a common manufacturing technology used to stabilize and prolong the shelf-life of pharmaceutical products, particularly injectable

solutions (Nireesha et al. 2013). The goal of this process is to reduce the amount of water to levels where biological growth and chemical reactions can no longer occur, thus keeping the product stable for extended periods until use. The three basic components of any freeze-dryer are drying chamber, condenser, and vacuum pump **(Figure 6)**. The main steps of the lyophilization process include (1) freezing of fresh product, (2) removal of free water molecules by sublimation (primary drying), and (3) removal of bound water molecules by desorption (secondary drying).

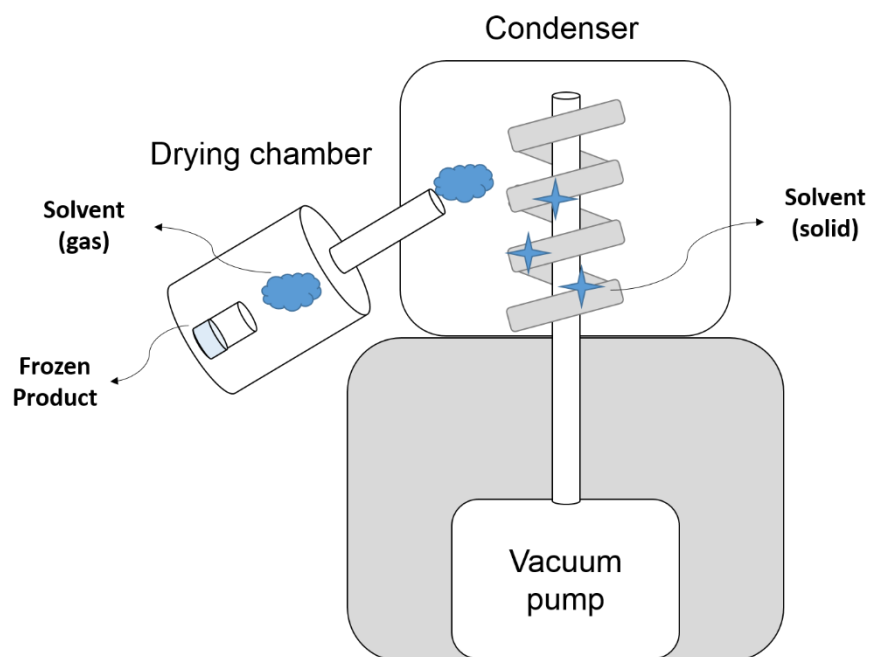


Figure 6: Scheme of freeze-dryer components.

Freezing is a critical step of lyophilization because the microstructure of the frozen product affects drying rates, freeze-dried cake morphology, and reconstitution properties (Nireesha et al. 2013). Products can be frozen directly in freeze-dryers equipped with cooling shelves, or frozen externally with liquid nitrogen and/or conventional freezers and quickly transferred to freeze-dryers for drying steps. During freezing, water molecules separate from solute to form ice crystals and solute is confined between solvent crystals. In general, rapid cooling results in the formation of small ice crystals while slow cooling generates larger crystals. Smaller crystals leave behind narrow spaces in the solute matrix as they sublime, creating high resistance to the passage of the remaining solvent. As a result, the drying time is often prolonged and rehydration of lyophilized cake might be challenging (Nireesha et al. 2013). Therefore, larger solvent crystals are usually preferred as they have shorter drying times and faster reconstitution (Nireesha et al. 2013). Some compounds undergo incomplete crystallization when first frozen and might require an additional thermal treatment called annealing. In this process, the product temperature is cycled a few times to allow higher molecule mobility and growth of larger crystals (Hottot, Vessot, and Andrieu 2007). Once products are properly frozen, they can proceed to the drying steps.

Sublimation is the passage of solvent molecules directly from the solid state to the gaseous state, without going through the liquid state. For this transition to take place, temperature and pressure conditions must be kept below the triple point, which in the case of water corresponds to 0.0099°C and 4.579 mmHg (**Figure 7**) (Nireesha et al. 2013). As the solvent crystals transform into gas, water vapor travels from the drying chamber to the condenser and solidifies, creating a concentration gradient of water

vapor that further drives the solvent removal (**Figure 6**). However, if the temperature of the product rises above a critical temperature – eutectic temperature for crystalline mixtures or glass transition temperature for amorphous mixtures – the drying material undergoes melt-back and collapse (Nireesha et al. 2013). The primary drying is completed once all free solvent molecules are removed and only bound water remains for the secondary drying.

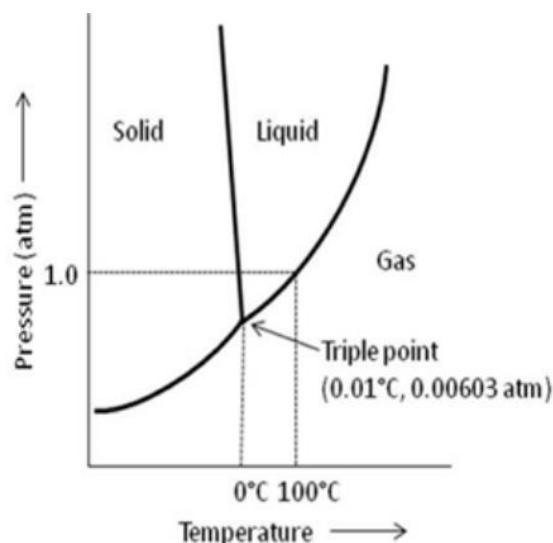


Figure 7: Phase diagram of water with the triple point.

Reprinted by permission from the International Journal of Novel Trends in Pharmaceutical Sciences (Licensed under CC BY 4.0), (Nireesha et al. 2013), Copyright 2013.

In the secondary drying, bound water is removed from the product by applying higher temperatures and lower chamber pressures (Nireesha et al. 2013). Since ice crystals are absent at this stage, the product is no longer at risk for melt back and can withstand higher temperatures. Care must be taken to not raise the temperature too high, otherwise, heat-labile compounds can degrade. At the end of the freeze-drying process, the resulting lyophilized product should be elegant and homogenous in appearance and contain large surface area, low residual moisture, and rapid reconstitution in water. The reconstituted product must be clear and free of particles other than drug-loaded micelles and exhibit acceptable drug potency. For long-term storage, the product vial can be flushed with inert gas and tightly sealed to protect the cake from the environment.

Freeze-dried pharmaceuticals usually required additional excipients to facilitate the lyophilization process and improve the properties of the final product. For example, cryoprotectants and lyoprotectants are commonly used agents to protect products against the stress of freezing and dehydration, respectively. During the freezing step, as the solvent separates from solutes to form ice crystals, the hydrophobic solutes may aggregate due to the increased concentration of ice crystals may induce mechanical stress over solutes, particularly nanoparticles and biologicals (Abdelwahed et al. 2006). To avoid this process, sugars such as trehalose, sucrose, lactose, and mannitol are often added to form a glassy matrix and immobilize solute in a stable state. These same sugars can also act as lyoprotectants by serving as “water substitutes” during the drying stages. As ice crystals are removed, the mechanical strength of the solid matrix is reduced, and the cake is at risk of collapsing. Lyoprotectants protect freeze-dried

products by providing bulk to the formulation and stabilizing solutes through hydrogen bonds (Abdelwahed et al. 2006).

Water is typically the only solvent removed by freeze-drying, but other organic solvents can also be present in smaller quantities (Teagarden and Baker 2002). These solvents can be residual solvents from a previous manufacturing step or intentionally added to improve product characteristics. Tert-butanol (TBA) is the most common organic solvent used in combination with water for lyophilization of pharmaceutical products because of its beneficial properties in the freeze-drying process.

TBA exhibits unique properties that make it an ideal co-solvent candidate for lyophilization (Teagarden and Baker 2002; Rey and May 2010). Firstly, TBA is completely miscible with water, forming a homogenous phase with aqueous solutions at any proportion. In addition, contrary to most organic solvents, TBA presents a relatively high freezing/melting point (24°C) which facilitates its solidification and removal by conventional condensers during lyophilization. The use of TBA in co-solvent systems also improve the solubility of hydrophobic drugs and excipients, increase the chemical stability of sensitive compounds in aqueous media, and promotes rapid solvent sublimation due to its high vapor pressure (26.8mmHg at 20°C). Furthermore, TBA is regarded as a safe solvent since its LD₅₀ is similar to other safe solvents (class 3) listed in the International Conference on Harmonization (ICH) guidance on impurities and residual solvents (Teagarden and Baker 2002; “Q3C - Tables and List Guidance for Industry” 2017). Still, special manufacturing processes and controls may be needed to ensure the safe handling of this flammable organic solvent.

Although lyophilization is often a costly and time-consuming process, freeze-drying cycle parameters (temperature, pressure, and time) can be optimized to reduce drying time, improve final product properties, and increase the cost-effectiveness of the process. In addition, freeze-drying employs lower temperature conditions than other dehydration methods, protecting heat-sensitive compounds and efficiently preserving pharmaceutical products for long-term storage.

3. Drug encapsulation by Fournier's method

Freeze-drying is conventionally used to stabilize aqueous formulations for long-term storage. However, in 2004, Fournier and colleagues reported the use of freeze-drying as part of the encapsulation method of hydrophobic drugs in poly(N-vinyl-2-pyrrolidone)-block-poly(D,L-lactide) (PVP-b-PDLLA) polymeric micelles (E. Fournier et al. 2004). The method consisted of first dissolving the micelle polymer in water and the hydrophobic drug in TBA. Next, the aqueous polymer solution was mixed with the organic drug solution at a final proportion of 30% TBA: water (v/v) and gently stirred at 4°C for 3h before freeze-drying. The lyophilized cake was reconstituted with 5% dextrose. According to the authors, TBA migrated to the hydrophobic core of micelles causing “swelling” (**Figure 8**) and facilitated the drug loading. The freeze-drying process was then employed to purify the formulation from the organic solvent and allow the rehydration with an injectable vehicle.

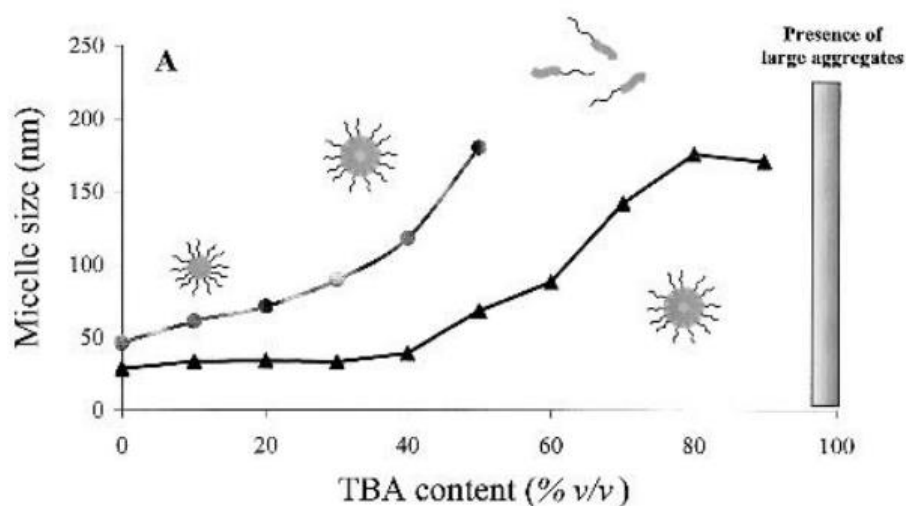


Figure 8: Swelling of PVP-b-PDLLA micelles with increases in TBA content. (●) PVP-b-PDLLA_{27%} and (▲) PVP-b-PDLLA_{38%} solutions. Reprinted by permission from Springer Nature, Pharmaceutical Research, (E. Fournier et al. 2004), Copyright 2004.

In this study, we adopted the Fournier's method to encapsulate TST in SSM (Figure 9), but we were unable to achieve similar drug loading as the thin-film hydration method. For this reason, we re-evaluated the principles of the method and developed it for our needs.

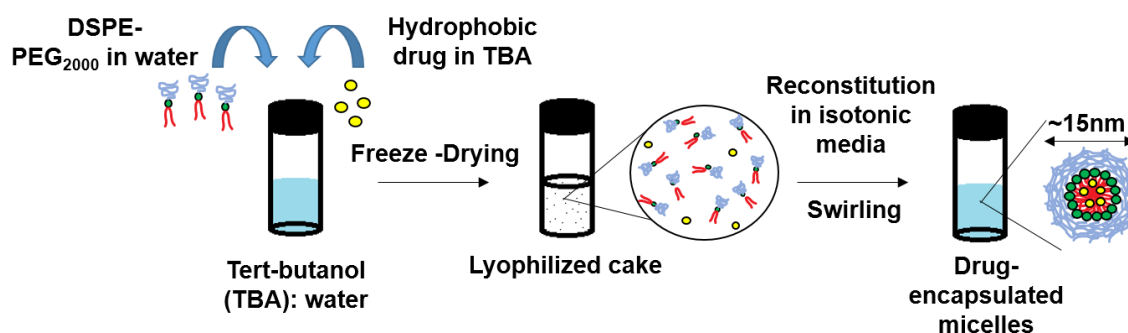


Figure 9: Scheme of co-solvent freeze-drying encapsulation method.

D. Staphylococcal pneumonia

1. Methicillin-resistant *Staphylococcus aureus* (MRSA)

Staphylococcus aureus is a Gram-positive, facultative anaerobic bacteria that cause an array of human diseases (Tong et al. 2015). Examples of diseases include superficial infections such as skin and soft tissue infections, systemic infections such as pneumonia, osteomyelitis, and bacteremia, and toxinoses such as food poisoning, scalded skin syndrome, and toxic shock syndrome (Sousa and Lencastre 2004). Approximately 30% of the global population is colonized with *S. aureus* on the skin or nares without any symptoms, but serious infections can arise if this microorganism overcomes immune barriers and reaches sterile sites (Krismer et al. 2017). According to the Center for Disease Control (CDC), more than 119,000 people suffered from bloodstream staphylococcal infections in the United States in 2017, leading to nearly 20,000 deaths (Kourtis et al. 2019). *S. aureus* is also an important cause of pulmonary infections, accounting for 1-10% of community-acquired pneumonia and 20-50% of hospital-acquired pneumonia (Hidron et al. 2009). Moreover, there is an increasing concern over the development of antibiotic resistance among these pathogens, limiting our ability to effectively treat staphylococcal infections.

Methicillin-resistance *S. aureus* (MRSA) is a subpopulation of *S. aureus* resistant to methicillin and most other β -lactams due to the acquisition of the *mecA* gene (**Figure 10**) (Gould et al. 2012). Although methicillin is no longer used in the clinics, the terms methicillin-sensitive *S. aureus* (MSSA) or methicillin-resistant *S. aureus* (MRSA) are still in use to these days. Surveillance reports indicate that more than 80,000 and 170,000 people contracted invasive MRSA infections in the United States and Europe,

respectively, of which 11,000 and 5,400 perished from MRSA-related complications (Norrby et al. 2009; CDC 2013). Since its first observation in 1961 (Jevons 1961), MRSA has been classically associated with healthcare-acquired infections, affecting patients with weakened immune systems or subjected to invasive medical procedures (Chambers and Deleo 2009; DeLeo et al. 2010). Recently, however, highly virulent MRSA has been identified in otherwise healthy individuals, leading to exceptionally severe infections (Chambers and Deleo 2009; Hidron et al. 2009).

In the mid-1990s, cases of MRSA infections were reported among young and healthy individuals who were in close physical contact (athletes, prisoners, children, and military recruits) (Tenover and Goering 2009). Because these infections were reported in populations without prior exposure to the healthcare environment, they were termed community-acquired MRSA (CA-MRSA). Since 2000, MRSA USA 300 has been the most predominant CA-MRSA in the United States (David and Daum 2017). Although skin and soft tissue are the most common type of infection observed, MRSA USA 300 is also linked with necrotizing pneumonia, particularly following influenza. In those cases, the pore-forming toxin Panton-Valentine leucocidin (PVL) seems to play a role in the pathophysiology of the disease (Labandeira-Rey et al. 2007; Diep et al. 2008), but evidence is still controversial (Peyrani et al. 2011; Olsen et al. 2010).

Staphylococcus aureus Drug Resistance and Epidemics

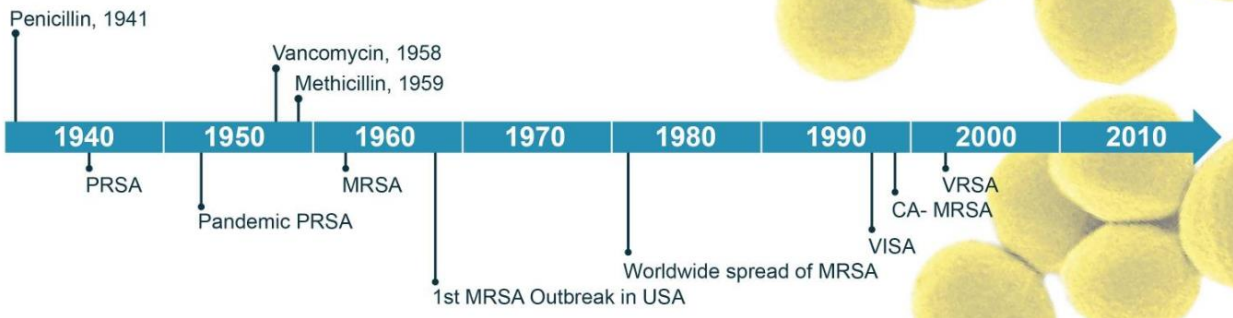


Figure 10: Historical evolution of methicillin-resistant *Staphylococcus aureus* (MRSA). PRSA: penicillin-resistant *S. aureus*; VISA: vancomycin intermediate-resistant *S. aureus*; CA-MRSA: community-acquired MRSA; VRSA: vancomycin-resistant *S. aureus*. Reprinted by permission from The Yale Journal of Biology and Medicine, (McGuinness, Malachowa, and Deleo 2017), Copyright 2017.

2. Pathogenesis of staphylococcal pneumonia

Staphylococcal pneumonia is an acute infection and inflammation of the pulmonary parenchyma caused by the invasion and colonization of *S. aureus*. The pathogen can reach the lungs by inhalation (aerogenous) or through the blood circulation as a result of spreading infection from other sites (hematogenous) (Farver 2019; Naraqi and McDonnell 1981). In both cases, the establishment and progression of this disease depend on complex interactions between the host and the pathogen (Azzopardi, Ferguson, and Thomas 2013; Abbas, Lichtman, and Pillai 2015).

The pathogenicity of *S. aureus* can be attributed to the coordinated actions of several cell wall-associated components and secreted bacterial proteins (**Figure 11**). *S. aureus* expresses adhesins on its surface which bind to host plasma or extracellular matrix components to promote pathogen attachment, colonization, and evasion from the

immune system (Gordon and Lowy 2008). Typical adhesins include fibronectin-binding proteins A and B, clumping factors A and B, collagen-binding protein, and staphylococcal protein A (SpA) (Bien, Sokolova, and Bozko 2011). Among virulent exoproteins, *S. aureus* secretes degrading enzymes, including nucleases, proteases, lipases, hyaluronidase, and collagenase which contributes to convert host molecules into nutrients that will promote bacterial growth (Bien, Sokolova, and Bozko 2011). Additionally, *S. aureus* produces and releases cytolytic toxins such as α -hemolysin, leucocidin, and PVL which cause host cell damage and weakens host defenses (Bien, Sokolova, and Bozko 2011; Gordon and Lowy 2008). *S. aureus* can produce potent toxins that stimulate the proliferation of T-cells and cause systemic effects. Those so-called superantigens include toxic shock syndrome toxin-1, staphylococcal enterotoxins, and the exfoliative toxins A and B (Gordon and Lowy 2008). Finally, *S. aureus* is able to form and reside in biofilms (Kiedrowski et al. 2018) or to invade and survive inside mammalian cells, allowing evasion of host defenses and increasing pathogen persistence and infection recurrence (Gordon and Lowy 2008).

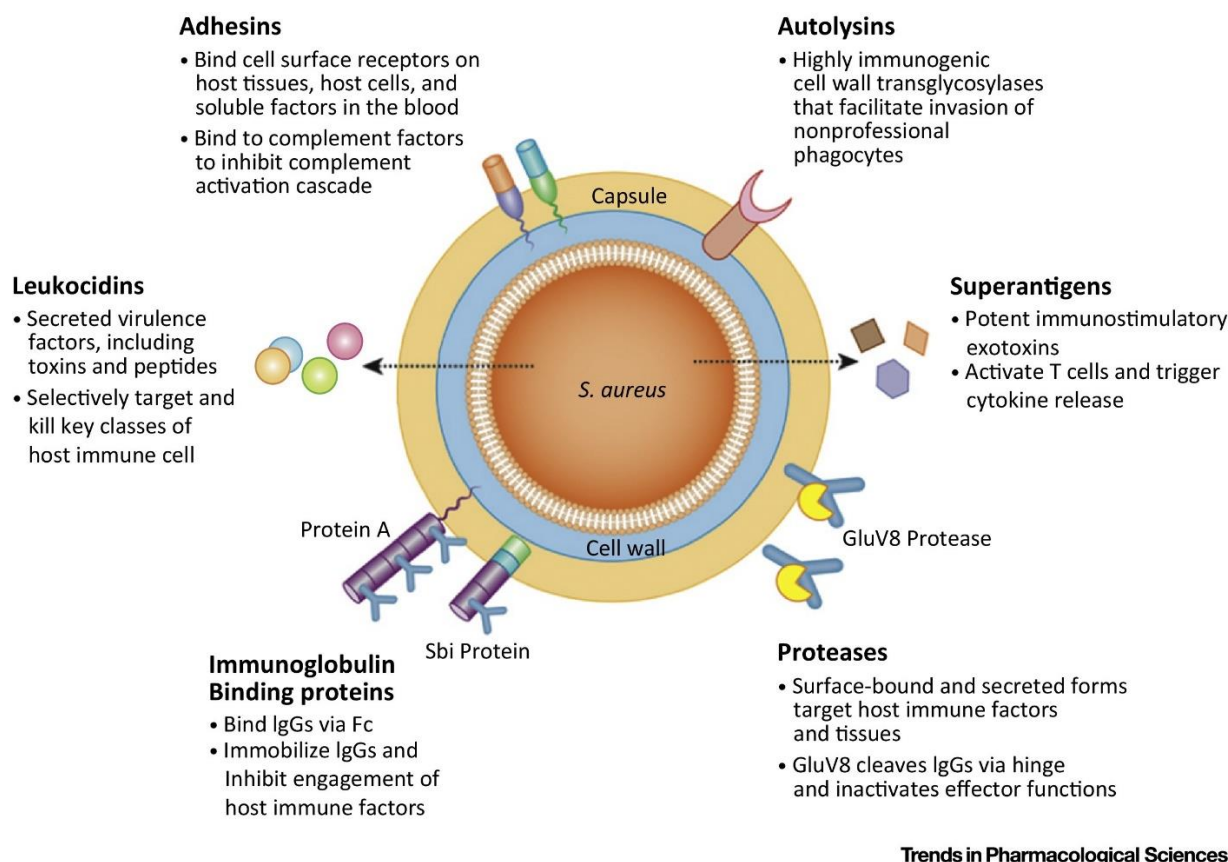


Figure 11: Virulence factors of *Staphylococcus aureus*.
Reprinted by permission from the Copyright Clearance Center: Elsevier, Trends in Pharmacological Sciences (Sause et al. 2016), Copyright 2016.

The host innate and adaptive immune systems work in conjunction to detain and resolve *S. aureus* infection. Plasma proteins called complement bind to the microbial surface and tag them for efficient phagocytosis (Fink and Campbell 2018). In addition, local tissue cells such as resident macrophages, dendritic cells, and epithelial cells express surface immune receptors including Toll-like receptors (TLRs) which recognize pathogen-associated molecular patterns (PAMPs) and initiate an appropriate immunological response (**Figure 12** and **Figure 13**). To date, 10 TLRs have been

identified in humans with different functions regarding PAMPs recognition and downstream response (Kawai and Akira 2010). TLR1, TLR2, TLR4, TLR5, and TLR6 are expressed on the cell surface and recognize microbial membrane components (lipids, lipoproteins, and proteins) (**Figure 12**), while TLR3, TLR7, TLR8, and TLR9 are located in intracellular vesicles and recognize microbial nucleic acids (**Figure 13**) (Kawai and Akira 2010). In the case of *S. aureus*, heterodimers of TLR2 with either TLR1 or TLR6 recognizes peptidoglycan and lipoteichoic acid on the bacterial cell wall and stimulate the production and release of pro-inflammatory cytokines such as tumor necrosis factor- α (TNF- α), IL-1 β , and IL-6 and chemoattractants including IL-8, macrophage/monocyte chemoattractant protein-1 (MCP-1), and macrophage inflammatory protein-1 (MIP-1) (B. Fournier and Philpott 2005). On the other hand, staphylococcal DNA – which as opposed to mammalian cells is rich in unmethylated cytosine-phosphate-guanosine (CpG) motifs – is processed by phagocytes and recognized by intracellular TLR-9, resulting in direct activation of dendritic cells, macrophages and B cells, and stimulating strong TH1 responses (adaptive immunity) (B. Fournier and Philpott 2005; Kawai and Akira 2010).

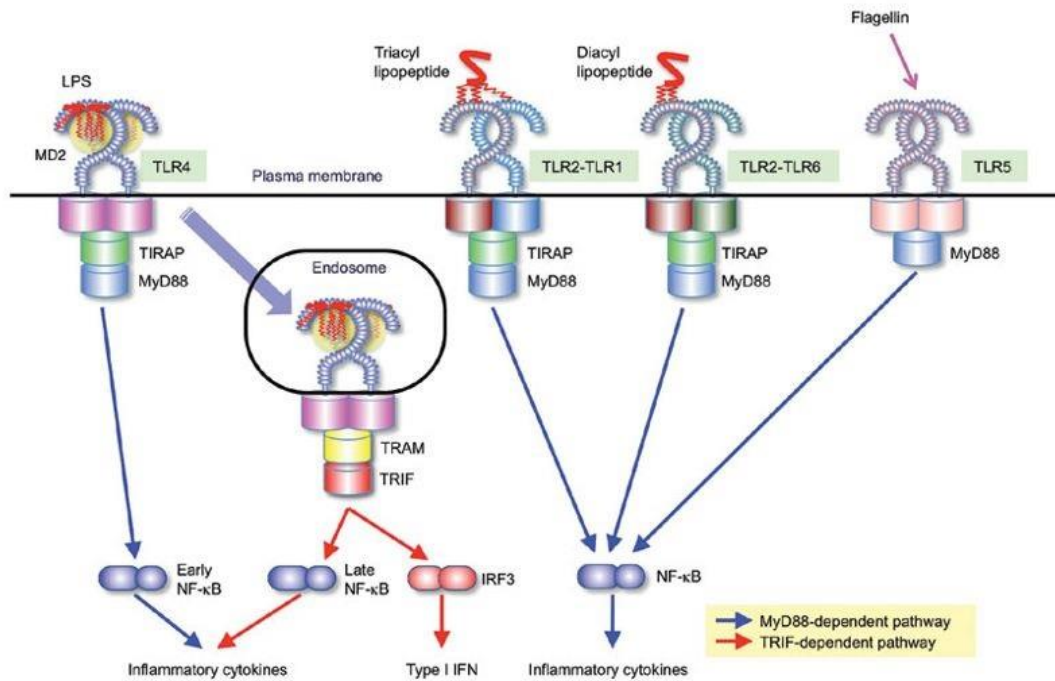


Figure 12: Extracellular Toll-like receptors (TLR).

Reprinted by permission from the Springer Nature Customer Service Centre GmbH: Springer Nature, Nature Immunology, (Kawai and Akira 2010), Copyright 2010.

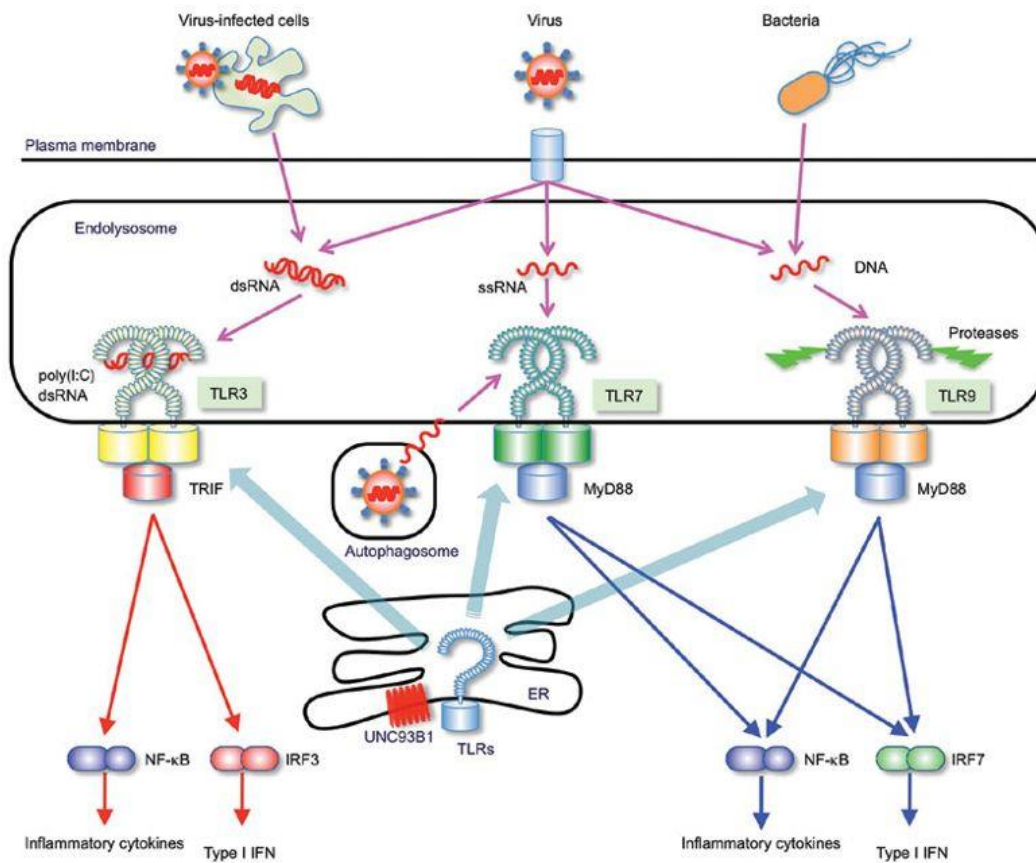


Figure 13: Intracellular Toll-like receptors (TLR).

Reprinted by permission from the Springer Nature Customer Service Centre GmbH: Springer Nature, Nature Immunology, (Kawai and Akira 2010), Copyright 2010.

Despite the elaborate human immunological response, bacterial infections can become complicated and elicit exacerbated immune response, damaging host tissue along with the pathogen. In the lungs, bacterial infection can progress with damage to both vascular endothelium and alveolar epithelium causing critical pulmonary edema and respiratory distress, a potentially deadly condition known as acute lung injury (Johnson and Matthay 2010). Another consequence of unresolved lung infection is the

translocation of bacteria to the bloodstream (bacteremia), which leads to sepsis, septic shock, and death. Alarming, septic shock caused by *S. aureus* has a fatality rate of more than 20% (Hal et al. 2012).

Signs and symptoms of staphylococcal pneumonia vary according to the severity of the infection. Patients often exhibit fever, chills, cough (with or without sputum production), chest pain, and dyspnea. Complications include empyema (collection of pus in the pleural space), respiratory failure, and bacteremia. Patients suffering from necrotizing pneumonia – the most severe manifestation of MRSA pneumonia – also display hypotension, hemoptysis (coughing up of blood), and pulmonary infiltrates and/or cavitation, which can rapidly progress to sepsis and death (Hidron et al. 2009). Older age, underlying lung diseases such as cystic fibrosis, intubation, and prior influenza infection are significant risk factors for staphylococcal pneumonia (David and Daum 2017). *S. aureus* infections can be transmitted directly by contact with an infected patient or indirectly through contaminated objects and surfaces (Chambers and Deleo 2009).

3. Current therapies against staphylococcal pneumonia

The management of *S. aureus* pneumonia often requires intravenous (IV) antibiotics for 7 days or longer depending on the severity of the disease. The current therapy for MSSA includes β -lactams such as oxacillin or nafcillin or cephalosporins such as cefazolin (David and Daum 2017). B-lactams are a broad class of antibiotics containing a β -lactam ring in their chemical structure (Gualerzi et al. 2014). This includes penicillin, cephalosporins, cephamycins, carbapenems, and monobactams (Letourneau 2017). Their mechanism of action consists of inhibiting a family of related

membrane-associated proteins called penicillin-binding proteins (PBPs) which are required for the biosynthesis of the bacterial cell wall (Gualerzi et al. 2014). The blocking of PBPs, particularly during cell division, activates the bacterial autolytic system which weakens the cell wall, causing cell lysis and lethal leakage of cytoplasmic content. Because of this mechanism of action, β -lactams are usually regarded as bactericidal agents (Letourneau 2017). Each microorganism expresses distinct sets of PBPs which confer them varying susceptibilities to β -lactams (Letourneau 2017). In addition, certain bacteria express mutated regulatory genes or absence of autolytic enzymes, which makes them tolerant of β -lactams. In the case of *S. aureus*, methicillin resistance is caused by the acquisition of *mecA* gene which encodes a PBP with a lower affinity to β -lactams called PBP2a (Peacock and Paterson 2015). On the other hand, penicillin resistance in *S. aureus* is often attributed to the acquisition of the *blaZ* gene, which encodes the hydrolytic enzyme β -lactamase (Mcguinness, Malachowa, and Deleo 2017). Such resistance infections are often associated with poor clinical outcomes and require alternative antibiotics for treatment (Mcguinness, Malachowa, and Deleo 2017).

Vancomycin is a glycopeptide antibiotic used intravenously to treat patients with suspected or confirmed invasive MRSA infections (C. Liu et al. 2011). This drug exerts its bactericidal effect by binding to precursors of peptidoglycan and interrupting essential cross-linking of the bacterial cell wall (Courvalin 2006; Perichon and Courvalin 2009). Although vancomycin is classically considered the first-line therapy for MRSA infections, vancomycin intermediate-resistant *Staphylococcus aureus* (VISA, MIC = 4-8 μ g/mL) and, less commonly, vancomycin-resistant *Staphylococcus aureus* (VRSA, MIC

> 16 µg/mL) have recently emerged leading to increasing therapeutic failure (Mcguinness, Malachowa, and Deleo 2017). The VISA subtype has been linked with several genetic mutations that lead to the thickened cell wall and increased sequestration and inactivation of vancomycin (Mcguinness, Malachowa, and Deleo 2017). On the other hand, VRSA is caused by the acquisition of the *vanA* gene which encodes a modified peptidoglycan precursor with low affinity to glycopeptides (Perichon and Courvalin 2009). Additionally, the use of vancomycin is limited by potential severe side effects of the drug. The red man syndrome is a serious dermatologic reaction on the face, neck, and upper torso caused by the release of histamine during the infusion of vancomycin (Sivagnanam and Deleu 2003). In rare cases, vancomycin is also associated with hypotension, ototoxicity, and acute renal failure, requiring immediate discontinuation (Bruniera et al. 2015).

Alternatively, the Infectious Diseases Society of America recommends the use of linezolid or clindamycin as a second-line treatment of MRSA pneumonia (C. Liu et al. 2011). Linezolid is an oxazolidinone drug that exerts its bacteriostatic activity by preventing the complexation of tRNA, mRNA, and ribosome, thus inhibiting the initiation of protein synthesis (Tsiodras et al. 2001). Resistance to linezolid has been observed in the clinical practice due to target modification of the mRNA induced by the *cfr* gene (Locke et al. 2014; Tsiodras et al. 2001). Clindamycin is a lincosamide that blocks bacterial growth by inhibiting the peptidyltransferase reaction on the 50S ribosomal subunit necessary for protein synthesis (Spizek and Rezanka 2004). Resistance to clindamycin is caused by *erm* genes that encode ribosome methyltransferases and modify the target site (Levin et al. 2005; Siberry et al. 2003; Spizek and Rezanka 2004).

In addition, *S. aureus* can enzymatically inactivate lincosamides through the expression of the *linA* gene (Brisson-noel et al. 1988).

In this study, we aimed to develop a new TST-SSM nanomedicine to provide a new therapeutic option to overcome at least partially some of the problems with current treatments of MRSA pneumonia.

4. Murine models of staphylococcal pneumonia

Mice are the main model organism used to study the pathogenesis and therapy of human staphylococcal pneumonia. Reasons for that include high cost-effectiveness, ease of handling, and shared genetic and biological functions which can be experimentally manipulated (Mizgerd and Skerrett 2008). Like the human infection, murine staphylococcal pneumonia can be induced via hematogenous spreading or through the airways. In the first case, the pathogen is incorporated in agar beads and injected intravenously. Due to their large size (~200 μm), infectious beads are entrapped in the pulmonary microvasculature, allowing colonization of the lung parenchyma. Other organs such as kidneys and liver are also affected in this model (Sawai et al. 1997). On the other hand, aerogenous infections are more localized and can be induced directly by instilling bacterial suspension in the lungs via nares or trachea, or indirectly by co-housing healthy animals with experimentally infected animals (Mizgerd and Skerrett 2008). Although the co-housing method mimics the natural transmission of respiratory pathogens, the weak cough reflex of mice and the generally lower infectivity of human pathogens in mice limit the efficiency of this method. In addition, the inoculum size, time of infection, and a number of infected animals are not controllable, creating a greater experimental variance. The direct introduction of

pathogens through nasal instillation is simple and non-invasive, but high variability can be encountered as the inoculum might leak out of the nares or be swallowed.

Another important variation of the staphylococcal pneumonia model is the use of immunosuppressed or immunocompetent mice. Since patients with compromised immune systems are particularly susceptible to staphylococcal pneumonia, investigators induce neutropenia in mice with cyclophosphamide a few days before the infection to predispose them to infection (Docobo-Pérez et al. 2012; Kidd, Abdelraouf, and Nicolau 2019). This state of immunosuppression usually lasts for at least 72h and allows the study of active infections for longer periods (Zuluaga et al. 2006). On the other hand, immunocompetent mice are more representative of patients that acquire infections in the community setting and exhibit peak expression of proinflammatory cytokines or chemokines after 6h of infection, but bacterial burden spontaneous decreases starting at 48h (Ventura et al. 2008).

More recently, humanized mice models have emerged as an alternative to better model staphylococcal infections using human-specific molecular targets (Parker 2017). Such models are particularly useful to understand host-pathogen interaction and in the development of vaccines because of the great number of virulence elements with human specificity. For example, Prince and colleagues demonstrated that irradiated mice engrafted with human CD34+ stem cells and thymic tissue express human leukocytes in the lung, blood, and bone marrow (Prince et al. 2017). These humanized mice were more susceptible to MRSA USA 300 pulmonary infection than non-humanized counterparts and produced robust human cytokine expression. Moreover, by comparing the infection with PVL-producing or PVL-deficient MRSA USA300, the

authors provided evidence that PVL expression results in more severe pulmonary infection, which can be ameliorated with anti-PVL antibodies. These observations would be impossible to obtain in non-humanized mice since PVL has high binding specificity for human C5aR and C5L2 receptors (Spaan et al. 2013).

In this dissertation study, we adopted the aerogenous infection model to create a more localized infection in the lungs rather than disseminated to other organs. In addition, we inoculated animals with bacterial suspension via intratracheal instillation to ensure complete dose administration in the distal regions of the lungs and minimize the involvement of the upper respiratory system. Lastly, since MRSA USA 300 is primarily a community-acquired infection affecting immunocompetent individuals, we employed immunocompetent mice to better represent the impact of the immune system in the pneumonia treatment and facilitate drug passive targeting through inflamed lungs.

E. Sepsis

1. Pathogenesis of sepsis

Sepsis is an acute, complex systemic syndrome caused by a dysregulated inflammatory response to infections that leads to multiple organ dysfunction syndrome (MODS) and death (Singer et al. 2016). On the other hand, septic shock is a severe subset of sepsis with persistent hypotension and hypoperfusion and a higher likelihood of death ($\geq 40\%$ versus $\geq 10\%$) (Singer et al. 2016). The Center for Disease Control estimates that 1.7 million adults develop sepsis with nearly 270,000 deaths each year in the United States ("Sepsis: Data and Reports" 2016). Although bacteria, viruses, and fungi can all cause sepsis and septic shock, bacterial sources are by far more common. In a multicenter prospective study conducted with over 7000 infected patients admitted

at intense care units across the globe, 62.2% of microbial isolates were Gram-negative bacteria, 46.8% Gram-positive bacteria, and 19.4% fungi (overlap represented polymicrobial infections) (Vincent et al. 2009). Among those isolates, *S. aureus* was the most prevalent microorganism (20.5%), followed by *Pseudomonas* species (19.9%) and *Candida* (17%) (Vincent et al. 2009). The most common source of infections were lungs (63.5%), abdominal organs (19.6%), bloodstream (15.1%), and urinary tract (14.3%), but other infected sites such as skin and central nervous system can also lead to sepsis (Ward and Levy 2017; Vincent et al. 2009).

The pathophysiology of sepsis is characterized by the dysregulated systemic immunological response against infection with life-threatening injury to the host (Ward and Levy 2017). Earlier definitions categorized sepsis into two phases termed systemic inflammatory response syndrome (SIRS) and compensatory inflammatory response syndrome (CARS) (Bone et al. 1992). In SIRS, the host innate immune system recognizes microbial patterns (PAMPs) or products of injured/dying cells and triggers intracellular signaling cascades that promote the excessive secretion of pro-inflammatory cytokines and other mediators such as TNF- α , IFN- γ , IL-1 β , IL-8, IL-6, and nitric oxide (NO). This “cytokine storm” prompt systemic inflammation by acting as endogenous pyrogens, activating the production of acute-phase proteins, increasing vascular permeability, recruiting effector cells (PMNs, macrophages, and natural killer cells), or stimulating the synthesis of secondary mediators (Chaudhry et al. 2013). An increase in vascular permeability causes generalized edema, hypovolemia, and compensatory tachycardia. In the meanwhile, antigen-presenting cells such as macrophages and dendritic cells present foreign antigens to T cells. The adaptive

immune system is activated and initiates antibody production by B cells or cytotoxicity by CD8+ cells, or it creates immunological memory for future use.

CARS is a hypo-inflammatory state created to offset the exacerbated inflammatory response of SIRS. In this phase, T regulatory cells, macrophages, PMNs, and other cells release anti-inflammatory cytokines such as IL-10, IL-4, and TGF- β to reduce inflammation and promote tissue healing. However, if CARS predominates over SIRS for a prolonged time, the primary infection can expand, and the patient becomes more susceptible to other opportunistic pathogens (**Figure 14**). In addition, a condition called disseminated intravascular coagulation can develop as a result of up-regulation of pro-coagulant mechanisms and downregulation of anticoagulant factors (Simmons and Pittet 2015). Intravascular thrombi can block blood vessels causing hypoxia damage in multiple organs and the depletion of clotting factors can lead to diffuse bleeding (Simmons and Pittet 2015). SIRS and CARS might also be present simultaneously, a condition termed mixed antagonist response syndrome (MARS). Given the severity of sepsis, early recognition and management are key to reduce sepsis-associated mortality (Ward and Levy 2017).

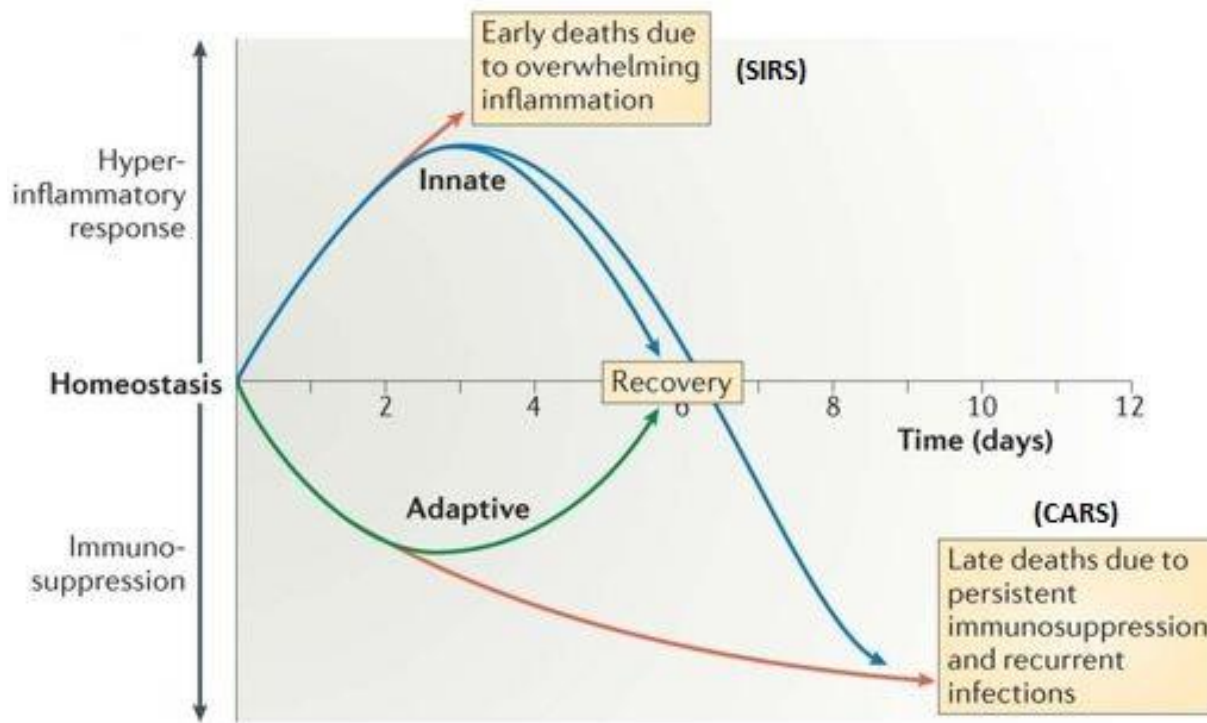


Figure 14: Pathogenesis of sepsis.

Adapted by permission from Springer Nature Customer Service Centre GmbH: Springer Nature, Nature Reviews Immunology, (Hotchkiss, Monneret, and Payen 2013). Copyright 2013.

The quick Sequential Organ Failure Assessment (qSOFA) is a predictive score system with three components that can be easily applied at patients' bedside to assess the risk of death from sepsis without the need of laboratory tests (Singer et al. 2016). Parameters of the qSOFA are respiratory rate $\geq 22/\text{min}$, altered level of consciousness with Glasgow coma score ≤ 13 , and systolic blood pressure $\leq 100 \text{ mmHg}$. Each positively identified parameter is assigned 1 point and a score of ≥ 2 is associated with poor outcomes and precludes immediate admission to critical care and initiation of supportive therapy.

2. Current therapies for sepsis

There are no specific drugs available targeting inflammatory events of sepsis. Therefore, the management of sepsis consists of antibiotic therapy to subside the source of infection and supportive measures to improve organ functions (Rello, Valenzuela-Sanchez, et al. 2017). The Surviving Sepsis Campaign has put forth a set of recommendations (bundles) in collaboration with the Institute of Healthcare Improvement to improve care and reduce sepsis mortality worldwide (Rhodes et al. 2017; Dellinger et al. 2008; Rello, Valenzuela-Sánchez, et al. 2017; M. M. Levy, Evans, and Rhodes 2018).

The resuscitation and management bundle are termed hour-1 bundle and must be implemented immediately after the patient's presentation (M. M. Levy, Evans, and Rhodes 2018). Elements of the bundle includes: (1) measurement of lactate levels and remeasure if lactate ≥ 2 mmol/L, (2) collection of blood for culture before administration of antibiotics, (3) administration of empiric broad-spectrum antibiotics to eliminate the source of infection, (4) initial IV fluid resuscitation with 30 mL/kg of crystalloid fluids for hypotension or lactate ≥ 4 mmol/L, and (5) administration of vasopressors during or after fluid resuscitation to maintain mean arterial pressure ≥ 65 mmHg. Commonly used vasopressors include noradrenaline, adrenaline, dobutamine or vasopressin. Serum lactate is a surrogate marker of tissue hypoperfusion because it is formed during the anaerobic breakdown of glucose in the tissues. The early administration of antibiotics is crucial, as a report indicates that every hour of delay in the first 6h after hypotension onset was implicated with reduced survival of 7.6% (Kumar et al. 2006). The choice of antibiotic must be reevaluated to better target the specific infection once the results of

the microbiological culture become available. Blood transfusion is recommended to patients with severe sepsis and hemoglobin levels below 7 g/dL (Rello, Valenzuela-Sánchez, et al. 2017). Administration of oxygen through a mask or mechanical ventilator is useful to reduce the work of breathing and optimize oxygen consumption (Rello, Valenzuela-Sánchez, et al. 2017). Unfortunately, therapies targeting inflammatory responses in sepsis has not been successful in clinical trials, thus they are not recommended (Riedemann, Guo, and Ward 2003).

3. Cecum ligation and puncture (CLP) sepsis mouse model

The cecum ligation and puncture (CLP) is the most frequently used animal model of sepsis because of its close resemblance to human sepsis (Dejager et al. 2011). In this model, mice are subjected to three insults that contribute to the development of sepsis: (1) tissue trauma during laparotomy, (2) necrosis due to the ligation of the cecum, and (3) polymicrobial infection due to the puncture of the cecum and leakage of intestinal content into the peritoneum. The severity of the inflammatory response depends on the extension of ligation of the colon, number, and location of punctures (necrotic or non-necrotic areas), the diameter of the puncture wound (determined by needle gauge), and amount of intestinal content extravasated during the procedure. The advantages of this method are the presence of a continuous infectious focus, the use of multiple host-derived microbes – similarly to the human peritonitis – and the presence of both hyper- and hypo-inflammatory phases. The main disadvantage of the method is the intra- and interlaboratory variability due to differences in personnel surgical skills/techniques and heterogeneity of the animal host responses. Other methods such as the systemic administration of lipopolysaccharide or bacterial inoculum models are

simpler and more controllable, but they do not reflect the microbiological diversity and complex pathophysiological changes commonly observed in human sepsis. Another less preferred method is called colon ascendens stent peritonitis (CASP) model, in which a stent is surgically inserted into the ascending colon for the continuous influx of intestinal bacteria into the peritoneum (Traeger et al. 2010). Although this model creates a strong inflammatory reaction, the immune response is thought to be more similar to endotoxemia instead of clinical sepsis with a surgical technique that is more challenging and variable than CLP (Dejager et al. 2011).

F. Limitations of therapies against staphylococcal infections and sepsis

Therapies specifically targeting inflammatory mechanisms of sepsis are an unmet medical need and are often referred to as a “graveyard” in the pharmaceutical field because of the multiple past clinical trial failures (Riedemann, Guo, and Ward 2003). The only drug specifically approved for sepsis, the recombinant human activated protein C (Xigris®, Eli Lilly) was withdrawn from the market in 2011 for not demonstrating a reduction in septic shock mortality in a follow-up clinical study (V. M. Ranieri et al. 2012). An incomplete understanding of sepsis pathophysiology along with the lack of consensus of sepsis definition leads to heterogeneous clinical testing populations and irreproducible outcomes, undermining the development of effective, life-saving therapies. Currently, antibiotics are the only therapy addressing the underlying cause of sepsis (infection), but its successful application is dependent upon the antimicrobial susceptibility.

Despite the availability of antibiotics to combat staphylococcal infections, the clinical failure of such therapies is still unacceptably high. In a retrospective,

observational study with patients suffering from ventilator-associated MRSA pneumonia, 15% of patients exhibited clinical failure after initiating treatment with linezolid versus 31% with vancomycin at day 14 (Peyrani et al. 2014). More dramatically, in a prospective, randomized, double-blind clinical trial including patients with MRSA healthcare-associated pneumonia, 42.4% and 53.4% of patients exhibited therapeutic failure at 7-30 days after the end of treatment with linezolid and vancomycin, respectively (Wunderink et al. 2012). Therapeutic failure of staphylococcal infections is often attributed to reduced drug susceptibility and lack of other antibiotic options and can lead to extended hospitalization and disease progression to bacteremia and sepsis (Nguyen and Graber 2010).

Although several policies have been implemented to reduce bacterial resistance – controlled antibiotic use, clinical surveillance, reduced veterinary use, among others – such measures are only effective over the long-term and do not substitute the need for new antibiotics (S. B. Levy and Marshall 2004). Paradoxically, despite the high demand for novel drugs to combat multidrug-resistant infections, the number of new antibiotics approved for clinical use has dropped in the past few years (Schäberle and Hack 2014; Shlaes et al. 2013). The pharmaceutical industry has shown diminished interest in developing antibiotics due to the low success rate in finding new compound leads in high-throughput screenings, strict clinical trial regulations, and the anticipated low return on investment (Schäberle and Hack 2014; Shlaes et al. 2013; Payne et al. 2007). Consequently, the global antibiotic crisis has prompted the reconsideration of old antimicrobial molecules which were previously disregarded due to their unfavorable physicochemical properties or unacceptable toxicity. Using current scientific knowledge

and modern technology, old drugs such as daptomycin and fidaxomicin were successfully introduced to the market decades after their discovery (Lewis 2013), and many other molecules such as thiostrepton (TST) remain to be revived.

G. Hypothesis and specific aims

We hypothesized that TST can be encapsulated into SSM using a scalable co-solvent freeze-drying method to provide a stable, safe, and effective nanomedicine against resistant staphylococcal pneumonia and sepsis. Despite several potential therapeutic uses, TST has been unable to reach the clinics because of its low water solubility and delivery issues. To address these challenges, we encapsulated TST in SSM nanocarrier for safe and efficacious intravenous delivery, developed a scalable drug encapsulation method, and evaluated the therapeutic value of the TST-SSM nanomedicine in animal models of MRSA pneumonia and CLP-induced sepsis. In specific aim 1, we used the conventional thin-film hydration method to determine the viability of the formulation and maximum drug loading, but developed a novel scalable method called co-solvent freeze-drying to enable large-scale production and facilitate future clinical translation of this nanomedicine. We optimized the new encapsulation method by systematically varying key parameters of the production process and assessed the short-term formulation stability after reconstitution of the lyophilized cake and sterilizing filtration, as well as long-term after storing the freeze-dried formulation at 5°C, 30°C/ 65% RH (relative humidity) or 40°C/ 75% RH. In specific aim 2, we investigated possible roles of SSM in improving the *in vitro* activity of TST against MRSA USA 300. We assessed the *in vitro* antimicrobial activity of TST-SSM nanomedicine against various Gram-positive microorganisms to define whether SSM

affected the drug accumulation intracellularly or the drug stability in the bacterial media at 37°C. In specific aim 3, we evaluated the therapeutic value of TST-SSM *in vivo* using models of staphylococcal pneumonia (MRSA USA 300) and polymicrobial sepsis induced by the cecum ligation and puncture (CLP) technique. In the first model we examined bacterial burden and drug accumulation in lungs, while in the second one we analyzed the survival rate, organs function, bacterial burden, and cytokine profile. Overall, results from this study provided us with new insights on how SSM can be used to enable the safe and effective delivery of TST using a production method that is amenable to scaling-up and more feasible for further clinical development.

The specific aims of this project were:

Specific aim 1: Develop and characterize TST-SSM nanomedicine

- 1.1. Determine the maximum TST loading in SSM using the conventional encapsulation method of thin-film hydration.
- 1.2. Develop and optimize the co-solvent freeze-drying method for the scalable preparation of TST-SSM nanomedicine.
- 1.3. Characterize TST-SSM formulation for particle size, drug concentration, residual TBA, and in-vitro antimicrobial activity.
- 1.4. Evaluate storage stability of freeze-dried and reconstituted TST-SSM nanomedicine.

Specific aim 2: Investigate mechanisms by which DSPE-PEG₂₀₀₀ micelles improve TST susceptibility against MRSA USA 300.

- 2.1. Assess the commonality of this phenomenon by evaluating TST-SSM susceptibility in other clinically relevant Gram-positive bacteria.

2.2. Evaluate if DSPE-PEG₂₀₀₀ micelles enhance TST uptake by MRSA USA 300.

2.3. Investigate if SSM prevents TST degradation in the experimental conditions of the microdilution assay.

Specific aim 3: Determine the *in vivo* efficacy of TST-SSM in mouse models of MRSA pneumonia and CLP-induced polymicrobial sepsis.

3.1. Evaluate the *in vivo* efficacy of TST-SSM nanomedicine in treating pneumonia caused by MRSA USA 300.

3.2. Compare drug accumulation in the lungs after treatment with free TST or TST-SSM formulation in MRSA pneumonia.

3.3. Evaluate the effect of TST-SSM nanomedicine on the survival rate of mice with CLP-induced polymicrobial sepsis.

3.4. Investigate underlying mechanisms of the TST-SSM effect in polymicrobial sepsis.

H. Significance of the project

Antibiotic resistance is a serious global concern because it limits our ability to treat life-threatening infections. Patients unresponsive to antibiotic therapy are at high risk for sepsis, septic shock, and death. Unfortunately, some previously discovered potent antibiotic drugs such as TST were not translated to clinical practice due to unfavorable physicochemical properties which restricted the practical, safe, and effective use of the drug.

Our study holds key innovative features that contribute to advance the development of TST for clinical use. **First**, we improved the aqueous solubility and stability of TST through encapsulation in SSM. This new TST-SSM nanomedicine can

be safely administered via intravenous route and delivered to target sites by passive targeting. **Second**, we developed a drug encapsulation method called co-solvent freeze-drying that, contrary to the conventional thin-film hydration, it can be easily scaled-up for industrial purposes with high reproducibility and efficiency. Due to the detailed evaluation performed on critical parameters of the co-solvent freeze-drying method for TST-SSM production, we believe this method can be adapted for other SSM nanomedicines such as paclitaxel, camptothecin, and curcumin to facilitate their clinical development. **Third**, this was the first time that an antibiotic drug has been successfully encapsulated in SSM without losing the *in vitro* antimicrobial activity. TST is a hydrophobic, uncharged molecule in physiological pH that does not rely on electrostatic charge for activity. For this reason, its antimicrobial activity was not impaired by SSM as reported for charged antibiotic molecules like polymyxin B. **Fourth**, we investigated a novel role of SSM in enhancing TST susceptibility against MRSA USA 300. We found that SSM protected the drug from the aqueous environment and prevented its inactivation at the *in vitro* conditions of the antimicrobial assay (incubation at 37°C for 24h). **Lastly**, we evaluated the therapeutic value of TST-SSM in animal models of MRSA pneumonia and CLP-induced polymicrobial sepsis. Although TST-SSM did not elicit antimicrobial activity *in vivo* at the tested conditions, we found that this nanomedicine improved the survival of septic animals and reduced systemic pro-inflammatory markers, possibly due to its reported anti-inflammatory activity via inhibition of TLR-9. This was the first time that TST has been tested as an anti-sepsis agent and further investigation is warranted to explore this notable therapeutic indication.

Altogether, findings of this study contributed to the development of a novel TST-SSM nanomedicine that can be produced in large-scale for the treatment of polymicrobial sepsis and possibly other anti-inflammatory diseases and cancers.

II. MATERIALS AND METHODS

A. Materials

1,2-Diastearoyl-sn-glycero-3-phosphoethanolamine-N-methoxy-poly(ethylene glycol 2000) (DSPE-PEG₂₀₀₀) sodium salt was purchased from LIPOID GmbH (Ludwigshafen, Germany). Thiostrepton (TST) (purity $\geq 98\%$) was purchased from EMD Millipore (Burlington, MA). Phosphate-buffered saline (PBS) 10X was purchased from Corning (Corning, NY) and diluted as needed with deionized water. Molecular biology grade water and PBS 1X was also obtained from Corning (Corning, NY). Sterile 0.9% saline were purchased from Baxter (Deerfield, IL). Water for injection and 0.9% saline for injection were from Hospira/Pfizer (Lake Forest, IL). Tert-butanol (TBA), chloroform, dichloromethane, hexane, diethyl ether, tryptic soy agar, tryptic soy broth, erythromycin, and vancomycin from *Streptomyces orientalis* were purchased from Sigma-Aldrich (St, Louis, MO). Nosiheptide was obtained from Cayman Chemical. HPLC-grade acetonitrile and dimethyl sulfoxide (DMSO) were obtained from Fisher Chemical (Fair Lawn, NJ). Scintillation glass vials of 4 mL and 20mL were obtained from Kimble-Chase (Vineland, NJ). Serum tube glass vials (20 mL), rubber stoppers, and flip-top caps were purchased from Fisher Scientific (Waltham, MA). Millex GP polyethersulfone (PES) sterile syringe filters (33 mm) were acquired from Millipore (Burlington, MA). The *Staphylococcus aureus* USA300 culture was kindly provided by Dr. Steven Dudek. *S. aureus* COL, *Bacillus anthracis* Sterne, *B. cereus* 14579, and *B. thuringiensis* konkukian 97-27 were kindly provided by Dr. Hyunwoo Lee from the Center for Biomolecular Sciences at UIC. Enzyme-linked immunosorbent assay (ELISA) kits for quantification of IL-6, IL-10, TNF- α , IL-1 β , and TGF- β were purchased from R&D Systems (Minneapolis, MN). Griess

reagent kit was obtained from Thermo Fisher Scientific (Waltham, MA). Nitrate reductase and nitrate reductase cofactor preparations were obtained from Cayman Chemical (Ann Arbor, MI). Isoflurane was obtained from Piramal Critical Care (Telangana, India). Lidocaine hydrochloride injection 20 mg/mL was obtained from APP Pharmaceuticals (Schaumburg, IL). Ketamine hydrochloride injection was obtained from West-Ward (Eatontown, NJ). Xylazine injection was obtained from Akorn (Lake Forest, IL). Heparin sodium injection (1000 USP units/mL) was from Aurobindo Pharma Limited (Pashamylaram, India).

B. Animals

Wild-type male C56BL/6 mice were purchased from the Jackson Laboratory (Bar Harbor, ME) and maintained in standard cages at the Biological Resources Laboratory (BRL) at UIC. Delivered animals were allowed at least 48h for acclimatization before use. Five mice were housed in each cage under a 12-hour light/dark cycle. Animals were fed with normal chow diet and drinking water ad libitum. Animal studies protocols were approved by the Animal Care Committee (ACC# 15-244 Mod. 16 and ACC# 17-138 Mod 2) and the Institutional Biosafety Committee (IBC# 16-006) at UIC. Approval letters can be found in **APPENDIX A**.

C. Methods

1. Preparation and characterization of TST-SSM nanomedicine

(Previously published as Esparza, K., Onyuksel, H. (2019) Development of co-solvent freeze-drying method for the encapsulation of water-insoluble thiostrepton in sterically stabilized micelles, *Int. J. Pharm.* 556, 21-29).

Most methods for preparation and characterization of TST-SSM have already been published elsewhere and will be adapted in this thesis (Esparza and Onyuksel 2019).

1.1. Determination of TST aqueous solubility by the modified shake-flask method

The aqueous solubility of free TST was determined by a modified shake flask method (Baka, Comer, and Takács-Novák 2008). We transferred approximately 2 mg of TST into 4 mL glass vials and added 2 mL of 1X PBS (triplicate). Samples were stirred with a magnetic bar in an incubator at 25°C protected from light. After 24 hours, we collected 1 mL of sample, separated undissolved drug using an Eppendorf model 5418 microcentrifuge at the maximum speed of 16873 g for 10 minutes. TST concentration was measured in the supernatant by HPLC, described in section 1.3.2.

1.2. Preparation of TST-SSM nanomedicine

1.2.1. Thin-film hydration method

We prepared stock solutions of TST and DSPE-PEG₂₀₀₀ in chloroform and combined fixed amounts of phospholipid (final concentration 2mM) with varying amounts of the drug (final concentration 30 to 240 μ M) in a 100 mL round bottom flask (**Figure 5**). Next, the organic solvent was removed by rotary evaporation at 650 mmHg vacuum pressure and water bath at 50°C. The resulting thin film was placed in a desiccator under vacuum overnight for removal of residual solvent. The thin film was reconstituted with 0.9% normal saline with 5 minutes of vortexing followed by 5 minutes of sonication. We transferred samples to a glass vial, flushed argon gas, and incubated for 2 hours at 25°C in the dark before characterization to equilibrate the system.

1.2.2. Co-solvent freeze-drying method

TST-SSM nanomedicine was prepared by the co-solvent freeze-drying method (**Figure 9**). Stock solutions of TST were prepared in TBA using a hot plate at 30°C to 35°C when necessary to maintain the TBA in a liquid state (melting point of 23°C to 26°C according to the manufacturer). We sonicated samples for about 10 seconds and stirred with a magnetic bar for 30 minutes to ensure complete drug dissolution. In the meanwhile, we prepared stock solutions of DSPE-PEG₂₀₀₀ in water or PBS using a water bath sonicator to dissolve the material. The quantity of salts in the PBS was adjusted as needed to ensure that the reconstituted formulation would have 1X PBS, which presents the optimal tonicity for intravenous administration (Naguib et al. 2016). We slowly added DSPE-PEG₂₀₀₀ solution to the TST solution under constant agitation with a magnetic stirrer to obtain the desired drug, phospholipid, and co-solvent combination (**TABLE III**). Samples were stirred for at least 15 minutes more before being aliquoted into smaller vials. Scintillation vials of 4 mL were filled with 1.5 mL of samples, while 20 mL vials were filled with 6 mL or 12 mL. Samples were placed in the -80°C freezer overnight and caps replaced with two layers of low-linting wipes attached with a rubber band. Samples were freeze-dried for 24h using a Labconco Freeze Dry System FreeZone® 4.5 floor model catalog number 77510-00 (Labconco, Kansas, MO) with default parameters available in the automatic mode of operation (≤ 0.133 mBar of vacuum pressure and condenser temperature at $\leq -40^\circ\text{C}$). In this freeze-dryer model, frozen vial samples are placed in glass containers and attached to manifold valves. Samples remained exposed to room temperature during the entire process. Primary and secondary drying cycle details could not be controlled or recorded. After freeze-drying,

samples prepared with TBA: water were reconstituted with 0.9% saline, while samples prepared with TBA: PBS were reconstituted with deionized water. In general, cake reconstitution was accomplished adding the diluent and gently swirling vials by hand. However, in some cases, we allow the sample to sit for 20 minutes without movement for a spontaneous reconstitution (low energy process) or sonicated for 5 minutes (high energy process). We flushed argon gas and incubated samples for 1h at 25°C protected from light before characterization.

TABLE III: COMPOSITION OF TESTED TST-SSM FORMULATIONS.

Sample	Number of TST molecules per micelle	Co-solvent system composition (v/v)	[TST] in lyo cake (μM)	[DSPE-PEG ₂₀₀₀] in lyo cake (mM)	Fill Volume (mL)	Reconstitution diluent	Volume of Reconstitution (mL)	[TST] in reconstituted sample (μM)	[DSPE-PEG ₂₀₀₀] in reconstituted sample (mM)
A	1	50% TBA: water	55.6	5	1.5	1X PBS	1.5	55.6	5
B	1	75% TBA: water	55.6	5	1.5	1X PBS	1.5	55.6	5
C	5	50% TBA: 2X PBS	277.8	5	1.5	Water	1.5	277.8	5
D	5	50% TBA: 2X PBS	555.6	10	1.5	Water	1.5	555.6	10
E	5	50% TBA: 2X PBS	833.4	15	1.5	Water	1.5	833.4	15
F	5	50% TBA: 0.667X PBS	277.8	5	6.0	Water	2.0	833.4	15

Reprinted by permission from the Copyright Clearance Center: Elsevier, International Journal of Pharmaceutics, (Esparza and Onyuksel 2019), Copyright 2019.

1.3. Characterization of TST-SSM nanomedicine

All TST-SSM samples were characterized regarding visual appearance, particle size, and drug concentration. Selected samples were further characterized based on reconstitution time, cake internal morphology, turbidity, residual TBA, and osmolality.

1.3.1. Particle size distribution by dynamic light scattering (DLS)

Particle size distributions of SSM formulations were evaluated using the Nicomp ZLS 380 particle sizer (Santa Barbara, CA) equipped with a 5mW helium-neon laser set at 632.8 nm and scattered light detection at an angle of 90°. A volume of 400 µL of each sample was carefully transferred into a drop-in vial for DLS analysis. The diffusion coefficient of particles in solution was derived from the autocorrelation function accumulated for at least 15 minutes and applied into the Stokes-Einstein relation (**Equation 1**) to determine the mean hydrodynamic particle diameter:

$$D = \frac{\kappa T}{3\pi d \eta} \quad (\text{Equation 1})$$

Where D is the particle translational diffusion coefficient, k is the Boltzmann constant (1.38×10^{-16} erg K⁻¹), T is the absolute temperature, d is the hydrodynamic diameter, and η is the media viscosity. We employed default parameters for aqueous solutions: temperature 23°C, viscosity (η) 0.933 cP, and refraction index 1.333. For TBA: water co-solvent systems, we determined viscosity values (**section 1.3**) and refractive indexes (**section 1.3.1.2**) using a Cannon-Fenske viscometer a digital refractometer, respectively, and readjusted the particle sizer parameters accordingly.

1.3.1.1. Viscosity of TBA: water co-solvent system

We measured the viscosity of 0 to 100% TBA: water co-solvent systems using the Cannon-Fenske capillary viscometer. This measurement technique is based on the time for the test liquid to pass through the capillary tube compared to a liquid with known viscosity, such as water. The conversion to viscosity at a given temperature is obtained with the following equation (**Equation 2**):

$$\frac{\eta_1}{\eta_2} = \frac{\rho_1 t_1}{\rho_2 t_2} \quad (\text{Equation 2})$$

Where η_1 and η_2 are the viscosities of unknown (1) and standard (2) liquids in centipoise (cP), ρ_1 and ρ_2 are the densities of the liquids (g/mL), and t_1 and t_2 are the times to pass between the two engraved marks (seconds). The density value of water at 25°C used was 0.9970479 g/mL and viscosity 0.8904 cP (Sinko 2011). To control the temperature during viscosity measurement, the capillary viscometer was immersed in a water bath with a controlled temperature. Since density is required for the calculation of viscosity, we measured the density of different proportions TBA: water by weighing the amount of water required to fill a 10 mL volumetric flask at a fixed temperature of 25°C. The densities of TBA: water solvent systems were calculated with the following equation (**Equation 3**):

$$\rho = (m / v) * \text{correction factor} \quad (\text{Equation 3})$$

Where ρ is the density of the liquid (g/mL), m is the mass of the liquid (g), and v is the volume of the liquid (mL). We calibrated the used volumetric flask with water at 25°C as a standard liquid. We weighed the amount of water required to fill the 10 mL volumetric flask in triplicate and calculated the real volume using the known density

value. The correction factor was obtained by dividing the average real volume by the theoretical volume.

1.3.1.2. Refractive index of TBA: water co-solvent system

The refractive indexes of 0 to 100% TBA: water co-solvent systems were obtained with the handheld, digital refractometer AR 200 (Reichert Technologies, Depew, NY). Calibration (distilled water) and sample measurements were performed in triplicate following equipment prompts. Prism surface of the refractometer was cleaned between measurements with methanol/ distilled water and dried with a dry tissue.

1.3.2. TST quantification by HPLC

The quantification of TST was performed by HPLC using a Shimadzu Prominence HPLC system (Kyoto, Japan) equipped with a diode array detector and Agilent SB-C18 (250 x 4.6mm, 5µm) column. Phase mobile consisted of 30 to 100% of acetonitrile in water with 0.1% trifluoroacetic acid for 15 minutes at ambient temperature and flow rate of 1 mL/min. The injection volume used was 10 µL with ultraviolet detection at 254 nm. Chromatographic peak areas were integrated using the software EZStart 7.4 SP2. The calibration curve was obtained with standard solutions of TST prepared in DMSO from 2.5 µg/mL to 100 µg/mL.

1.3.3. Internal morphology of lyophilized cake

Internal structures of lyophilized cakes were analyzed by SEM at the Electron Microscopy Service facility (Research Resource Center, University of Illinois at Chicago). Glass vial necks were cut, and lyophilized cakes were carefully removed to prevent mechanical damage. Extracted cakes were cut in half with a sharp blade and mounted on aluminum stubs with the cross-sections facing up. Silver paint and carbon

tabs were used to adhere samples to aluminum mounts. Samples were sputter-coated with 10 nm of gold/palladium at a low-pressure argon atmosphere. Morphology was examined using a Hitachi S-3000N Variable Pressure SEM. Samples were analyzed with a secondary electron detector, varying accelerating voltages, and different magnifications.

1.3.4. Reconstitution time of the lyophilized cake

To measure the reconstitution time of TST-SSM freeze-dried cakes, we added the reconstitution diluent (water or 0.9% saline, depending on the experiment) and recorded the time necessary to obtain a visually clear product using a digital timer. We evaluated reconstitution times in triplicate samples.

1.3.5. Turbidity of reconstituted TST-SSM

We measured the turbidity of selected TST-SSM samples by absorbance at using microplate reader Synergy 4 (Biotek Instruments, Winooski, VT) to compare reconstitution methods. Samples were aliquoted into a clear 96-well plate (200 μ L of sample per well) in triplicate and absorbance measured at 400 nm wavelength.

1.3.6. Determination of the number of encapsulated drug molecules per micelle

The number of drug molecules encapsulated in each micelle (X) was estimated based on three parameters: (1) aggregation number of DSPE-PEG₂₀₀₀ micelles prepared in isotonic aqueous media, which was previously reported as 90 monomers per micelle (Ashok et al. 2004), (2) the dissolved TST drug concentration in 1X PBS ($C_{\text{TST free}}$) determined by the shake-flask method (**Section 1.1**), and (3) the maximum drug concentration that can be incorporated in a fixed concentration of phospholipid

(C_{Lipid}) without the formation of large drug particles ($C_{\text{TST in SSM}}$), as determined by HPLC and DLS. We subtracted the drug solubility ($C_{\text{TST free}}$) from the total concentration of TST in the micellar system ($C_{\text{TST total}}$) to obtain the concentration of the encapsulated drug ($C_{\text{TST in SSM}}$) (**Equation 4**). Next, we calculated the saturation molar ration of lipid: drug by dividing the lipid molar concentration (C_{Lipid}) by the maximum encapsulated drug molar concentration ($C_{\text{TST in SSM}}$) (**Equation 5**). The concentration of DSPE-PEG₂₀₀₀ in the monomeric form is negligible ($\text{CMC} = 1 \mu\text{M}$) and was disregarded in the calculation. The lipid: drug molar ratio informed us the number of phospholipid molecules that were associated with each drug molecule. Considering that each micelle is composed of approximately 90 monomers, we divided 90 by the molar ratio to determine the number of drug molecules associated with each micelle (X) (**Equation 6**).

$$C_{\text{TST in SSM}} = C_{\text{TST total}} - C_{\text{TST free}} \quad (\text{Equation 4})$$

$$\text{Saturation Molar Ratio} = C_{\text{Lipid}} / C_{\text{TST in SSM}} \quad (\text{Equation 5})$$

$$X = 90 / \text{Saturation Molar Ratio} \quad (\text{Equation 6})$$

1.3.7. Residual tert-butanol concentration

The residual TBA in the freeze-dried TST-SSM optimized formulation was analyzed by headspace gas chromatography-mass spectroscopy (GC-MS) at the Analytical Forensic Testing Laboratory at the University of Illinois at Chicago in collaboration with Dr. Albert Karl Larsen. Three batches of TST-SSM samples were weighed (25mg) into 10mL vials, reconstituted in 2mL of water, and sealed with aluminum caps with PTFE/silicone septa. Samples were equilibrated to 50°C for 5 minutes, pressurized with helium gas, and injected into the column for 0.2 minutes. Samples were assayed using an Agilent 7890B system (Agilent Technologies, Santa

Clara, CA) equipped with a DB-ALC 1 capillary column (30 m × 320 µm × 1.8 µm), a flame ionization detector, and a mass spectrometer using selected ion monitoring. We used the mass-to-charge ratios of 31, 41, and 59 to confirm the identity of TBA. The oven temperature was set at 55°C for 2 minutes, ramped at 30°C/min until 110°C and hold it for 2.17 minutes. Standard samples of TBA were prepared in deionized water at concentrations between 0.05% and 5% (w/w) of the expected TBA per 25 mg of freeze-dried material.

1.3.8. Osmolality

Osmolality was measured by the freezing point depression technique using Micro-osmometer Model 3MO Plus (Advanced Instruments, Norwood, MA). A volume of 20 µL of samples was drawn with a disposable sampler tip and loaded in the equipment for analysis. Calibration was conducted with 50 and 850 mOsm/kg standard solutions (Advanced Instruments, Norwood, MA). Three independent samples were used for measurements.

1.3.9. Moisture Analysis

The moisture content in selected lyophilized cake samples was analyzed using Sartorius moisture analyzer Model MA50XX20A (Göttingen, Germany). This technique is based on the solvent evaporation and weight loss promoted by the even application of infrared heat on the sample. The moisture is automatically calculated using the following equation (**Equation 7**):

$$\text{Moisture (\%)} = \frac{\text{Initial weight} - \text{Final weight}}{\text{Initial weight}} * 100 \text{ (Equation 7)}$$

We weighed approximately 0.5 g of samples on the tared aluminum dish and started the equipment selecting the fully automatic pre-set program “Progr 0”. In this

setting, the moisture analyzer applies heat for samples to reach about 150°C and monitors the sample weight until no significant changes are observed.

1.3.10. Minimum inhibitory concentration (MIC)

Microbiological assays were performed in collaboration with Dr. Hyunwoo Lee from the Center for Biomolecular Sciences at the University of Illinois at Chicago. To evaluate the antimicrobial activity of TST-SSM formulations, we performed the microdilution assay using MRSA USA 300 as a target pathogen. A single colony of MRSA USA300 grown in tryptic soy agar plate was transferred into a sterile 15 mL Falcon tube containing 2 mL of tryptic soy broth. The cell suspension was incubated in the shaker at 37°C and 250rpm overnight. The next morning, we transferred 100 µL of overnight suspension into a sterile 50 mL Falcon tube containing 9.9 mL of tryptic soy broth (1:100 dilution) and incubate bacterial suspension in the shaker for 3 hours at 37°C and 250rpm. We centrifuged bacterial suspension at 2880 g for 10 minutes, removed supernatant, and resuspended pellet in 1mL of PBS. The bacterial suspension was transferred to Eppendorf tube and centrifuged at 16.1 g for 5 minutes. We removed the supernatant and washed the bacteria with 1X PBS twice. We resuspended the bacterial pellet in 1mL of PBS and performed a 1:20 dilution of the stock suspension (50 µL of bacteria + 950 µL of PBS) to measure the optical density at 600 nm (OD₆₀₀). We diluted bacteria suspension stock in tryptic soy broth to obtain the OD₆₀₀ of 0.1. We confirmed the bacterial load by plating 10-fold dilutions of the bacterial suspension in TBA and calculating the CFU/mL in the following day. For the microdilution assay, we diluted TST-SSM formulation 15-fold (50 µL of sample + 700 µL of PBS), added 200 µL of treatment samples in triplicate on the first row and added 100 µL of PBS to remaining

wells. We performed 2-fold serial dilution by transferring 100 μL of concentrated sample to the next well containing 100 μL of PBS successively. We added 100 μL of bacterial suspension of $\text{OD}_{600} = 0.1$ to all wells. The final concentration range of TST-SSM after adding the pathogen was 0.014 μM to 27.78 μM of TST and 0.24 μM to 500 μM of DSPE-PEG₂₀₀₀. Plates were incubated for 24 hours at 37°C and visual bacterial growth observed in the next day. The minimum inhibitory concentration (MIC) was defined as the lowest concentration of drug capable of visually inhibiting the growth of bacteria. Vancomycin (concentration range 0.0625 - 16 $\mu\text{g/mL}$ or 0.043 - 11.04 μM) was selected as positive control. As a negative control, we used DSPE-PEG₂₀₀₀ at the same concentration range as TST-SSM samples (0.24 μM to 500 μM). For comparison, we also included TST dissolved in 2% of DMSO in 1X PBS ranging from 0.014 μM to 1.736 μM . The maximum drug concentration is below the TST solubility in water, therefore, is expected to be in its molecular form.

1.4. Short-term stability of reconstituted TST-SSM nanomedicine

We assessed the short-term stability of the optimized reconstituted TST-SSM nanomedicine for 7 days when stored at 4°C or 25°C. The purpose was to establish the amount of time that the reconstituted formulation remains stable and suitable for use after reconstitution. We prepared 3 batches of TST-SSM formulation containing 277.8 μM of TST and 5 mM of DSPE-PEG₂₀₀₀ using the co-solvent freeze-drying method and reconstituted the lyophilized cake with deionized water at 1/3 of the fill volume. This resulted in reconstituted samples that were 3 times more concentrated (833.4 μM of TST and 15 mM of DSPE-PEG₂₀₀₀). Samples were flushed with Argon gas and incubated at 4°C or 25°C. We analyzed samples regarding particle size by DLS

(**Section 1.3.1**), drug concentration by HPLC (**Section 1.3.2**), and antimicrobial activity against MRSA USA300 (**Section 1.3.10**) at timepoints 0, 1, 3, 5, and 7 days.

1.5. Long-term stability of freeze-dried TST-SSM nanomedicine

The long-term stability of optimized freeze-dried TST-SSM nanomedicine was assessed based on the adaptation of the Q1A(R2), a guideline developed by the “International Council for Harmonization of Technical Requirements for Pharmaceuticals for Human Use” (“Stability Testing of New Drug Substances and Products Q1A(R2)” 2003). Samples were prepared by the co-solvent system method as described in **Section 1.2.2** and aliquoted to 20 mL glass vials (fill volume 6mL). After freeze-drying, samples were flushed with Argon gas and closed with a rubber stopper and aluminum crimp cap. Samples were stored under three environmental conditions: (1) $5 \pm 3^{\circ}\text{C}$, (2) $30 \pm 2^{\circ}\text{C} / 60 \pm 5\% \text{ RH}$, and (3) $40 \pm 2^{\circ}\text{C} / 75 \pm 5\% \text{ RH}$. To control the temperature and humidity, we placed samples in a glass desiccator containing a saturated solution of cupric chloride (60% RH) or sodium chloride (75% RH) and kept them inside incubators set at 30°C or 40°C , respectively. At pre-established time points, samples were retrieved from incubators and reconstituted with deionized water (1/3 of the fill volume) for a final concentration of $833.4 \mu\text{M}$ of TST and 15 mM of DSPE-PEG₂₀₀₀. We let samples rest for at least one hour before analyzing them regarding reconstitution time (**Section 1.3.4**), particle size by DLS (**Section 1.3.1**), drug concentration by HPLC (**Section 1.3.2**), and antimicrobial activity against MRSA USA300 (**Section 1.3.10**) at timepoints 0, 1, 3, and 7 months (**TABLE IV**).

TABLE IV: LONG-TERM STABILITY OF TST-SSM NANOMEDICINE.

Timepoint	Storage Condition	Reconstitution time	Particle size	TST quantification	Antimicrobial activity	Freeze-dried cake moisture	Total number of vials
Initial	-	X	X	X	X	X	8
1 month	5°C	X	X	X	X		3
	30°C, 65% RH	X	X	X	X		3
	40°C, 75% RH	X	X	X	X		3
3 months	5°C	X	X	X	X		3
	30°C, 65% RH	X	X	X	X		3
	40°C, 75% RH	X	X	X	X		3
7 months	5°C	X	X	X	X	X	8
	30°C, 65% RH	X	X	X	X	X	8
	40°C, 75% RH	X	X	X	X	X	8
TOTAL							54

2. In-vitro efficacy of TST-SSM against Gram-positive bacteria

Microbiological assays were performed in collaboration with Dr. Hyunwoo Lee from the Center for Biomolecular Sciences at the University of Illinois at Chicago.

2.1. Minimum inhibitory concentration (MIC) of TST-SSM nanomedicine

The minimum inhibitory concentration of TST-SSM was determined by the microdilution assay similarly as described in **Section 1.3.10**. The microorganisms tested were *S. aureus* COL, *Bacillus anthracis* Sterne, *B. cereus* 14579, and *B. thuringiensis* *konkukian* 97-27 from Dr. Hyunwoo Lee's collection.

2.2. TST accumulation in MRSA USA 300

We determined the accumulation of TST in *S. aureus* USA 300 in the presence or absence of micelles using a method adapted from the literature (Furneri et al. 2000; Mombeshora and Mukanganyama 2017). We prepared an overnight culture of *S. aureus* USA 300 in TSB and diluted 1:100 in fresh media. The culture was grown in the shaker at 200 rpm and 37°C until it reached $OD_{600} \approx 0.5$. We centrifuged the bacterial suspension at 2880 g for 5 minutes, washed the cells twice with PBS and resuspended them in TSB in half of the original volume to obtain a culture with $OD_{600} \approx 1.0$. We added TST in DMSO, TST + DSPE-PEG₂₀₀₀ in DMSO, or TST-SSM for a final drug concentration of 6 μ M and placed samples in the shaker at 200 rpm and 37°C. At time points 0, 10, 20, 30, 60, and 120 minutes we collected 1 mL of each sample, centrifuged at 21100 g for 5 minutes, removed the supernatant, washed cells once with PBS, and resuspended in 1.1 mL of 1 M glycine hydrochloric acid pH 3. We left samples at room temperature overnight, centrifuged at 21100 g for 15 minutes to separate cell debris and transferred 1 mL of supernatants into glass vials. For drug extraction, we added 2.44 μ L

of 0.05 mg/mL nosiheptide in DMSO (internal standard) and 3 mL of tri-solvent (dichloromethane, hexane, and diethyl ether (1:1:1)). We tumbled samples for 5 minutes and centrifuge at 2880 g for 5 minutes to separate phases. The supernatant (organic phase) was transferred to glass tubes and dried in a warm water bath under a nitrogen stream. Dried samples were reconstituted with 0.1 mL of 50% methanol: water and analyzed by liquid chromatography with tandem mass spectroscopy LC-MS/MS.

2.2.1. TST quantification by LC-MS/MS

Quantification of TST by LC-MS/MS was performed at the Analytical Forensic Testing Laboratory at the University of Illinois at Chicago in collaboration with Dr. Albert Karl Larsen. We prepared 100 μ M (166 μ g/mL) of TST stock solution in DMSO, diluted the stock solution with water to 1 μ M, and prepare 5-level standard solutions with spiked nosiheptide as an internal standard (**TABLE V**). Enough nosiheptide was added to obtain a molar concentration similar to TST standard solution level 3 (middle point of calibration curve). Nosiheptide is a member of the thiopeptide antibiotic class and was selected as an internal standard because of its similar chemical properties as TST and commercial availability (Just-Baringo, Albericio, and Álvarez 2014). Lung homogenates (1 mL) were thawed, transferred to glass vials, and spiked with the same amount of nosiheptide as standard solutions.

TABLE V: STANDARD SOLUTIONS OF TST FOR QUANTIFICATION BY LC-MS/MS.

Level	[TST] (μM)	[Nosiheptide] (μM)	Total Volume (μL)
1	0.01	0.1	1000
2	0.05	0.1	1000
3	0.1	0.1	1000
4	0.5	0.1	1000
5	1	0.1	1000

The chemical extraction of TST and nosiheptide was performed with 3 mL of trisolvent (dichloromethane, hexane and diethyl ether (1:1:1)). Samples were homogenized by tumbling for 5 minutes. We centrifuged samples for 5 minutes to separate phases and collected supernatants (organic phase) into glass tubes. We dried samples in the hood using a water bath and nitrogen stream and resuspended the material with 0.1 mL of 50% methanol: water.

Samples were analyzed with the 1200/6460 series Triple Quad LC/MS/MS system using Agilent Poroshell C18 column (2.1 \times 100 mm, 2.7 μm) (Agilent Technologies, Santa Clara, CA) with mobile phase A (0.2% formic acid in water) and mobile phase B (9:1 acetonitrile: water). The flow rate was 0.5 mL/min. The linear gradient was as follows: 0.2-0.8 min, 90% mobile phase A; 0.8-2.5 min, 100% mobile phase B. The autosampler was set at 30 $^{\circ}\text{C}$. The injection volume was 10 μL . Mass spectra were acquired with positive electrospray ionization at the ion spray voltage of

3500 V. The source temperature was 250 °C. TST (precursor ion m/z 832.8) and nosiheptide (precursor ion m/z 1222.2) were analyzed with fragmentor voltage of 175 V and 220 V, respectively. Collision energy of fragments were as follow: TST (m/z 1160.7) 30 V, TST (m/z 1125.1) 35 V, TST (m/z 763.7) 16 V, nosiheptide (m/z 1204.2) 32 V, and nosiheptide (m/z 1194.2) 32 V.

2.3. Stability of TST-SSM nanomedicine in spent media of MRSA USA

300

The stability of TST in the presence or absence of SSM was tested in fresh TSB media or spent media of MRSA USA 300 culture (**Figure 15**). We prepared an exponential culture of MRSA USA 300 ($OD_{600} \approx 1$) from an overnight culture and centrifuged it at 2880 g for 5 minutes. We transferred the supernatant into two different Falcon tubes and added TST dissolved in DMSO or TST-SSM nanomedicine (final drug concentration = 50 μ M, final volume = 2 mL). Tubes were placed in the shaker at 200 rpm and 37°C for 24 hours. The next day, we collected 0.5 mL of samples, added 0.5 mL of acetonitrile, and centrifuge at 21100 g for 20 minutes to remove any debris. We quantified TST by HPLC using the same conditions as described in **Section 1.3.2**.

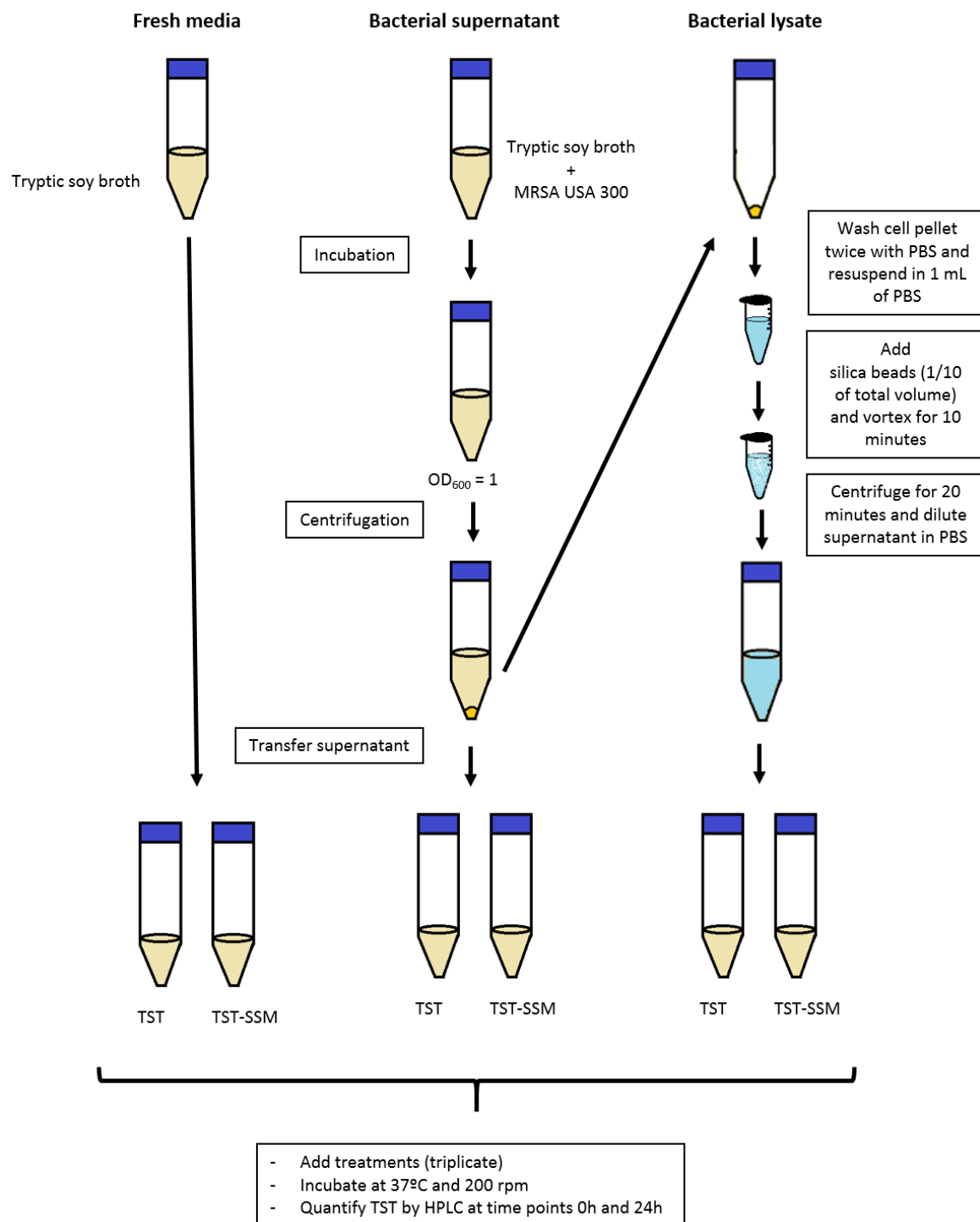


Figure 15: Experimental procedures for drug stability in spent media.

3. *In vivo* efficacy of TST-SSM nanomedicine

3.1. Filtration of TST-SSM nanomedicine

We investigated the stability of reconstituted TST-SSM after filtration through a 0.22 μm PES syringe filter to ensure the quality of the filtered drug product for animal studies. We prepared 3 batches of TST-SSM containing 6 mL per vial of 277.8 μM of TST and 5mM of DSPE-PEG₂₀₀₀ and reconstituted the freeze-dried cake in one-third of the fill volume (2 mL) with deionized water to obtain a final formulation with 833.4 μM of TST and 15mM of DSPE-PEG₂₀₀₀. We measured the particle size by DLS (**Section 1.3.1**), drug concentration by HPLC (**Section 1.3.2**), and antimicrobial activity against MRSA USA300 (**Section 1.3.10**) before and immediately after filtration.

3.2. Staphylococcal pneumonia

Studies using the MRSA USA300 pneumonia animal model were performed in collaboration with Dr. Steven Dudek's research group (ACC# 15-244 Mod 16).

3.2.1. Preparation of drug treatments

Optimized TST-SSM nanomedicine was prepared by the co-solvent freeze-drying method and maintained at -80°C until use. Samples were reconstituted on the day of the experiment with water for a final concentration of 833 μM of TST and 15 mM of DSPE-PEG₂₀₀₀. Empty SSM was prepared on the day of the experiment by simple dissolution of DSPE-PEG₂₀₀₀ in 1X PBS using sonication for final phospholipid concentration of 15 mM. Vancomycin was freshly prepared by dissolving the drug in 1X PBS for a final concentration of 21.2 mg/mL. Free TST was prepared in 10% DMSO by first dissolving the drug in DMSO at concentration of 13.875 mg/mL and diluting it 10-fold in 1X PBS to obtain 1.3875 mg/mL TST in 10% DMSO. The final product was a fine

suspension of drug particles. All solutions, except the TST in 10% DMSO, were filtered through a 0.22 μ m PES syringe filter for sterilization.

3.2.2. Preparation of MRSA USA300 inoculum

MRSA USA300 inoculum was freshly prepared on the day of the animal experiment. The pathogen was streaked from a frozen stock onto tryptic soy agar plates and growth overnight at room temperature. We picked one colony and transferred to a 15 mL Falcon tube containing 3 mL of TSB for an overnight incubation in the shaker at approximately 200 rpm and 37°C. The next morning, we transferred 1 mL of bacterial suspension into an Erlenmeyer flask containing 50 mL of TSB and return it to the shaker. The bacterial suspension was grown until OD₆₆₀ of 0.5, adjusting with fresh TSB when necessary. We centrifuged 25 mL of the bacterial suspension for 10 min at 7000 rpm (Beckman centrifuge model J2-21), removed the supernatant, and washed the cells with PBS twice. The bacterial pellet was resuspended in 1X PBS to a final concentration of 1×10^8 CFU/30 μ , following the equation previously generated in a regression analysis of MRSA USA 300 OD₆₀₀ vs CFU/mL (**Figure 16**). Bacterial inoculum was kept on ice until use in animals. We also serially diluted an aliquot of the bacterial inoculum and plated on tryptic soy agar plates to confirm the bacterial count on the following day.

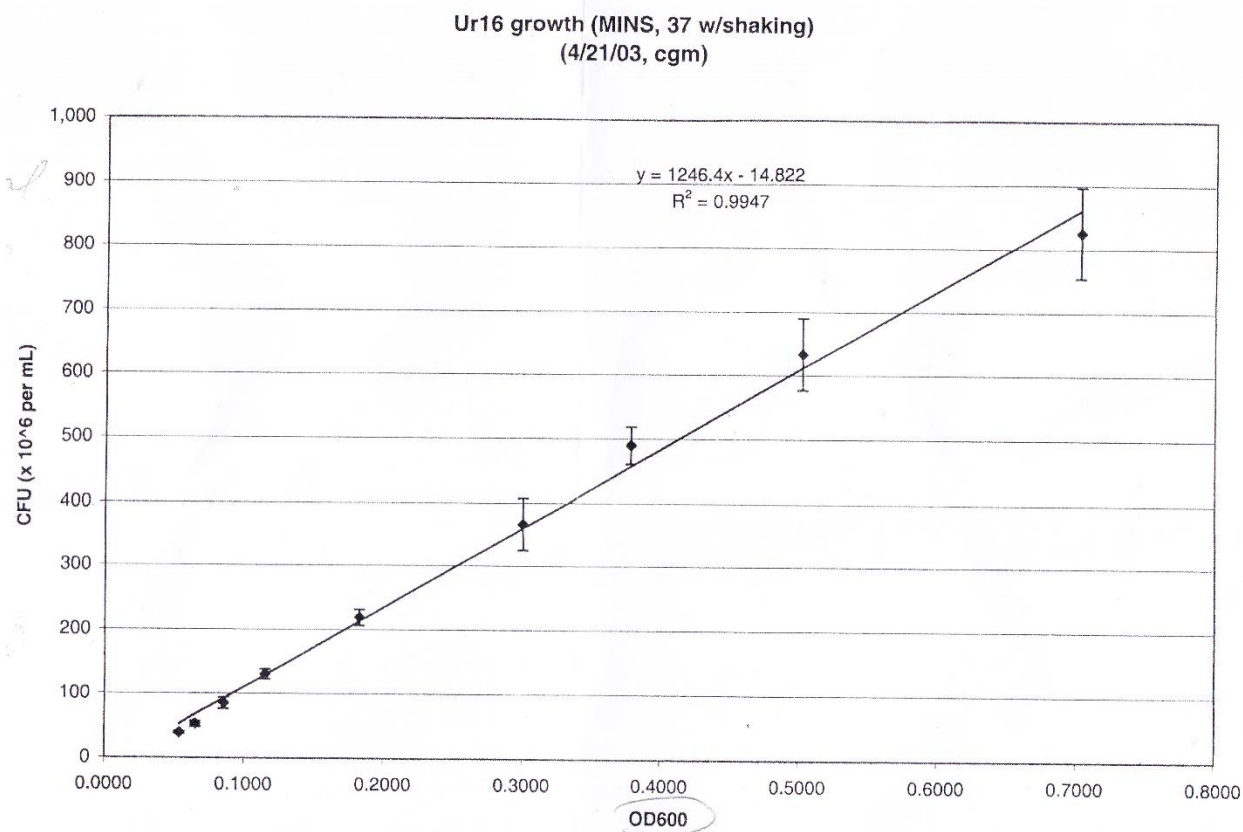


Figure 16: Regression analysis of OD₆₀₀ vs CFU of MRSA USA300. Data obtained from Dr. Dudek's research group.

3.2.3. Induction of MRSA pneumonia in mice

Mice were weighed and anesthetized with ketamine (100 mg/kg) and xylazine (5 mg/kg) intraperitoneally and the depth of anesthesia confirmed by non-responsiveness to toe pinching. We restrained anesthetized animals on the surgical board and shaved the frontal neck area with an electric shaver and disinfect the area with 70% ethanol pads. Using sterile surgical scissors, we made a small cut in the skin approximately 12mm below the lower incisor and gently pulled the skin and muscles away with forceps to visualize the trachea wall. We pulled the tongue to the side with tweezers and

inserted a commercial one-inch long 20G IV cannula in the mouth and direct it into the trachea. We visualize the cannula in the trachea through the skin cut. Using a gel loading pipette tip, we administered 1×10^8 CFU of MRSA USA300/ 30g animal or an equal volume of PBS (vehicle) via intratracheal (IT) route with a maximum volume of 40 μ L per administration. We inflated 0.6 mL of air into the cannula using a 1 mL syringe to ensure the proper distribution of bacteria inoculum into the lungs. Next, we removed the cannula, closed the skin incision with cyanoacrylate adhesive. Animals were returned to cages and monitored for their recovery from anesthesia. After 6 h from bacterial instillation, we administered treatments intravenously via retro-orbital injection (**Figure 17**). In a separate set of experiments, the second dose of treatment was administered at 16h (**Figure 18**). After 24h, animals were anesthetized and euthanized by cardiac puncture and exsanguination. We collected blood in heparinized tubes and harvested lungs for bacterial count and drug quantification.

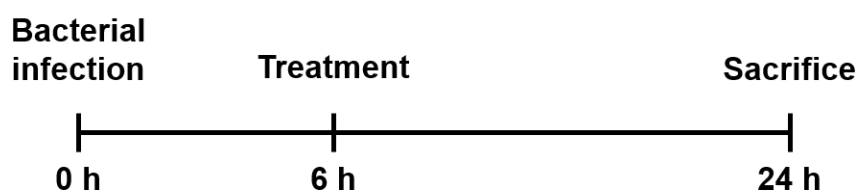


Figure 17: Staphylococcal pneumonia mouse model with single-dose treatment.

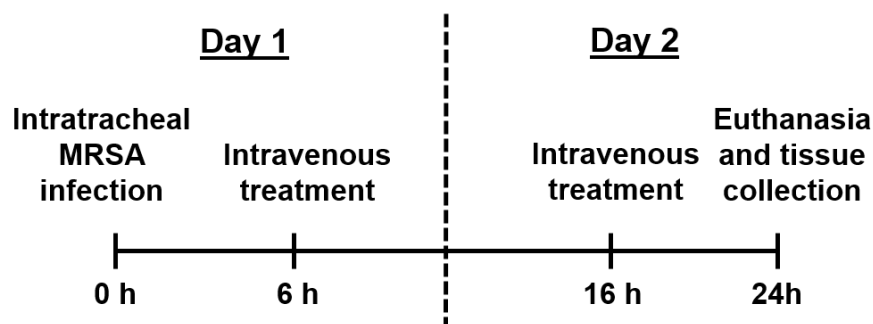


Figure 18: Staphylococcal pneumonia mouse model with two doses of treatment.

3.2.4. Bacterial burden in lungs

Microbiological assays were performed in collaboration with Dr. Hyunwoo Lee from the Center for Biomolecular Sciences at the University of Illinois at Chicago. Harvested lungs were kept on ice to be processed on the same day of collection. We weighed and homogenized lungs in 1 mL of 1X PBS by pressing samples with a roller in a sterile sample bag. The lung homogenate was serially diluted in 1X PBS and plated on tryptic soy agar plates. After incubation at 37°C for 18-24h, we counted the colony-forming units (CFU) and calculate the CFU/g of lung tissue. The remaining lung homogenates were frozen at -80°C and used later for drug quantification.

3.2.5. TST concentration in lungs

The quantification of TST in the lungs was performed at the Analytical Forensic Testing Laboratory in collaboration with Dr. Albert Karl Larsen. We extract TST from lung homogenates with the tri-solvent mixture and quantified the drug by LC-MS/MS following same procedures as described in **Section 2.2.1**.

3.3. Polymicrobial sepsis

Studies using CLP-induced polymicrobial sepsis were performed in collaboration with Dr. Richard Minshall's research group (ACC# 17-138 Mod 2).

3.3.1. Preparation of drug treatments

Optimized TST-SSM nanomedicine was prepared by the co-solvent freeze-drying method and maintained at -80°C until use. Samples were reconstituted on the day of the experiment with water for a final concentration of 833 µM of TST and 15 mM of DSPE-PEG₂₀₀₀. Empty SSM was prepared on the day of the experiment by simple dissolution of DSPE-PEG₂₀₀₀ in 1X PBS using sonication for final phospholipid concentration of 15 mM.

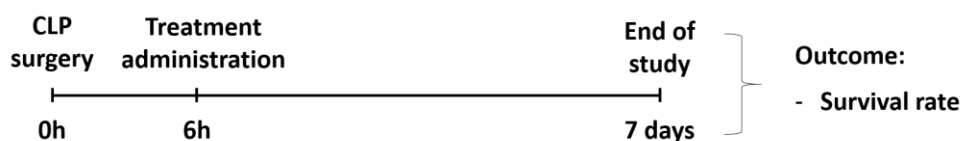
3.3.2. Induction of sepsis in mice by the cecal ligation and puncture (CLP) method

The CLP model was used to assess the therapeutic value of TST-SSM nanomedicine in treating polymicrobial sepsis in mice based on a previously published method (Herrmann et al. 2013). The study was divided into two parts: survival study and physiological status (**Figure 19** and **TABLE VI**). Animals were anesthetized with ketamine (100mg/kg) and xylazine (10 mg/kg) IP and immobilized on their back on a flat surface. The abdomen was shaved and rubbed with povidone-iodine antiseptic solution before making a 1cm skin incision on the left side. The underlying abdominal muscle was incised with scissors and the cecum exposed. The distal 20% of the cecum was ligated with a 6-0 suture between the first and the second groove from the tip to interrupt blood circulation. Punctures were made once in the ligated area and twice in the non-ligated area with a 20-gauge needle. The cecum was lightly pressed to

extravasate the intestinal content and placed back in the abdominal cavity. The peritoneal cavity was closed in two layers (muscle and skin) with 6-0 sutures. SHAM animals underwent the same procedure without ligation and puncture of the cecum. All mice received 0.5 mL of warmed PBS via SC on the left flank after surgery as support therapy. The CLP procedure was performed within 1.5 h to reduce variations in the experimental results.

Cecum ligation and puncture sepsis model

Study 1:



Study 2:

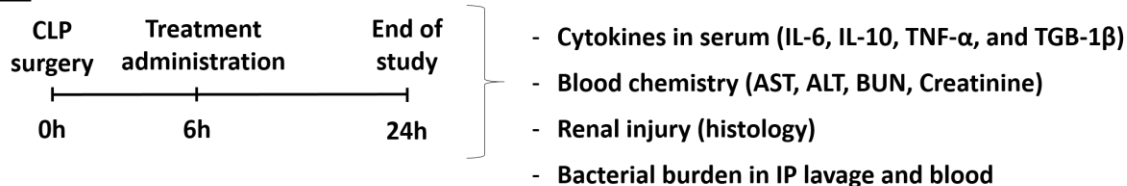


Figure 19: Study design of sepsis animal experiments.

Animals presenting sepsis were treated 6 hours after the CLP surgery via intraperitoneal injection (IP) (max. volume 0.5 mL) with empty micelles (negative control) or 20 mg/kg TST-SSM (treatment). This time point of treatment was selected to

allow time for the establishment of systemic inflammation after the CLP procedure (Wen 2013). The TST dose was fixed in 20 mg/kg which is below the reported IV LD₅₀ of 41 mg/kg (“Toxnet - Thiostrepton USP,” n.d.). Animals were monitored every 6 hours for the first 24 hours, and twice-daily afterward.

For the survival study, animals were monitored for 7 days. Euthanasia was performed by isoflurane overdose and cervical dislocation once animals achieved humane endpoints (labored breathing and lack of purposeful movement) or at the end of the study. For the physiological status study, animals were euthanized at 24h after CLP surgery.

TABLE VI: TREATMENT GROUPS FOR SEPSIS STUDY.

Treatment group	Number of animals	
	Survival study	Physiological status study
Sham surgery	12	6
Septic + empty micelles (SSM)	12	6
Septic + 20 mg/kg TST-SSM	12	6
Total	36	18

To collect the blood, we injected 50 μ L of heparin (1,000 units/mL) into the inferior vena cava and allowed it to circulate for a minute before drawing the blood. We immediately transferred 10 μ L of blood into a sterile Eppendorf tube containing 90 μ L of 1X PBS in triplicate for the bacterial count. The remaining blood was centrifuged at 3000 g for 15 minutes. Plasma samples were analyzed immediately or stored at -80°C until assayed.

Finally, we instilled 1 mL of sterile 0.9% saline into the peritoneal cavity and massaged the abdomen gently for a few seconds. We opened the abdominal cavity with sterile scissors and recovered peritoneal lavage (~0.5 ml) for the bacterial count.

3.3.3. Cytokine profile in plasma

Pro-inflammatory (IL-6 and TNF- α) and anti-inflammatory (IL-10 and TGF-1 β) cytokines were quantified in plasma samples using ELISA kits. Procedures were carried out following the manufacturer's protocols.

3.3.4. Nitric oxide derivatives (NOx) in plasma

The total nitric oxide (NOx) was determined spectrophotometrically in plasma samples with Griess reagent kit. NO is a labile molecule that rapidly converts into nitrite (NO₂⁻) and nitrate (NO₃⁻) in aqueous solution. Since Griess reagent detects nitrite only, we converted nitrate to nitrite first using NADH-dependent enzyme nitrate reductase. We mixed 80 μ L of the sample, 10 μ L of cofactors preparation, and 10 μ L of nitrate reductase, followed by 3h incubation at room temperature. The Griess reaction was performed according to the manufacturer's protocol.

3.3.5. Blood chemistry

Biomarkers of renal function (blood urea nitrogen (BUN) and serum creatinine) and hepatic function (alanine transaminase (ALT), and aspartate transaminase (ASP)) were analyzed in fresh plasma samples with a Beckman Coulter AU480 chemistry analyzer (Brea, CA) at the BRL facilities.

3.3.6. Bacterial burden

The bacterial burden was assessed in fresh peritoneal lavage and blood. We performed 10-fold dilutions of the peritoneal lavage in sterile 1X PBS and plated 10 μ L of each dilution on tryptic soy agar plates. Plates were incubated at 37°C for 18-24h for CFU count.

4. Statistical analysis

Data were expressed as mean \pm standard deviation. Studies with two groups were compared with Student's t-test. Studies with 2 or more groups and one independent variable were analyzed by one-way ANOVA with Tukey's multiple comparisons test. Studies with 2 or more groups and two independent variables were analyzed by two-way ANOVA with Tukey's multiple comparisons test. Survival curves were created using the Kaplan-Meier method and differences compared with the log-rank (Mantel-Cox) test. Bacterial burden results in blood and peritoneal lavage were log-transformed and analyzed by a one-tailed Mann-Whitney test (non-parametric). We used the software GraphPad Prism 7.01 and 8.0 (San Diego, CA). A p-value < 0.05 was considered statistically significant.

III. RESULTS

A. Development of TST-SSM nanomedicine

(Previously published as Esparza, K., Onyuksel, H. (2019) Development of co-solvent freeze-drying method for the encapsulation of water-insoluble thioestrepton in sterically stabilized micelles, *Int. J. Pharm.* 556, 21-29).

The development and optimization of TST-SSM nanomedicine were mostly published at the International Journal of Pharmaceutics (Esparza and Onyuksel 2019). The content of the study will be adapted to fit the thesis dissertation format.

1. TST solubility in aqueous media

We determined the aqueous solubility of TST to use it in our calculations of drug loading in the phospholipid nanocarrier. We applied a modified shake-flask method for 24h and found that the solubility of TST was 3.5 μM in 1X PBS and 3.8 μM in 0.9% saline (**TABLE VII**). The TST solubility value 3.5 μM was used in all subsequent calculations of TST loading in SSM.

TABLE VII: TST SOLUBILITY IN AQUEOUS MEDIA

Replicate	TST concentration (μM)	
	1X PBS	0.9% saline
1	3.0	3.6
2	5.4	3.5
3	3.1	4.4
Average	3.8	3.8
SD	1.4	0.5

2. Maximum loading capacity of TST in SSM by the thin-film hydration

method

The maximum loading capacity of TST in SSM was determined by the conventional encapsulation method of thin-film hydration. By fixing the concentration of DSPE-PEG₂₀₀₀ at 2 mM and gradually increasing the concentration of TST, we found that the SSM nanocarrier system accommodated approximately 120 μM of TST (diameter ~ 16 nm) without forming large drug particles (**Figure 20**). This proportion corresponded to a molar ratio of phospholipid: drug of 17.2 ($2000 \mu\text{M} / (120 \mu\text{M} - 3.5 \mu\text{M})$) and a maximum loading of approximately 5 drug molecules per micelle ($90/17.2$).

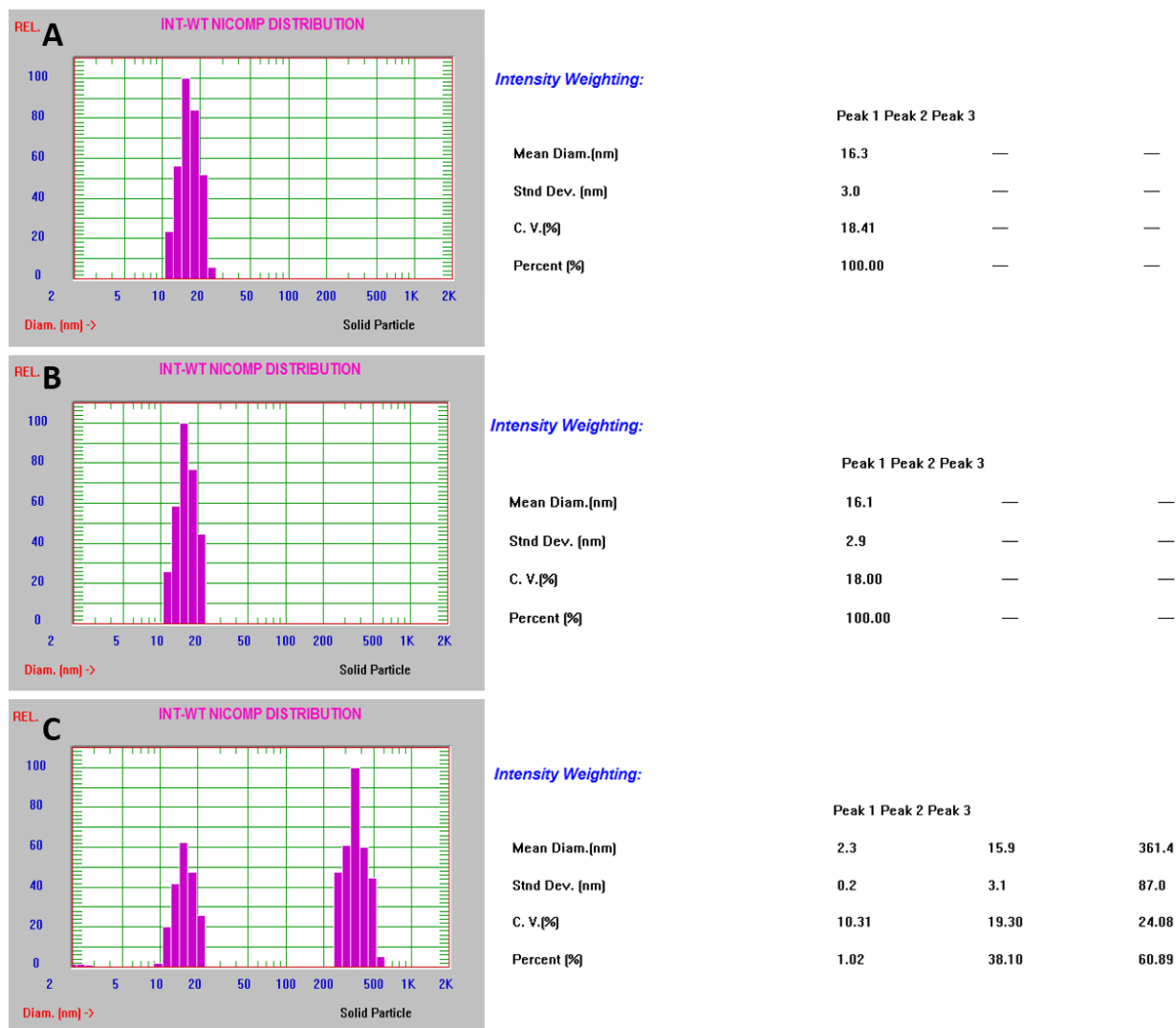


Figure 20: Particle size of SSM or TST-SSM prepared by the thin-film hydration method.

(A) 2mM DSPE-PEG₂₀₀₀, (B) TST-SSM containing 120 μ M of TST and 2 mM of DSPE-PEG₂₀₀₀, (C) TST-SSM containing 180 μ M of TST and 2 mM of DSPE-PEG₂₀₀₀.

Adapted by permission from the Copyright Clearance Center: Elsevier, International Journal of Pharmaceutics, (Esparza and Onyuksel 2019), Copyright 2019.

3. Preparation of TST-SSM nanomedicine by the co-solvent freeze-drying method

We employed co-solvent freeze-drying as a scalable and more practical method to produce TST-SSM nanomedicine for clinical and commercial uses. Our goal was to encapsulate 5 drug molecules per micelle, which was the maximum drug loading observed with the thin-film hydration method (**Section A-2**). We adopted a previously published freeze-drying method developed to encapsulate hydrophobic taxane derivatives in PVP-b-PDLLA polymeric micelles (E. Fournier et al. 2004). In this method, drug and polymer are combined in 30% TBA: water co-solvent, freeze-dried, and reconstituted in dextrose 5% or saline. The principle of this method is that TBA infiltrates in the hydrophobic core of micelles and makes them swollen, allegedly facilitating the drug loading process. The co-solvent is removed by freeze-drying and replaced by a biocompatible diluent. However, when Fournier's method was applied to encapsulate TST in SSM (proportion of approximately 5 drug molecules per micelle), we observed additional large drug particles by DLS indicating poor drug loading in SSM (**Figure 21**).



Figure 21: Particle size of SSM and TST-SSM prepared by the co-solvent freeze-drying with 30% TBA: water (v/v) and reconstituted in 0.9% saline. (A) 5 mM DSPE-PEG₂₀₀₀, (B) TST-SSM containing 120 μ M of TST and 5 mM DSPE-PEG₂₀₀₀.

3.1. Effect of TBA on DSPE-PEG₂₀₀₀ micelle formation

Since we failed to obtain a clean TST-SSM formulation using Fournier's method, we decided to investigate the behavior of DSPE-PEG₂₀₀₀ micelles in the co-solvent system. We measured the particle size by DLS of 5mM DSPE-PEG₂₀₀₀ micelles prepared in various proportions of TBA: 0.9% saline to determine the effect of TBA on phospholipid micelle formation. However, since TBA considerably affects the viscosity

and refractive index of the media, we measured those parameters to adjust them in the particle sizer. The results are summarized in **TABLE VIII**.

TABLE VIII: REFRACTIVE INDEX, DENSITY, AND VISCOSITY OF DIFFERENT PROPORTIONS OF TBA IN WATER AT 25°C.

TBA (%)	Refractive Index	Viscosity (cP)	Density (g/mL)
0	1.3322	0.8904	0.9934
10	1.3387	1.3459	0.9791
20	1.3465	2.0190	0.9694
30	1.3538	2.7383	0.9529
40	1.3621	3.4177	0.9310
50	1.3678	3.9697	0.9085
60	1.3727	4.3563	0.8852
70	1.3770	4.7178	0.8610
80	1.3807	4.5775	0.8354
90	1.3830	4.4575	0.8102
100	1.3849	4.4121	0.7763

Using these adjusted parameters, we found that the particle size of DSPE-PEG₂₀₀₀ prepared in 0.9% saline was approximately 16 nm (intensity-weighted) (**Figure 22** and **Figure 23**). However, as we increased the content of TBA in the system, we observed gradual micelle size reduction and complete micelle disruption above 40% TBA: 0.9% saline (v/v). The emerging particle population between 1.2 nm and 4.7 nm could be an artifact of the measurement since the Nicomp equipment is less reliable for particles smaller than 5 nm (Vukovic et al. 2011). At 90% TBA, an additional particle population with a mean diameter of 7.6 nm was observed, possibly corresponding to reversed micelles (hydrophilic core and hydrophobic surface). Particle size analysis was not performed in 100% TBA because DSPE-PEG₂₀₀₀ did not dissolve in pure TBA.

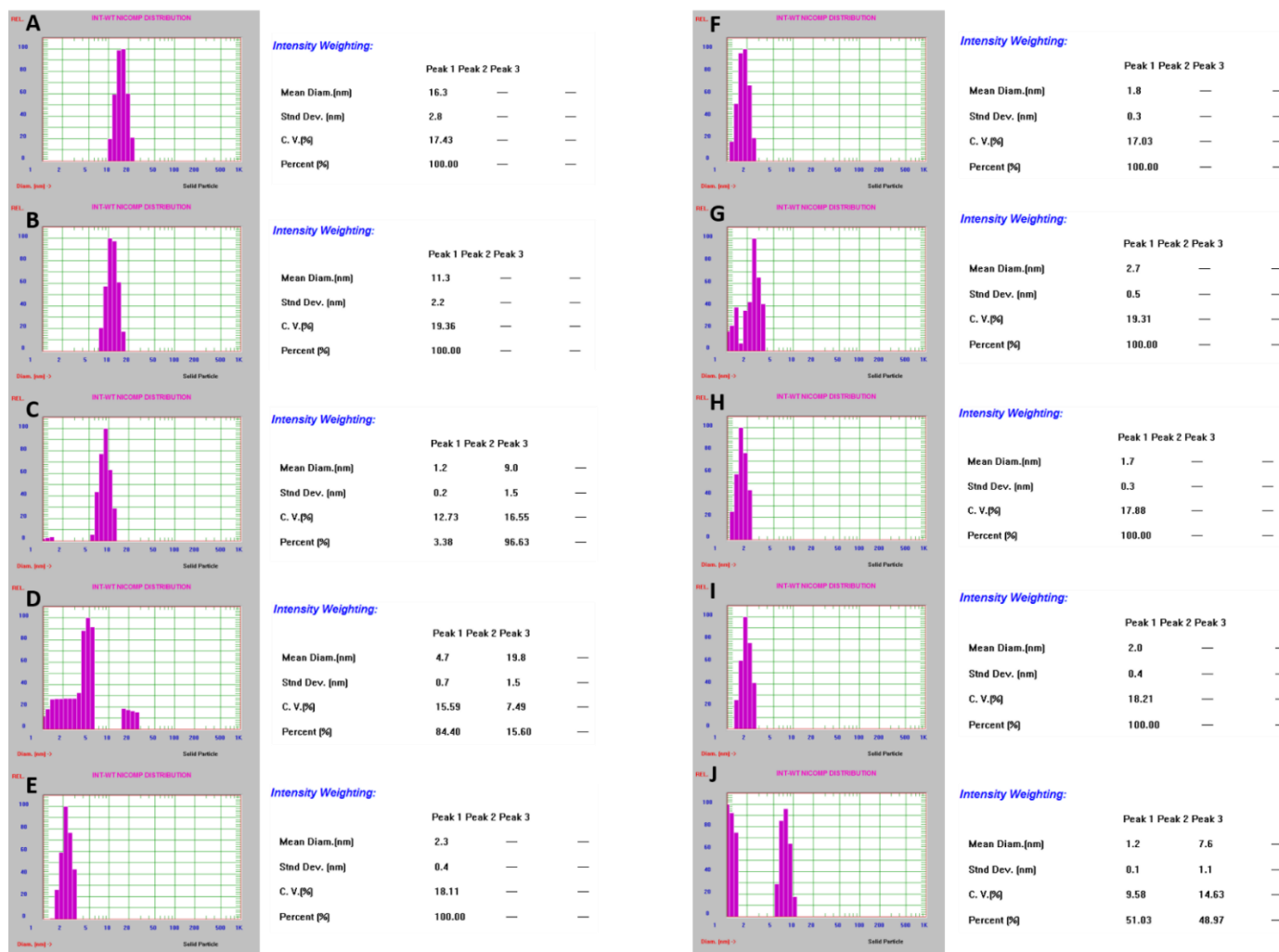


Figure 22: Particle size of DSPE-PEG2000 micelles in TBA: 0.9% saline co-solvent system.

(A) 0% TBA, (B) 10% TBA, (C) 20% TBA, (D) 30% TBA, (E) 40% TBA, (F) 50% TBA, (G) 60% TBA, (H) 70% TBA, (I) 80% TBA, and (J) 90% TBA.

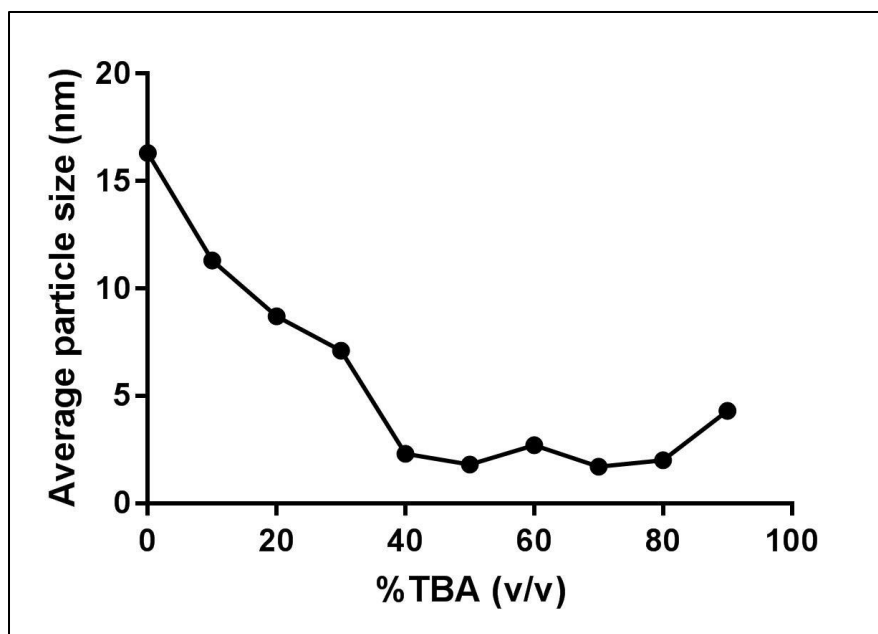


Figure 23: Average particle size of DSPE-PEG2000 micelles in TBA: 0.9% saline co-solvent system.

Reprinted by permission from the Copyright Clearance Center: Elsevier, International Journal of Pharmaceutics, (Esparza and Onyuksel 2019), Copyright 2019.

Since DSPE-PEG₂₀₀₀ micelles are disrupted in the presence of TBA instead of presenting the swelling properties of PVP-b-PDLLA micelles (E. Fournier et al. 2004), we concluded that the encapsulation model proposed by Fournier is not applicable to SSM. Therefore, we decided to modify Fournier's method and investigate a new encapsulation model of TST in SSM using co-solvent freeze-drying.

We prepared TST-SSM samples by co-solvent freeze-drying varying method parameters systematically (TBA proportion, reconstitution method, presence of PBS salts, phospholipid concentration, and fill volume) (**TABLE III**). Based on these results, we were able to establish our new model of drug encapsulation in SSM using co-solvent freeze-drying.

3.2. Effect of TBA proportion on drug loading

We prepared stock solutions of TST in TBA and DSPE-PEG₂₀₀₀ in water and combined them at the final proportion of 50% TBA: water (v/v). After freeze-drying, we reconstituted samples in 0.9% saline. These lyophilized samples took approximately 2 minutes and 48 seconds to reconstitute. In addition, we were only able to encapsulate 54 μM of TST in 5 mM of DSPE-PEG₂₀₀₀ micelles without having the formation of other larger particles (**Figure 24**), which corresponds to one TST molecule per micelle (molar ratio of phospholipid: drug was 99 ($5000 \mu\text{M} / (54 \mu\text{M} - 3.5 \mu\text{M})$)) and maximum loading was one drug molecules per micelle (90/99)). We increased the proportion of TBA to 75% in water (v/v) to reduce the polarity of the co-solvent solvent and prevent the formation of drug particles before freeze-drying. However, the increase of TBA proportion slightly increased the reconstitution time to 3 minutes and 7 seconds and it failed to improve the drug loading beyond 1 drug molecule per micelle (**Figure 24**). Since no difference in drug loading was observed with the increase of TBA proportion, we decided to explore if drug aggregation was occurring during the reconstitution step.

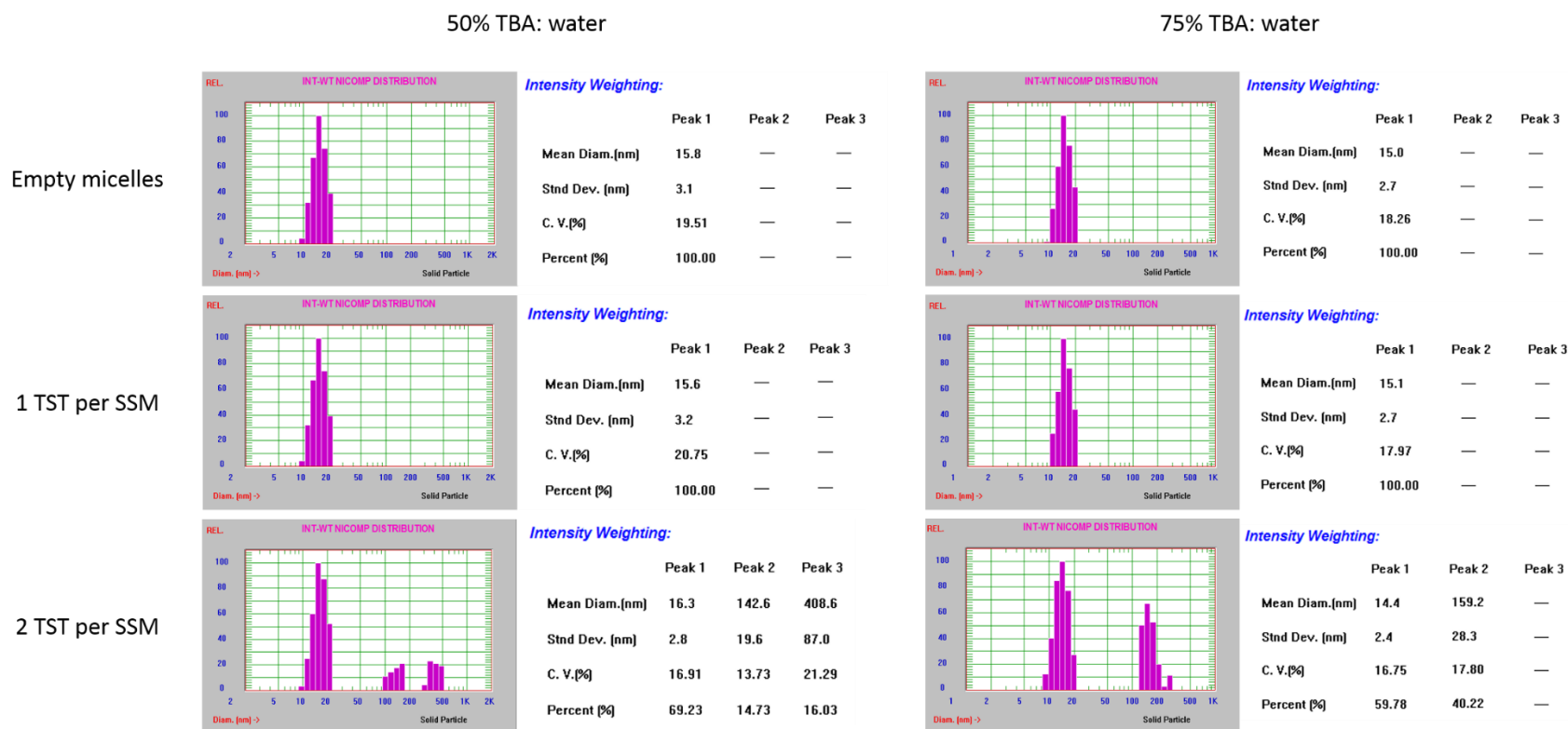


Figure 24: Particle size of SSM or TST-SSM prepared by the co-solvent freeze-drying method with 50% or 75% TBA: water (v/v) and reconstituted with 0.9% saline.

Adapted by permission from the Copyright Clearance Center: Elsevier, International Journal of Pharmaceutics, (Esparza and Onyuksel 2019), Copyright 2019.

3.3. Effect of reconstitution method on drug loading

We prepared TST-SSM formulations using 75% TBA: water (v/v) co-solvent system and compared three reconstitution methods from low to high mechanical energy: spontaneous, swirling, or sonication. All samples with low drug concentration (1 TST per micelle) were clear without visible drug precipitates regardless of the reconstitution method (**Figure 25**). However, samples with higher drug concentration (5 TST per micelle) and reconstituted with sonication were considerably less turbid than samples reconstituted by other methods. This result supports the idea that the reconstitution step can still be critical for drug encapsulation in SSM.

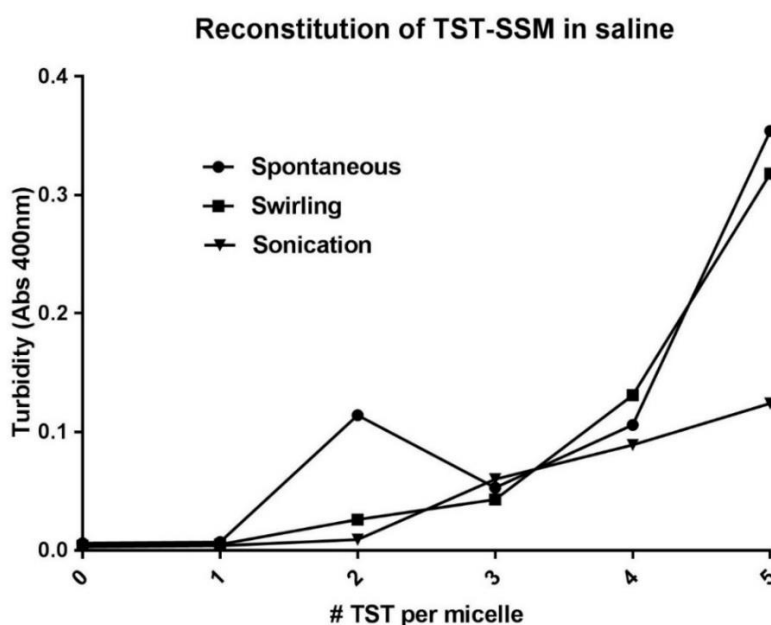


Figure 25: Turbidity of TST-SSM samples using different reconstitution methods. TST-SSM samples containing 0 to 5 TST molecules per micelle were prepared with 75% TBA: water co-solvent system and reconstituted in 0.9% saline. Reprinted by permission from the Copyright Clearance Center: Elsevier, International Journal of Pharmaceutics, (Esparza and Onyuksel 2019), Copyright 2019.

3.4. Effect of PBS salts on reconstitution time and drug loading

Considering that most of the ingredients in the TST-SSM lyophilized cake were hydrophobic and therefore difficult to reconstitute in water, we decided to add salts before freeze-drying to enhance the hydrophilicity of the cake. We adjusted the PBS concentration in the co-solvent system to obtain a reconstituted final product with 1X PBS. However, as we added the aqueous phase containing DSPE-PEG₂₀₀₀ into the organic phase to a final proportion of 75% TBA: 4X PBS (v/v), even in the absence of drug, we observed cloudiness of the solution suggesting phospholipid precipitation (**Figure 26**). This forced us to change the co-solvent composition to 50% TBA: 2X PBS (v/v) to maintain both drug and phospholipid in solution prior to the lyophilization. Using those conditions, we reproducibly obtained a clear solution prior to freeze-drying (**Figure 26**) which originated uniform and elegant lyophilized cakes. Those cakes rapidly reconstituted in water (approximately 19 seconds) and contained 277.8 μM of TST in 5 mM of DSPE-PEG₂₀₀₀ micelles without the presence of other particles as confirmed by HPLC and DLS, respectively (**Figure 27**). This proportion corresponded to a molar ratio of phospholipid: drug of 18.2 ($5000 \mu\text{M} / (277.8 \mu\text{M} - 3.5 \mu\text{M})$) and a maximum loading of approximately 5 drug molecules per micelle ($90/18.2$).

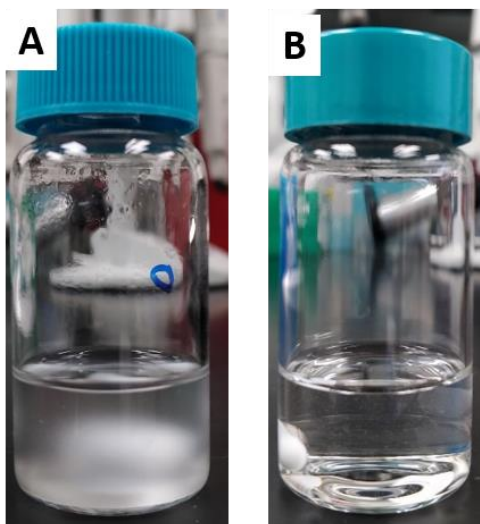


Figure 26: Visual appearance of 5mM of DSPE-PEG₂₀₀₀ dispersed in different co-solvent systems before freeze-drying. (A) 75% TBA: 4X PBS (v/v) and (B) 50% TBA: 2X PBS (v/v). Reprinted by permission from the Copyright Clearance Center: Elsevier, International Journal of Pharmaceutics, (Esparza and Onyuksel 2019), Copyright 2019.

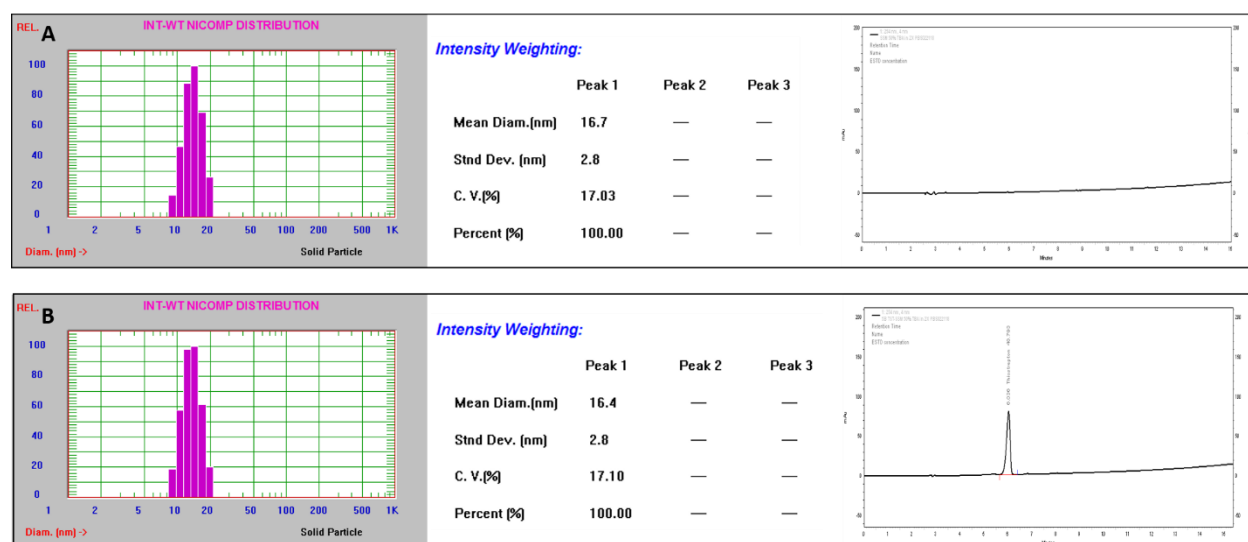


Figure 27: Particle size and TST quantification of SSM or TST-SSM prepared by the co-solvent freeze-drying method with 50% TBA: 2X PBS (v/v) and reconstituted with deionized water.

(A) Empty SSM, (B) 5 TST molecules per micelle.

3.5. Effect of phospholipid concentration on reconstitution time and drug loading

We decided to improve the strength of the formulation by increasing the phospholipid concentration to 10 mM and 15 mM while still maintaining the ratio of 5 TST molecules per micelle. Using 50% TBA: 2X PBS co-solvent system, we observed that the increase of phospholipid concentration impaired with the cake reconstitution and led to the formation of drug aggregates (**Figure 28**). The reconstitution time of cakes containing 10 mM and 15 mM of DSPE-PEG₂₀₀₀ were approximately 1 minute and 9 seconds and 3 minutes and 40 seconds, respectively.

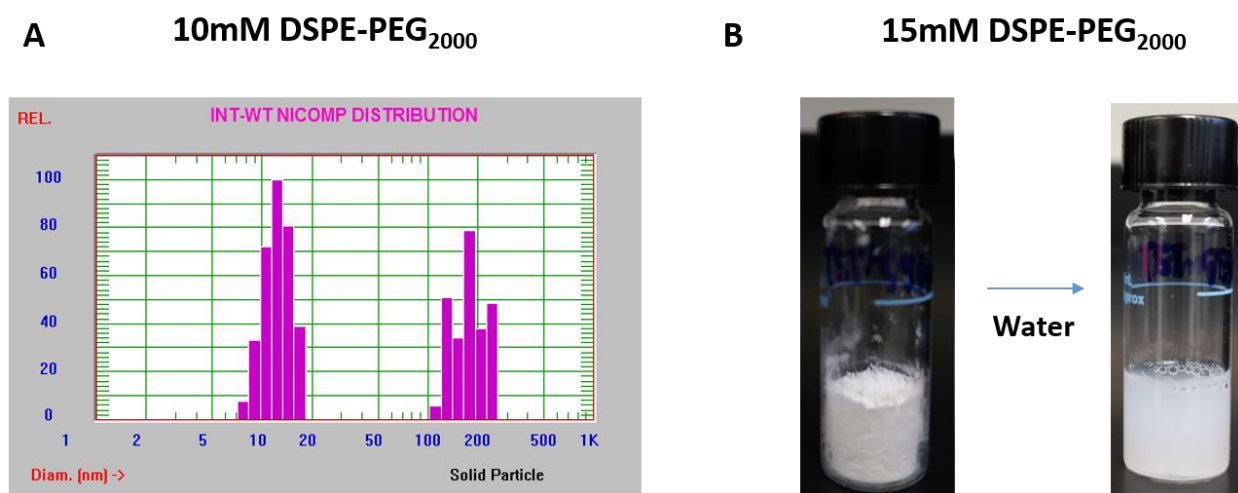


Figure 28: Formation of drug aggregates due to the increase of phospholipid concentration in formulations containing 5 TST molecules per micelle. Particle size of TST-SSM containing 10 mM of DSPE-PEG₂₀₀₀ showing an additional large particle population. (B) TST-SSM containing 15 mM of DSPE-PEG₂₀₀₀ showing turbidity after reconstitution due to drug precipitation. Reprinted by permission from the Copyright Clearance Center: Elsevier, International Journal of Pharmaceutics, (Esparza and Onyuksel 2019), Copyright 2019.

3.6. Effect of fill and reconstitution volumes on drug loading

Given the challenges to prepare TST-SSM with 15 mM DSPE-PEG₂₀₀₀, we decided to concentrate the formulation by reconstituting the freeze-dried formulation using a smaller volume of water. We prepared samples containing 5 mM of phospholipid, 5 TST molecules per micelle, and 50% TBA: 0.667X PBS co-solvent, and fill 6 mL or 12 mL of this formulation into 20 mL glass vials. After freeze-drying, we reconstituted cakes with 2 mL or 4 mL of water, respectively, which correspond to one-third of fill volumes. As a result, samples filled with 6 mL and reconstituted with 2 mL were visually clear exhibiting a single micelle particle population of 12.7 ± 0.5 nm and containing TST at the expected concentration (833.4 μ M) (**Figure 29**). This formulation exhibited a drug concentration 238 times higher than the drug intrinsic aqueous solubility and presented a reconstitution time of approximately 1 minute and 45 seconds. On the other hand, samples filled with 12 mL of formulation and reconstituted in 4 mL exhibited an additional particle population besides micelles, indicating the presence of large drug aggregates. This observed effect was probably due to the reduced space inside the vial which impaired with the proper agitation of samples and drug loading. Therefore, the fill volume of 6mL and reconstitution volume of 2 mL was selected as our final optimized formulation.

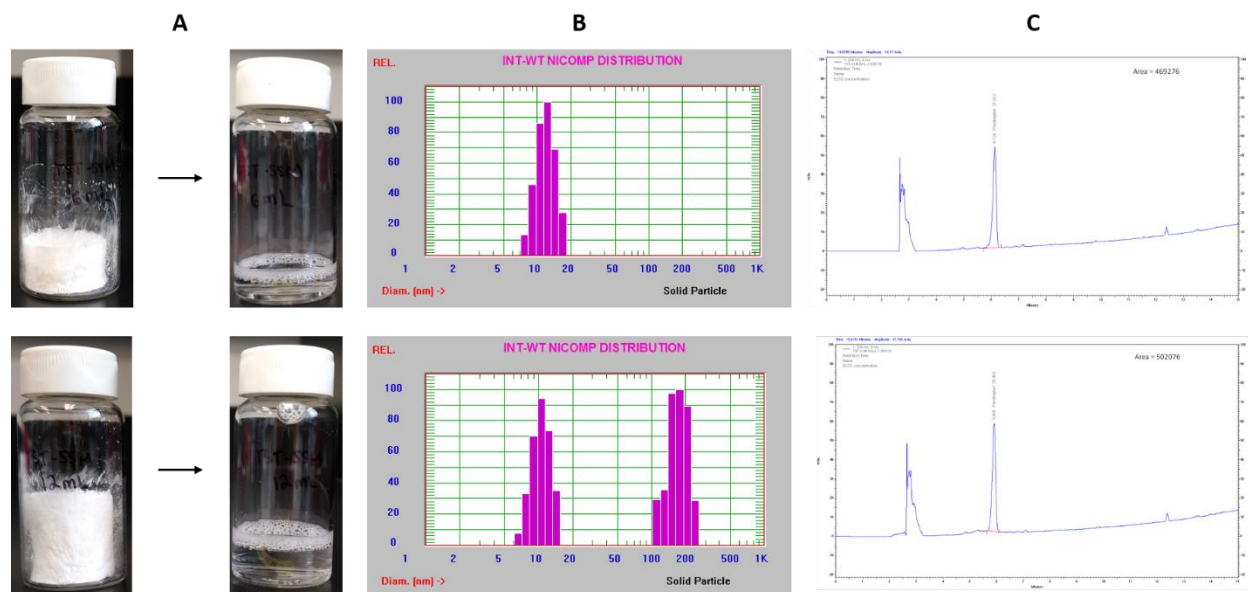


Figure 29: TST-SSM samples with a fill volume of 6 mL (top) or 12 mL (bottom) and reconstituted in one-third of the volume. (A) Representative picture of lyophilized cake (left) and reconstituted nanomedicine (right). (B) Intensity-weighted particle size distribution. (C) HPLC chromatogram confirming the presence of TST in the formulation. Reprinted by permission from the Copyright Clearance Center: Elsevier, International Journal of Pharmaceutics, (Esparza and Onyuksel 2019), Copyright 2019.

3.7. Residual TBA in the TST-SSM lyophilized cake

We measured the residual levels of TBA in three batches of optimized TST-SSM formulations to ensure that the organic solvent was effectively removed during lyophilization. All samples tested exhibited levels below 0.03% (**TABLE IX**).

TABLE IX: RESIDUAL TERT-BUTANOL (TBA) IN OPTIMIZED TST-SSM LYOPHILIZED CAKES.

Replicate	Tert-butanol concentration (% in 25mg of cake)
1	0.0193
2	0.0236
3	0.0264

3.8. Osmolality of reconstituted TST-SSM nanomedicine

The osmolality of the optimized TST-SSM formulation (833.4 μ M of TST in 15 mM of DSPE-PEG₂₀₀₀) was approximately 312 mOsm/kg which is in the range of physiological osmolality desirable for safe IV administration (**TABLE X**) (W. Wang 2015).

TABLE X: OSMOLALITY OF TST-SSM RECONSTITUTED IN ONE-THIRD OF FILL VOLUME.

Samples	Average Osmolality (mOsm/kg)
1X PBS	298
15 mM SSM	327
6 mL TST-SSM	312 \pm 20.7

Reproduced by permission from the Copyright Clearance Center: Elsevier, International Journal of Pharmaceutics, (Esparza and Onyuksel 2019), Copyright 2019.

3.9. Internal lyophilized cake morphology and reconstitution time

We compared the external and internal morphology of TST-SSM lyophilized cakes (**TABLE III**) to understand differences in reconstitution time and drug loading efficiency (**Figure 30**). The increase in TBA proportion from 50% (sample A) to 75% v/v (sample B), in the absence of salts, improved the cake stability during freeze-drying and prevented its collapse. However, contrary to our expectations, SEM analysis revealed only a modest increase in cake porosity which was associated with long reconstitution time and inefficient drug loading. On the other hand, we observed that the presence of PBS salts (sample C) remarkably increased the internal porosity of the cake and reduced the reconstitution time, resulting in efficient high drug loading. We did not observe obvious differences in internal morphology among samples with increasing concentration of drug and phospholipid by SEM, even though their reconstitution times were remarkably different (samples D and E). The optimized TST-SSM formulation containing initially 5 mM of DSPE-PEG₂₀₀₀ and reconstituted with one-third of the fill volume (final DSPE-PEG₂₀₀₀ concentration of 15 mM) (sample F) exhibited longer reconstitution time than samples reconstituted with the full fill volume (sample C), but the internal morphology was not noticeably different.

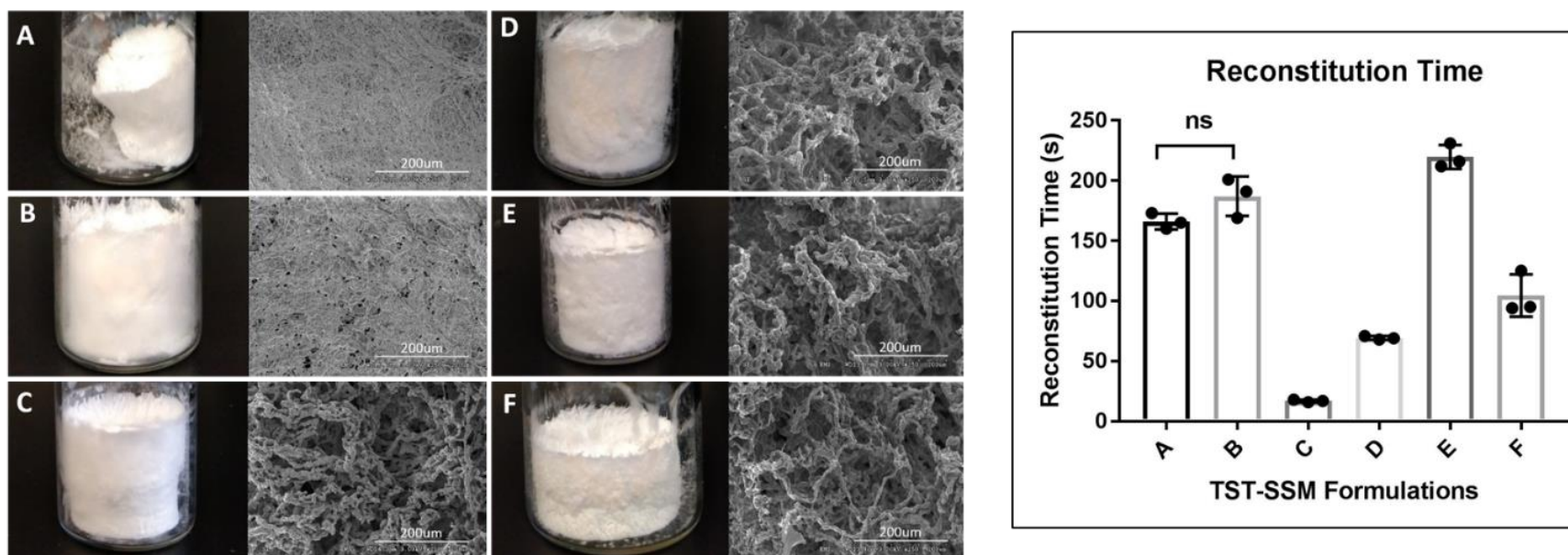


Figure 30: Scanning electron microscopy and reconstitution time of different preparations of TST-SSM. Samples preparation details are described in **TABLE III**. (A) 55.6 μM of TST and 5 mM DSPE-PEG₂₀₀₀ prepared in 50% TBA: water, (B) 55.6 μM of TST and 5 mM DSPE-PEG₂₀₀₀ prepared in 75% TBA: water, (C) 277.8 μM of TST and 5mM DSPE-PEG₂₀₀₀ prepared in 50% TBA: 2X PBS, (D) 555.6 μM of TST and 10 mM DSPE-PEG₂₀₀₀ prepared in 50% TBA: 2X PBS, (E) 833.4 μM of TST and 15mM DSPE-PEG₂₀₀₀ prepared in 50% TBA: 2X PBS, (F) 277.8 μM of TST and 5mM DSPE-PEG₂₀₀₀ prepared in 50% TBA: 0.667X PBS. The average of three samples was analyzed by one-way ANOVA with Tukey's multiple comparisons with p-value < 0.05 considered statistically significant. Reproduced by permission from the Copyright Clearance Center: Elsevier, International Journal of Pharmaceutics, (Esparza and Onyuksel 2019), Copyright 2019.

4. Stability of TST-SSM nanomedicine

4.1. Short-term stability of reconstituted TST-SSM nanomedicine

We evaluated the short-term stability of TST-SSM to define the maximum period that the nanomedicine remains suitable for use after reconstitution in water. We found that the particle size ($p=0.5547$) (**Figure 31** and **Figure 32**) and drug concentration ($p=0.8480$) (**Figure 33**) did not change significantly during storage at 4°C and 25°C for up to 7 days. In addition, HPLC analysis revealed no changes in TST retention time or the formation of detectable degradation products in both storage conditions (**Figure 34**).

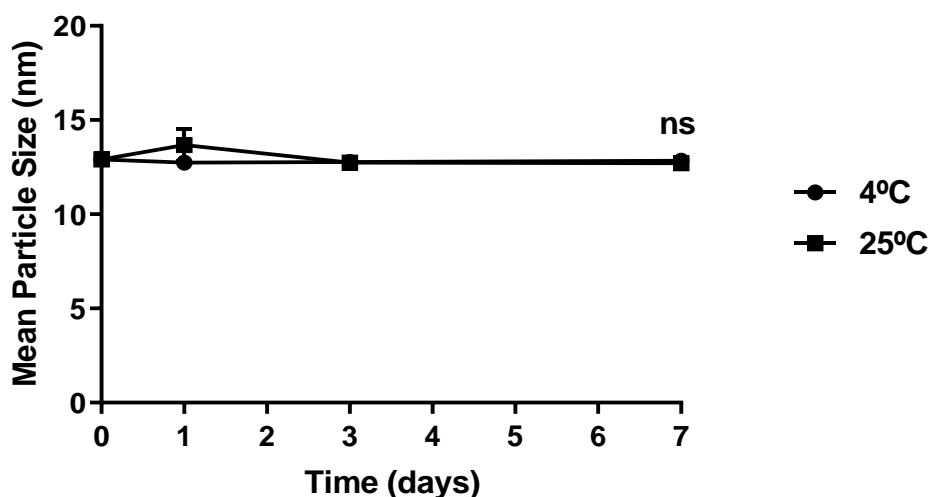


Figure 31: Particle size of reconstituted TST-SSM stored at 4°C or 25°C. Results are mean \pm standard deviation ($n=3$). Data analyzed by one-way ANOVA with $p<0.05$ considered statistically significant. Ns = not significant compared to time zero.

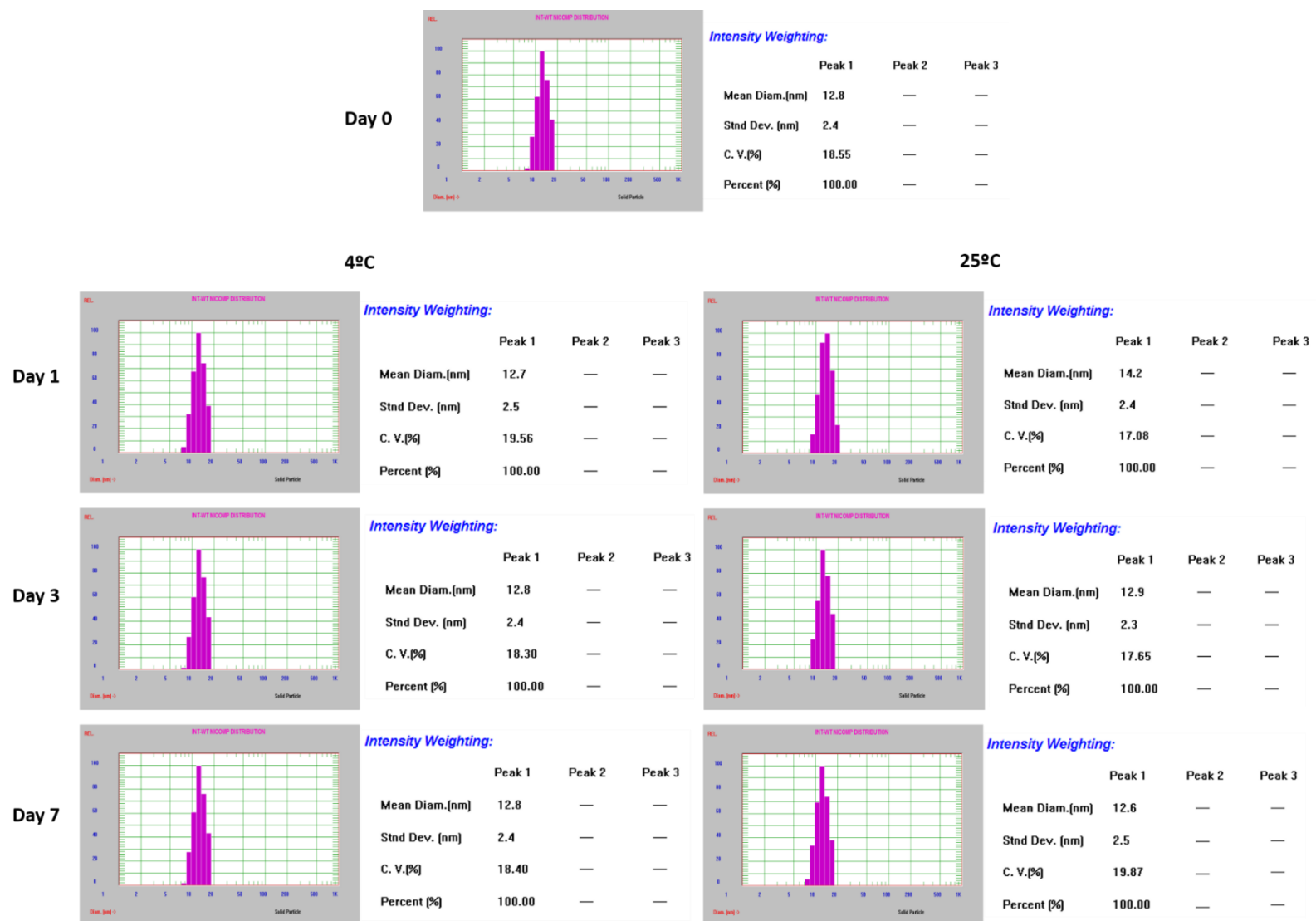


Figure 32: Representative particle size analysis of reconstituted TST-SSM after short-term storage.

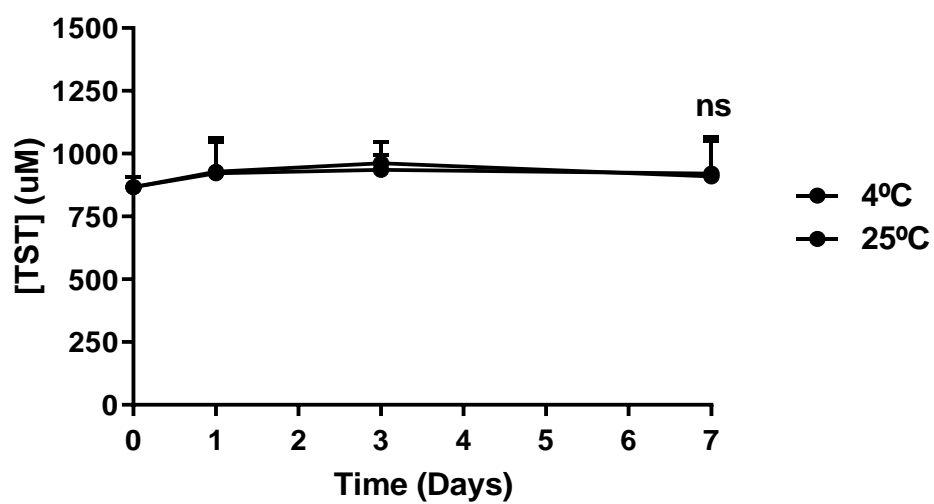
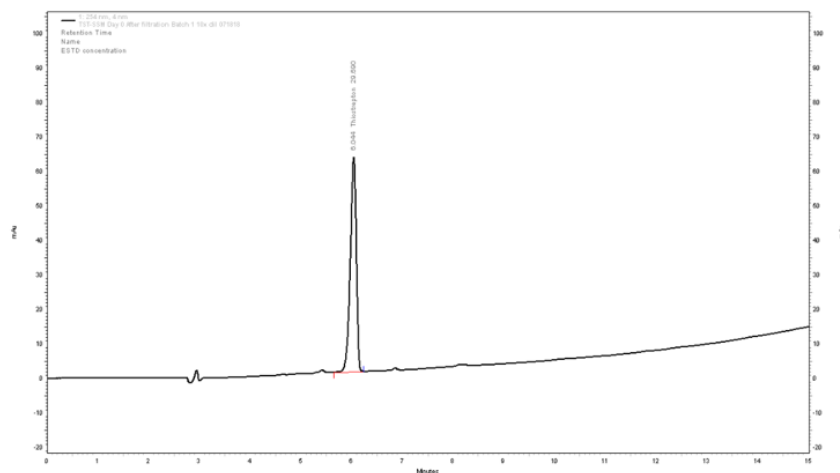
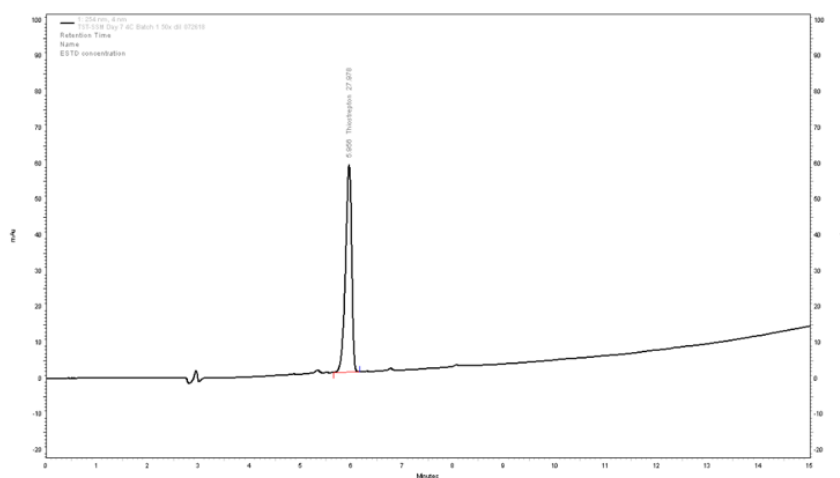


Figure 33: Drug concentration of reconstituted TST-SSM stored at 4°C or 25°C. Results are mean \pm standard deviation ($n=3$). Data analyzed by a one-way ANOVA test with $p<0.05$ considered statistically significant. Ns = not significant compared to time zero.

Day 0



Day 7 / 4°C



Day 7 / 25°C

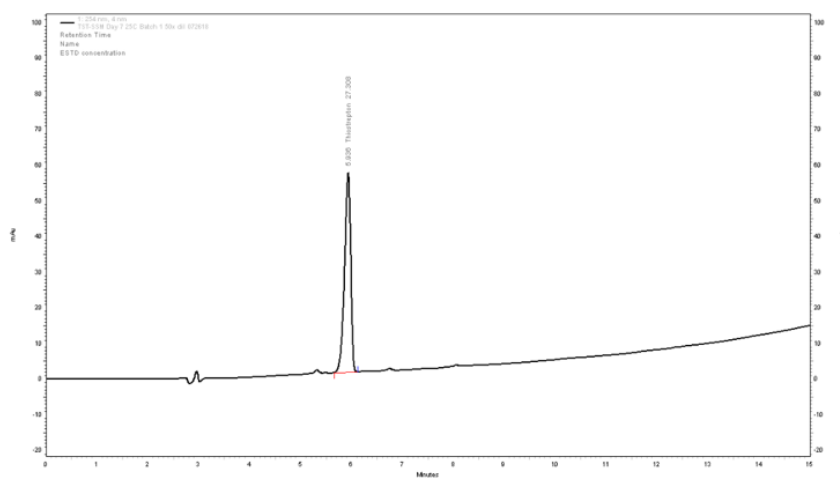


Figure 34: Representative chromatogram of TST-SSM at day 0 and day 7 of storage at 4°C or 25°C.

Reconstituted TST-SSM lost its antimicrobial activity against MRSA USA300 when stored at 25°C for longer than a day (**TABLE XI**).

TABLE XI: MINIMUM INHIBITORY CONCENTRATION (MIC) OF RECONSTITUTED TST-SSM STORED AT 4°C OR 25°C.

Samples	MIC (μM)					
	Exp 1		Exp 2		Exp 3	
	4°C	25°C	4°C	25°C	4°C	25°C
TST in 2% DMSO	-	0.2	-	0.2	-	0.2
Day 0	-	0.03	-	0.05	-	0.03
Day 1	0.05	0.05	0.03	0.05	0.03	>28
Day 3	0.05	>28	0.05	>28	0.03	>28
Day 7	0.05	0.05	0.05	>28	0.03	>28

4.2. Long-term stability of freeze-dried TST-SSM nanomedicine

The long-term stability of lyophilized TST-SSM nanomedicine was evaluated during storage at 5°C, 30°C/60% RH and 40°C/75% RH for 7 months. The purpose was to establish the maximum period that the formulation retains its properties when stored in the freeze-dried form in different temperature and humidity conditions. We found that

in all cases, the moisture of TST-SSM nanomedicine slightly increased during storage for over 7 months (**TABLE XII**). Although the reconstitution time remained below 90 seconds for all samples (**Figure 35**), formulations stored at 40°C exhibited secondary larger particles indicative of drug aggregation or micellar destabilization (**Figure 36** and **Figure 37**). This change in particle size at 40°C was accompanied by a reduction of drug concentration of about 16% compared to the initial time (**Figure 38**) and appearance of degradation products in the chromatogram (**Figure 39**). However, contrary to our expectations, all samples, including the ones stored at 40°C exhibited similar antimicrobial activity for up to 7 months (**TABLE XIII**).

TABLE XII: MOISTURE IN TST-SSM LYOPHILIZED CAKES AFTER STORAGE AT 5°C, 30°C/60% RH OR 40°C/75% RH FOR 7 MONTHS.

Storage conditions	Moisture (%)	
	Initial	7 months
5°C	0.07	0.65
30°C/60% RH	0.07	1.17
40°C/75% RH	0.07	0.56

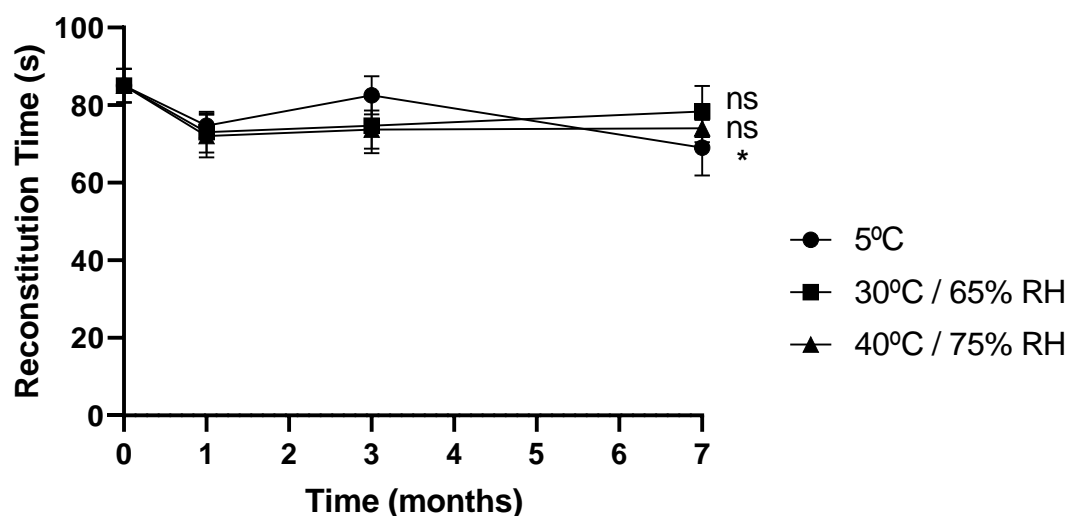


Figure 35: Reconstitution time of TST-SSM lyophilized cakes after long-term storage. Results are mean \pm standard deviation ($n=3$). Data analyzed by one-way ANOVA with Tukey's multiple comparisons. $P<0.05$ considered statistically significant. * $p<0.05$, ns=not significant compared to time zero.

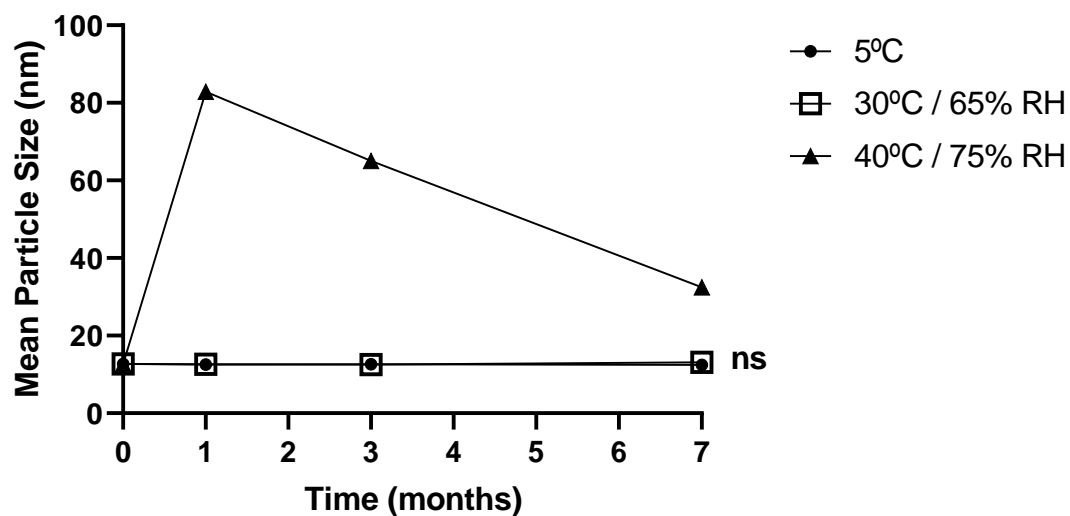


Figure 36: Particle size of TST-SSM after long-term storage of lyophilized cake. Results are mean \pm standard deviation ($n=3$). Data analyzed by one-way ANOVA with $p<0.05$ considered statistically significant. Ns = not significant compared to time zero.

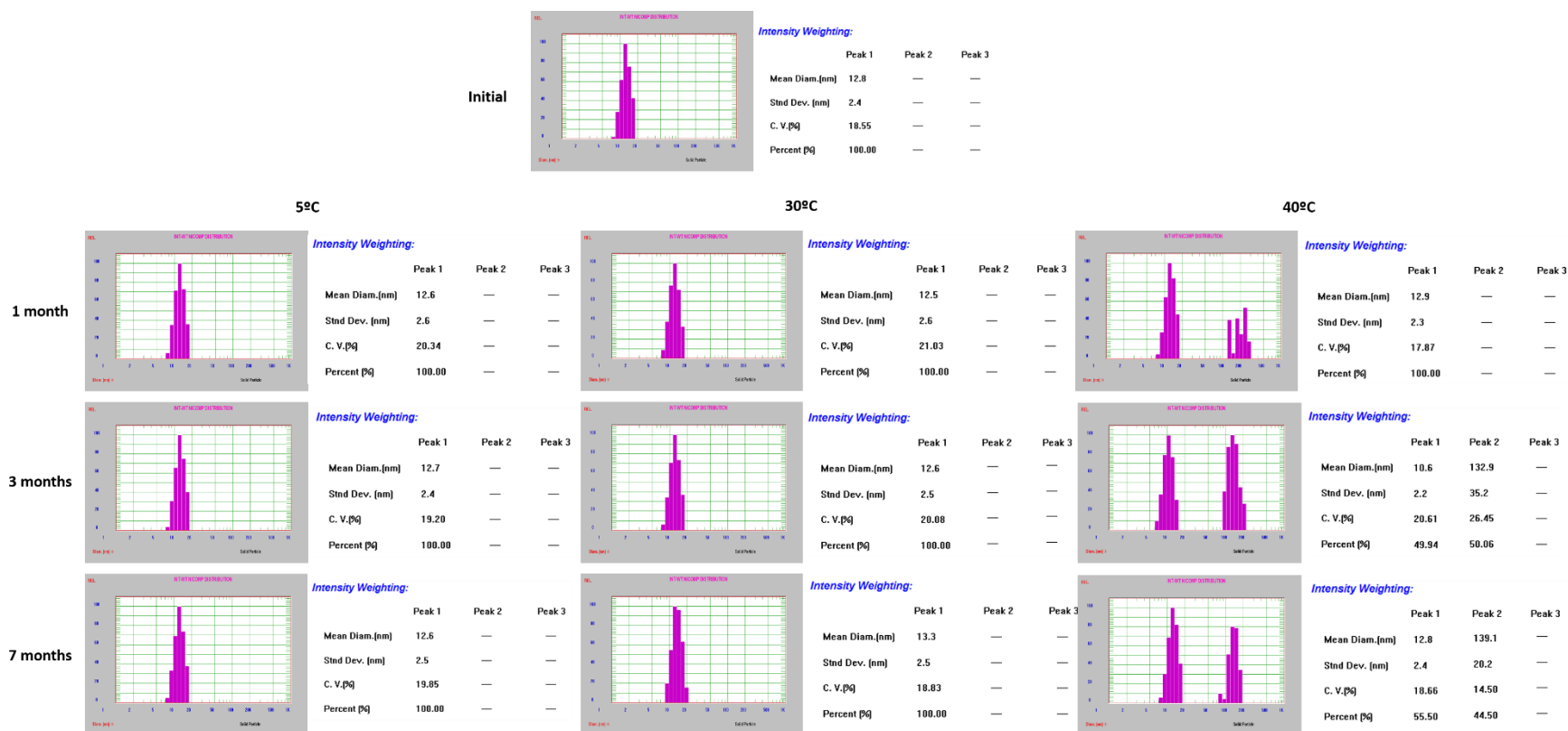


Figure 37: Representative particle size of TST-SSM after long term storage of lyophilized cake.

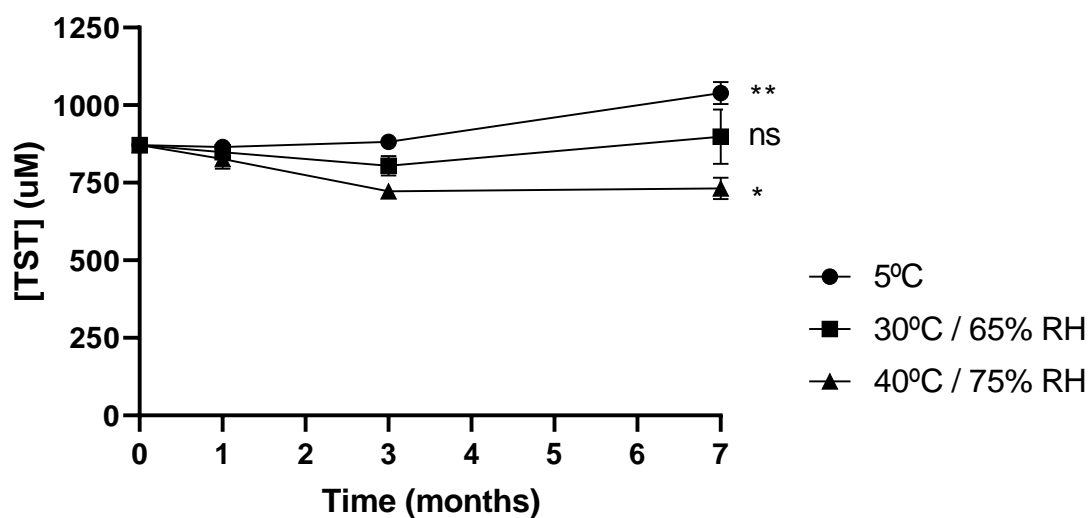
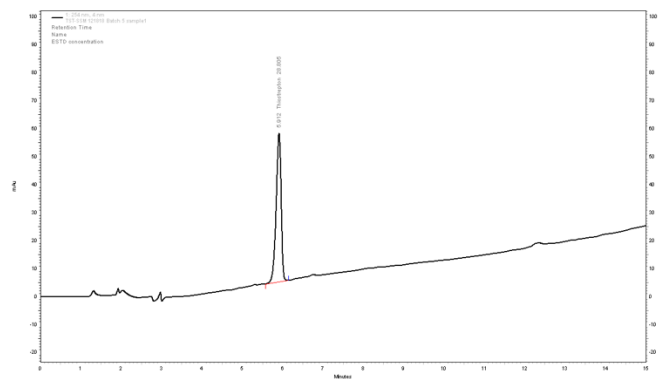
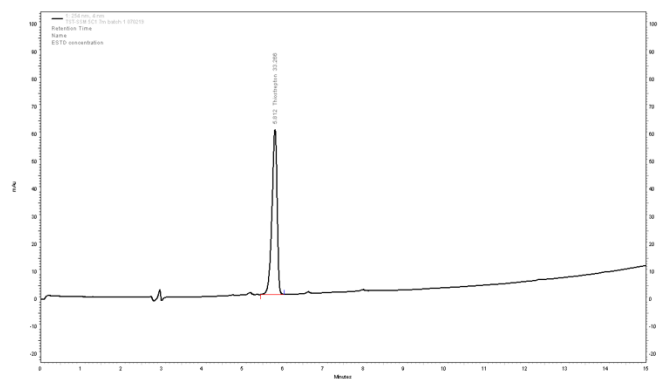


Figure 38: Drug concentration of TST-SSM after long-term storage of lyophilized cake. Results are mean \pm standard deviation (n=3). Data analyzed by one-way ANOVA with Tukey's multiple comparisons. $P < 0.05$ considered statistically significant. * $p < 0.05$, ** $p < 0.01$, ns = not significant compared to time zero.

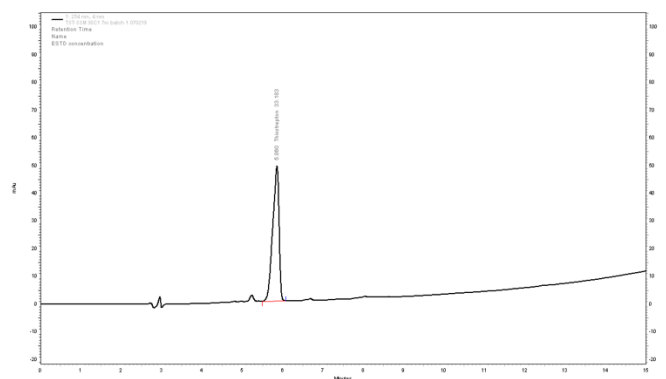
Time 0



**7 months
5 ± 3°C**



**7 months
30 ± 2°C
RH 65 ± 5%**



**7 months
40 ± 2°C
RH 75 ± 5%**

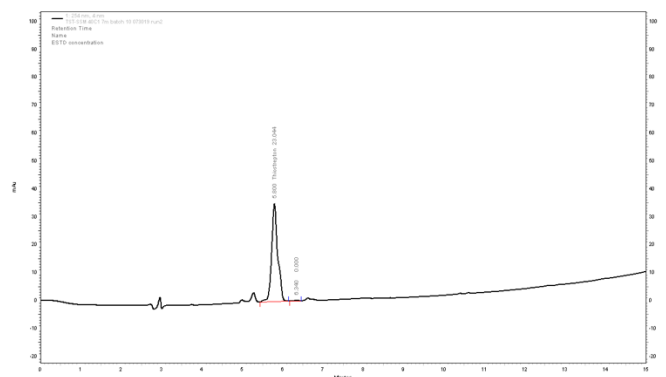


Figure 39: Chromatogram of TST-SSM after long-term storage of lyophilized cake at 5°C, 30°C/60% RH and 40°C/75% RH.

TABLE XIII: MINIMUM INHIBITORY CONCENTRATION (MIC) OF TST-SSM AFTER STORAGE OF LYOPHILIZED CAKE AT 5°C, 30°C/60% RH OR 40°C/75% RH.

Timepoint	Storage Condition	MIC (μM)		
		Exp 1	Exp 2	Exp 3
Initial	-	0.054	0.027	0.027
	5°C	0.027	0.027	0.027
1 month	30°C/60% RH	0.027	0.027	0.027
	40°C/75% RH	0.027	0.054	0.027
	5°C	0.027	0.027	0.027
3 months	30°C/60% RH	0.027	0.027	0.027
	40°C/75% RH	0.054	0.027	0.054
	5°C	0.027	0.027	0.027
7 months	30°C/60% RH	0.054	0.027	0.054
	40°C/75% RH	0.054	0.054	0.027

B. In vitro activity of TST-SSM nanomedicine

1. Antimicrobial activity of TST-SSM nanomedicine against several Gram-positive bacteria

We tested the antimicrobial activity of the optimized TST-SSM formulation (833.4 μM TST and 15 mM DSPE-PEG₂₀₀₀) against various Gram-positive microorganisms using the microdilution assay. We observed the MIC of TST-SSM was 2 to 8-fold lower than TST dissolved in 4% DMSO, indicating that TST-SSM nanomedicine has better

activity than free TST in all cases (**TABLE XIV**). Also, TST-SSM was active at lower concentrations than reference antibiotics vancomycin and erythromycin. The largest difference was observed with MRSA USA300, in which TST-SSM exhibited antimicrobial activity at a concentration 100-fold lower than the gold-standard antibiotic vancomycin.

TABLE XIV: MINIMUM INHIBITORY CONCENTRATION OF TST, TST-SSM OR POSITIVE CONTROLS AGAINST GRAM-POSITIVE PATHOGENS.

Microorganism	Minimum Inhibitory Concentration (μM)			
	Erythromycin	Vancomycin	TST in 4% DMSO	TST-SSM
<i>Staphylococcus aureus</i> USA 300	-	5.4	0.2	0.03 – 0.05
<i>Staphylococcus aureus</i> COL	0.4	-	0.2 – 0.4	0.05
<i>Bacillus anthracis</i> Sterne	1.4 – 2.7	-	0.4 – 0.9	0.1 – 0.2
<i>Bacillus cereus</i> 14579	0.3 – 0.7	-	0.2	0.03
<i>Bacillus thuringiensis</i> konkukian 97-27	0.7	-	0.4 – 0.9	0.05

2. Accumulation of TST-SSM in MRSA USA300

We evaluated the accumulation of TST inside MRSA USA 300 in the presence and absence of micelles. Our purpose was to investigate reasons for improved drug activity of the nanomedicine compared to the free drug (**TABLE XIV**). We hypothesized that SSM might improve the drug penetration across the bacterial cell and expose the bacteria to higher concentrations in the cytoplasm where target ribosomes are located. To test this hypothesis, we incubated MRSA USA 300 ($OD_{600}=1$) with 6 μ M of TST dissolved in 4% DMSO, TST + DSPE-PEG₂₀₀₀ or optimized TST-SSM formulation and collected samples periodically for 2h. Cells were lysed overnight with glycine hydrochloride, cell debris removed by centrifugation, and drug extracted with organic solvents for quantification by LC-MS/MS. We observed that there were no significant differences in drug accumulation among groups (**Figure 40**). Despite that, TST seems to accumulate in MRSA USA300 more rapidly and to a greater extent than TST-SSM, but more studies are needed to confirm this behavior.

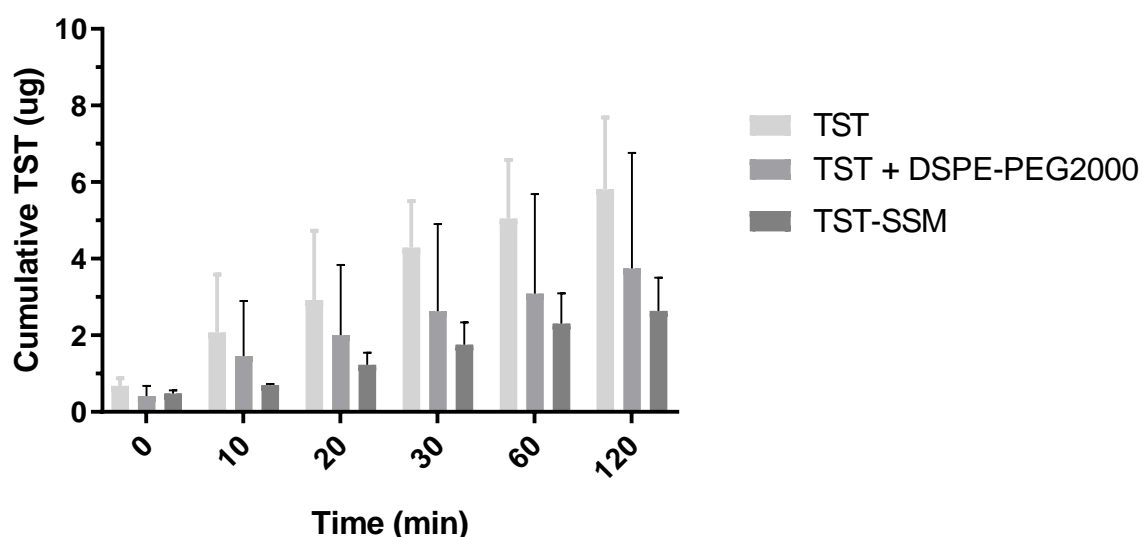


Figure 40: Accumulation of TST in MRSA USA 300 bacterial cells. Results are mean \pm standard deviation (n=2). Data analyzed by one-way ANOVA with $p < 0.05$ considered statistically significant.

3. Stability of TST-SSM in spent media of MRSA USA300

Since SSM does not improve the drug accumulation in bacterial cells, we hypothesized that SSM protects TST from degradation that might occur at the conditions of the antimicrobial assay. To test this hypothesis, we compared the stability of TST-SSM in fresh media, spent media from MRSA USA300, and bacterial lysate at 37°C for 24h. We observed that 84% to 94% of the original dose of TST remained stable when encapsulated in SSM, but this recovery decreased to 53%-74% when TST is incubated in its free form (**Figure 41**). This result confirms that SSM protects TST in the conditions of the microdilution assay.

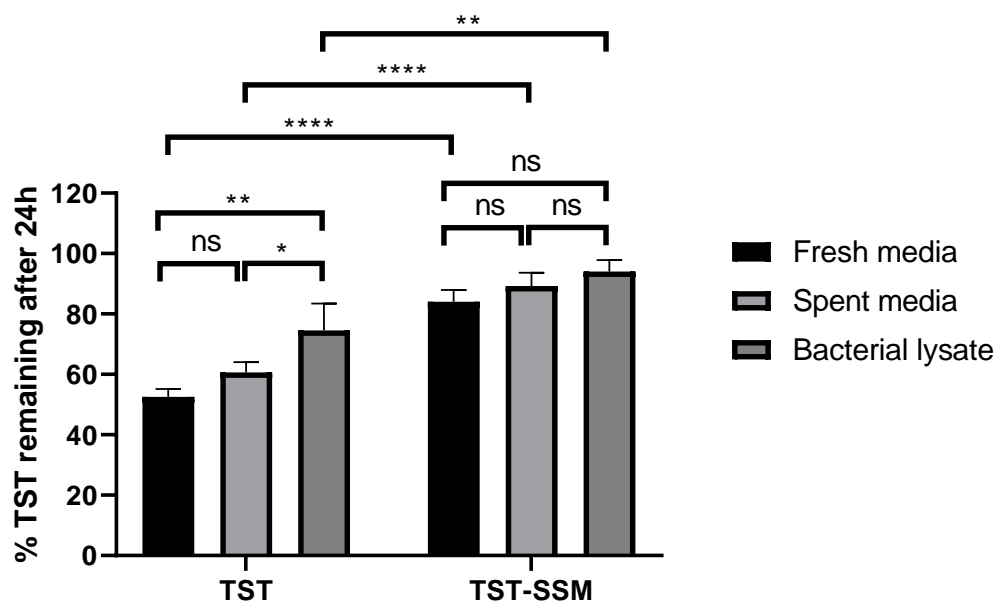


Figure 41: Remaining TST (%) after incubation in fresh media, MRSA USA300 spent media, or MRSA USA 300 lysate for 24h at 37°C.

Results are mean \pm standard deviation (n=3). Data analyzed by two-way ANOVA with Tukey's multiple comparisons. $p < 0.05$ was considered statistically significant. ns = not significant, * $p < 0.05$, ** $p < 0.01$, **** $p < 0.0001$.

C. In vivo efficacy of TST-SSM nanomedicine

1. Filtration of reconstituted TST-SSM nanomedicine

We assessed if sterilizing filtration through 0.22 μ m PES membrane affected the properties of TST-SSM nanomedicine. We found that filtration of reconstituted TST-SSM did not affect the particle size ($p = 0.5543$) (**Figure 42** and **Figure 43**), drug concentration ($p = 0.6556$) (**Figure 44**), or antimicrobial activity (**TABLE XV**). Therefore, sterilizing filtration of reconstituted TST-SSM through a 0.22 μ m PES membrane can be performed without altering the properties of the nanomedicine.

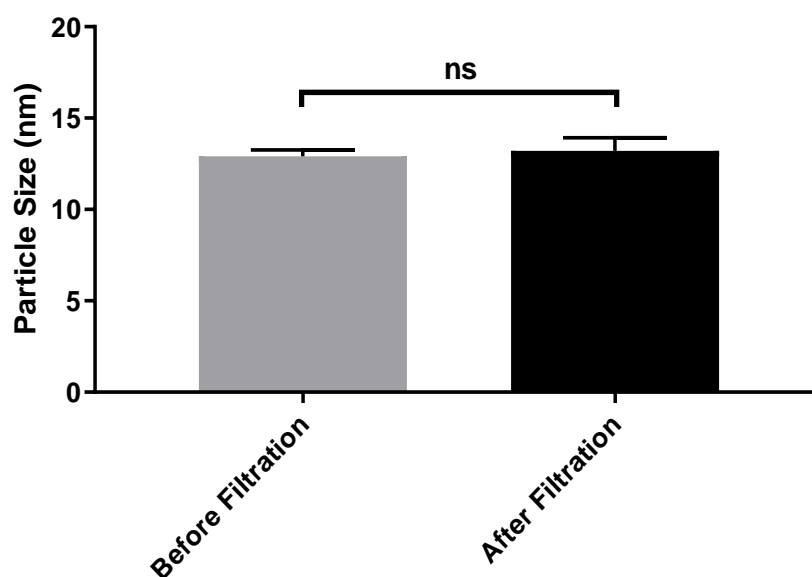
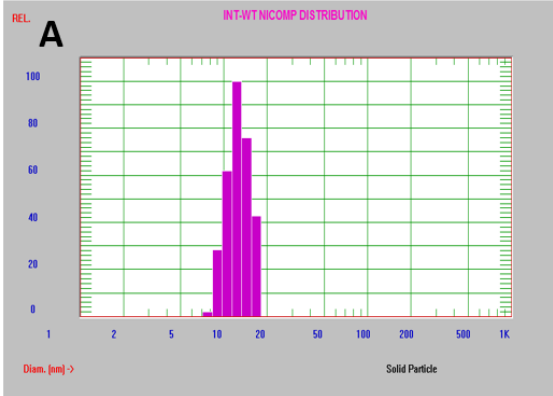
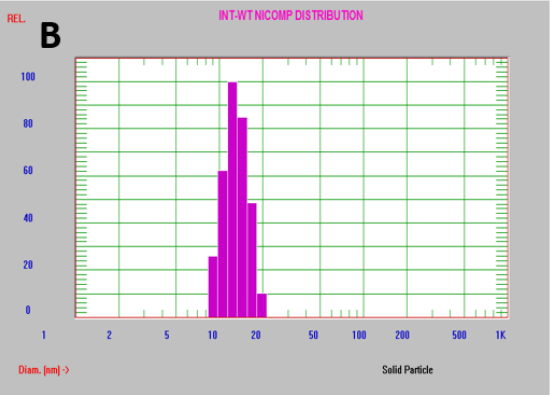


Figure 42: Particle size of reconstituted TST-SSM before and after filtration. Filtration was performed through a 0.22 μm PES syringe filter. Results are mean \pm standard deviation (n=3). Data were analyzed by Student's t-test with $p < 0.05$ considered statistically significant. Ns = not significant.



Intensity Weighting:

	Peak 1	Peak 2	Peak 3
Mean Diam.(nm)	12.8	—	—
Std Dev. (nm)	2.4	—	—
C. V.(%)	18.55	—	—
Percent (%)	100.00	—	—



Intensity Weighting:

	Peak 1	Peak 2	Peak 3
Mean Diam.(nm)	13.0	—	—
Std Dev. (nm)	2.6	—	—
C. V.(%)	20.30	—	—
Percent (%)	100.00	—	—

Figure 43: Representative particle size analysis of TST-SSM (A) before and (B) after filtration.

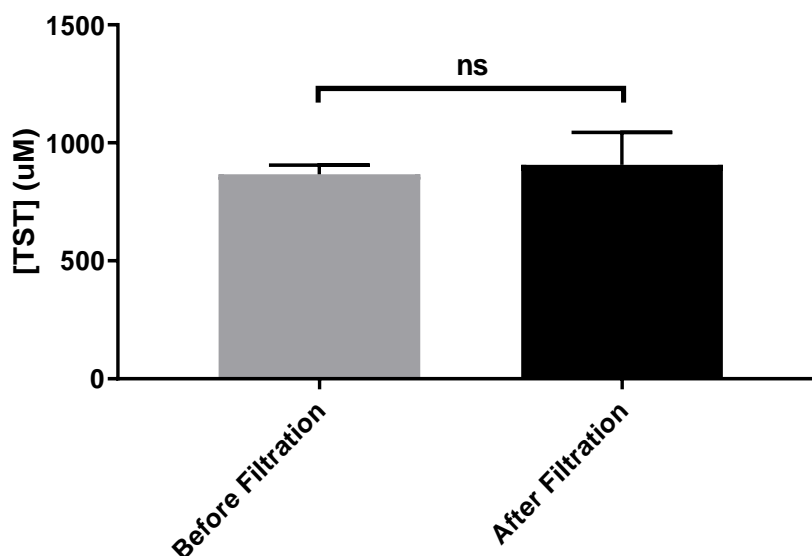


Figure 44: Drug concentration of reconstituted TST-SSM before and after filtration. Filtration was performed through a 0.22 µm PES syringe filter. Results are mean ± standard deviation (n=3). Data were analyzed by Student's t-test with $p < 0.05$ considered statistically significant. Ns = not significant.

TABLE XV: MINIMUM INHIBITORY CONCENTRATION (MIC) OF RECONSTITUTED TST-SSM BEFORE AND AFTER FILTRATION.

Samples	MIC (µM)		
	Exp 1	Exp 2	Exp 3
TST in 2% DMSO	0.2	0.2	0.2
TST-SSM Before Filtration	0.03	0.05	0.03
TST-SSM After Filtration	0.03	0.05	0.03

2. Staphylococcal pneumonia

2.1. Bacterial burden

We evaluated the therapeutic value of TST-SSM nanomedicine in the treatment of pneumonia caused by MRSA USA 300. We performed a total of 5 independent experiments summarized below (**Figure 45**). The bacterial inoculum was intended to be around 1×10^8 CFU/30 μ L, but the culture of these inoculums revealed a variation from 0.12 to 2.25×10^8 CFU/30 μ L. In all cases, we were unable to observe a significant difference in bacterial burden in the lungs of animals treated with empty micelles or TST-SSM nanomedicine. Similarly, vancomycin – the gold standard therapy for MRSA pneumonia – also failed to show therapeutic effect in experiment 4 at the tested dose of 110 mg/kg, which is the necessary dose to provide similar AUC as humans who received a therapeutic dose of 1 g twice daily (Docobo-Pérez et al. 2012). The addition of a second dose of TST-SSM (experiments 3, 4, and 5) did not improve the bacterial clearance in the lungs. In addition, in experiment 3, we administered a bacterial inoculum that was more concentrated than expected. As a result, animals became excessively sick and several died before the end of the study (24h). Interestingly, 2 out of 3 animals who received empty micelles died compared to 1 out of 3 who received TST-SSM. Although the number of animals was too low to confidently achieve any conclusions, this observation prompted us to investigate the possible role of TST-SSM in sepsis management. Severe pneumonia can lead to sepsis, septic shock, and death. The fact that TST-SSM seems to reduce mortality in animals with severe pneumonia, could be because of its anti-inflammatory role in sepsis.

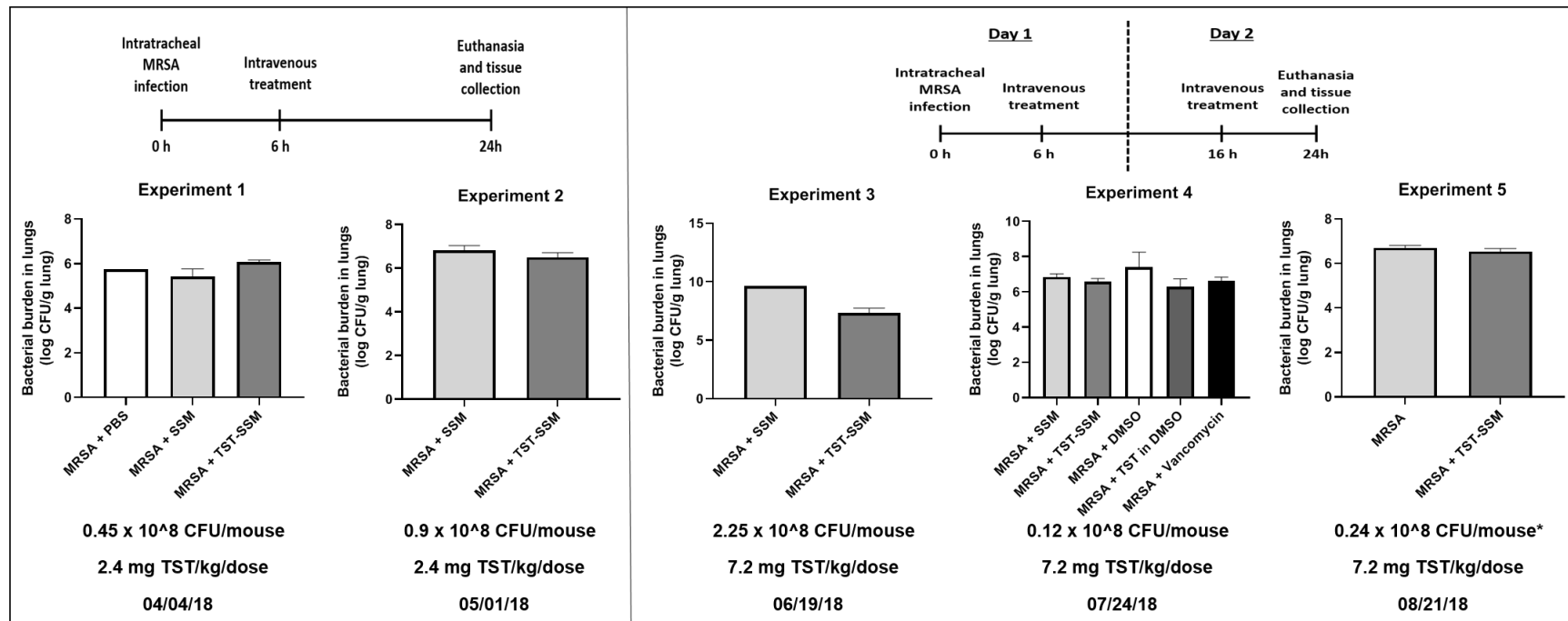


Figure 45: Bacterial burden in the lungs of mice with MRSA pneumonia.

C57BL/6 mice (1-4 per group) received MRSA USA 300 intratracheally to induce pneumonia. Treatment was administered retro-orbitally at 6h and 16h after infection and animals were euthanized at 24h. Lung homogenates were serially diluted and cultured for the bacterial count. Values are mean \pm standard deviation. Results were log-transformed and analyzed by one-tailed Mann-Whitney test. $P < 0.05$ was considered statistically significant.

2.2. Drug concentration

We measured the concentration of TST in the lung homogenate to confirm the drug delivery to the inflamed tissue (**TABLE XVI**). In experiments 1 and 2, the levels of TST in lung homogenates were undetectable. TST was only detectable after adding a second dose of nanomedicine 8h before euthanasia in experiments 3, 4, and 5. The drug concentration in experiment 3, where animals were sicker because of the higher bacterial inoculum, the drug concentration was also 3 to 5-fold higher. In experiment 4, we compared the drug concentration between nanomedicine and drug suspension. The drug accumulation in the lungs for the drug suspension was considerably higher than TST-SSM nanomedicine (over 18-fold), possibly due to the entrapment of drug particles in the pulmonary capillaries. Despite this increase in drug concentration, the bacterial burden was still the same because the drug was in a precipitated form and not available to exert its biological activity.

TABLE XVI: TST CONCENTRATION IN LUNG HOMOGENATE.

Animal #	[TST] (ng/g tissue)					
	Exp 1	Exp 2	Exp 3	Exp 4	TST in 10% DMSO	Exp 5
	TST-SSM	TST-SSM	TST-SSM	TST-SSM		TST-SSM
1	*	*	162	56.3	1559.2	60.2
2	*	*	140	48.8	544.8	5.77
3	*	*	194	85.3	1447	56.11
4	-	-	-	-	-	0
Average	-	-	165.3	63.5	1183.7	30.5
SD	-	-	27.2	19.3	556.1	32.0

*Undetectable

3. Polymicrobial sepsis

TST is a bacteriostatic agent that requires the joint effort of the host immune system to eliminate the pathogen from the body. Since TST-SSM nanomedicine did not elicit antimicrobial activity in the MRSA pneumonia animal model, we hypothesized that the anti-inflammatory activity of TST impaired with the ability of the immune system in clearing the infection. TST has been reported as a potent TLR-9 inhibitor (Lai et al. 2015), which is a known molecular target to reduce the exacerbated inflammatory response of sepsis (Yasuda et al. 2008; Hu et al. 2015; L. Liu et al. 2012). Therefore, we tested for the first time if TST-SSM could be a useful anti-sepsis nanomedicine in a mouse model of CLP-induced polymicrobial sepsis.

3.1. Survival study

We evaluated the *in-vivo* efficacy of TST-SSM nanomedicine in treating C56BL/6 mice with CLP-induced sepsis. Our purpose was to investigate if TST-SSM could be a useful anti-inflammatory/antibiotic therapy to improve the survival in polymicrobial sepsis. We observed that TST-SSM treatment significantly improved the survival of septic animals compared to empty micelles (median survival time of 44h versus 31h) (**Figure 46**). All sham-operated animals survived until the end of the study.

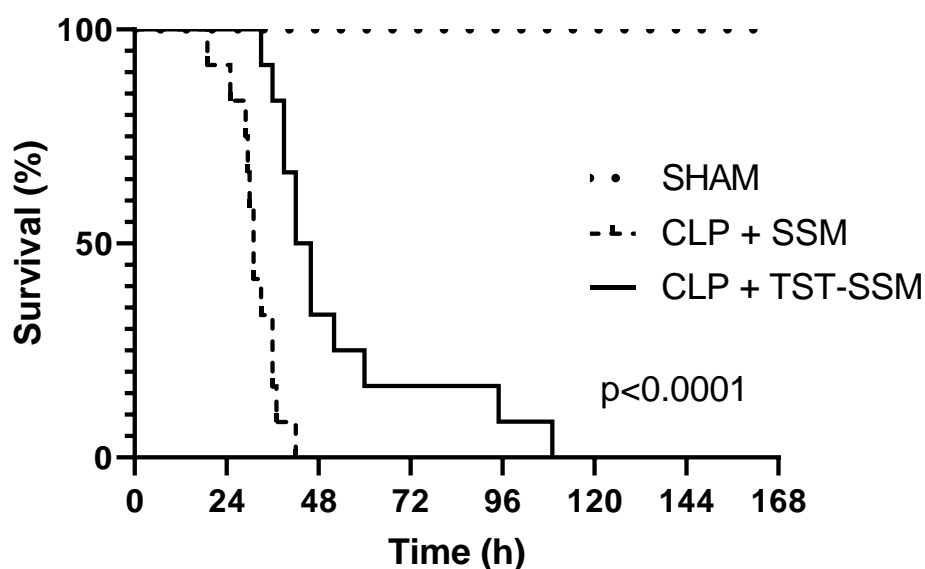


Figure 46: Survival rate of mice with CLP-induced sepsis. C57BL/6 mice (12 per group) were subjected to CLP or SHAM surgery. CLP animals were treated 6h after surgery with empty micelles (SSM) or TST nanomedicine (TST-SSM) IP and monitored for survival for 7 days. Survival rates were compared using the Log-rank (Mantel-cox) test. $P < 0.05$ was considered statistically significant.

3.2. Cytokine profile in plasma

We evaluated the cytokine profiles in plasma of sham or treated CLP animals euthanized at 24h. Our purpose was to verify the anti-inflammatory effects of TST-SSM in septic animals. We found that TST-SSM treatment significantly reduced the levels of pro-inflammatory cytokines TNF- α and IL-6, but had no effect on anti-inflammatory cytokines IL-10 ($p=0.1761$) and TGB-1 β ($p=0.4010$) (**Figure 47**).

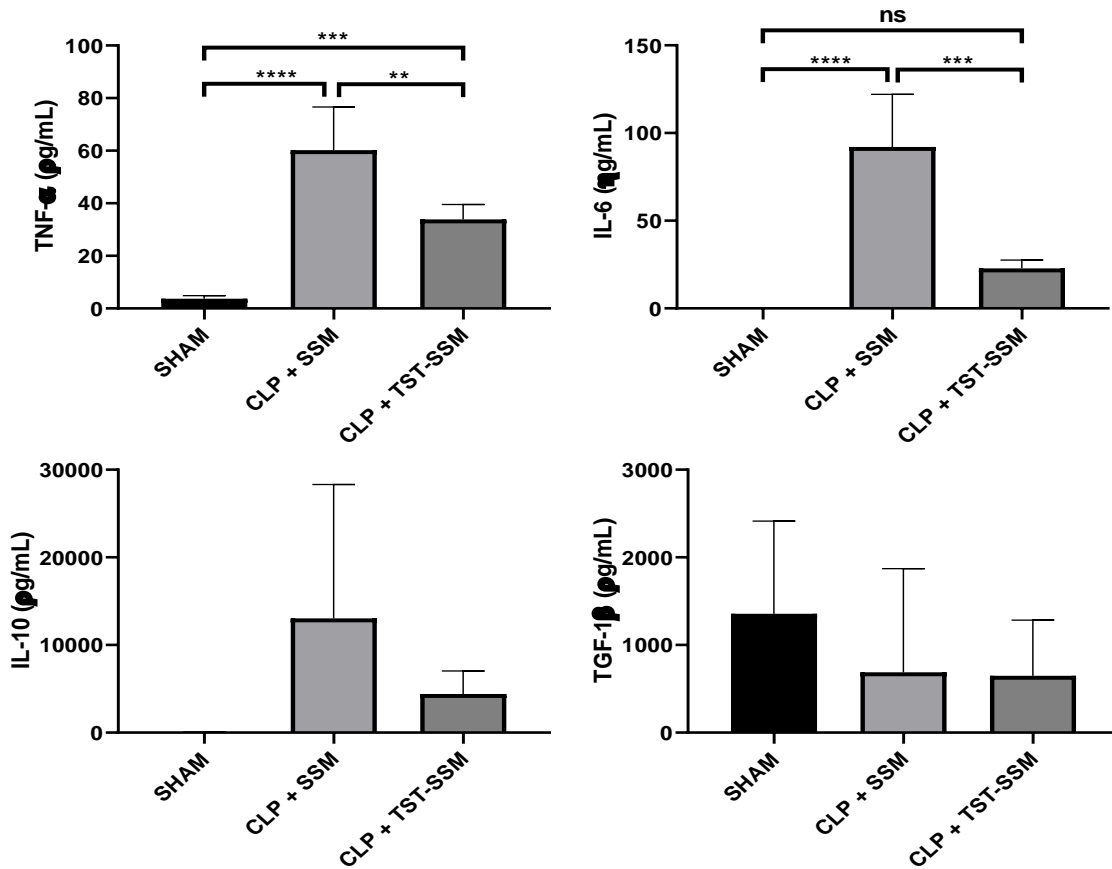


Figure 47: Cytokine profile in plasma of mice with CLP-induced sepsis. C57BL/6 mice (3-6 per group) were subjected to CLP or SHAM surgery. CLP animals received empty micelles (SSM) or TST nanomedicine (TST-SSM) IP at 6h and all animals were euthanized at 24h. Cytokines were quantified from heparinized plasma samples using ELISA kits. Values are mean \pm standard deviation. Results were analyzed by one-way ANOVA with Tukey's multiple comparisons. $P < 0.05$ was considered statistically significant. Ns = not significant, * $p < 0.05$, *** $p < 0.001$, **** $p < 0.0001$.

3.3. Nitric oxide derivatives (NOx) in plasma

We measured the levels of NOx in plasma of sham or treated CLP animals euthanized at 24h. NO is a vasodilator overproduced during sepsis which contributes to the development of hypotension and circulatory shock. Since NO is short-lived, we measured derivative products nitrite and nitrate using Griess reaction. We found septic mice treated with empty micelles had significantly higher levels of NOx in plasma compared to sham-controls (**Figure 48**). No statistical difference in plasma NOx was observed between CLP + TST-SSM treatment and sham-controls groups.

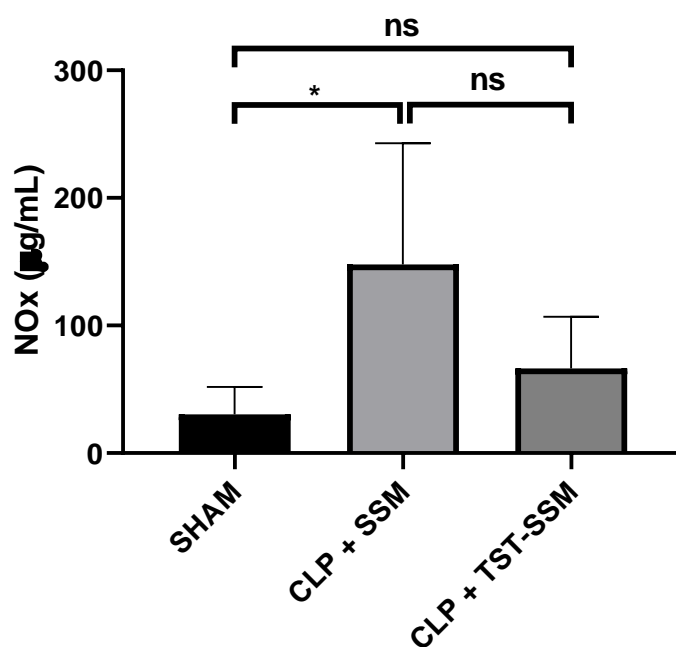


Figure 48: Total nitrite and nitrate levels in plasma and peritoneal lavage. C57BL/6 mice (4-6 per group) were subjected to CLP or SHAM surgery. CLP animals received empty micelles (SSM) or TST nanomedicine (TST-SSM) IP at 6h and all animals were euthanized at 24h. Total nitrite and nitrate levels were quantified from heparinized plasma samples using Griess reaction. Values are mean \pm standard deviation. Results were analyzed by one-way ANOVA with Tukey's multiple comparisons. * $P < 0.05$ was considered statistically significant.

3.4. **Biomarkers of hepatic and renal injury**

We compared plasma levels of hepatic and renal function biomarkers of sham or treated CLP animals euthanized at 24h. Our purpose was to define if TST-SSM treatment contributes to the improvement of organ damage commonly observed in sepsis. Hepatic marker AST was significantly higher in septic mice treated with empty micelles compared to sham-control but unaltered in animals treated with TST-SSM (**Figure 49**). ALT levels were unchanged among all groups ($p=0.9588$). We observed mixed results regarding renal biomarkers. TST-SSM significantly reduced plasma creatinine levels compared to empty micelles, but it failed to improve BUN levels.

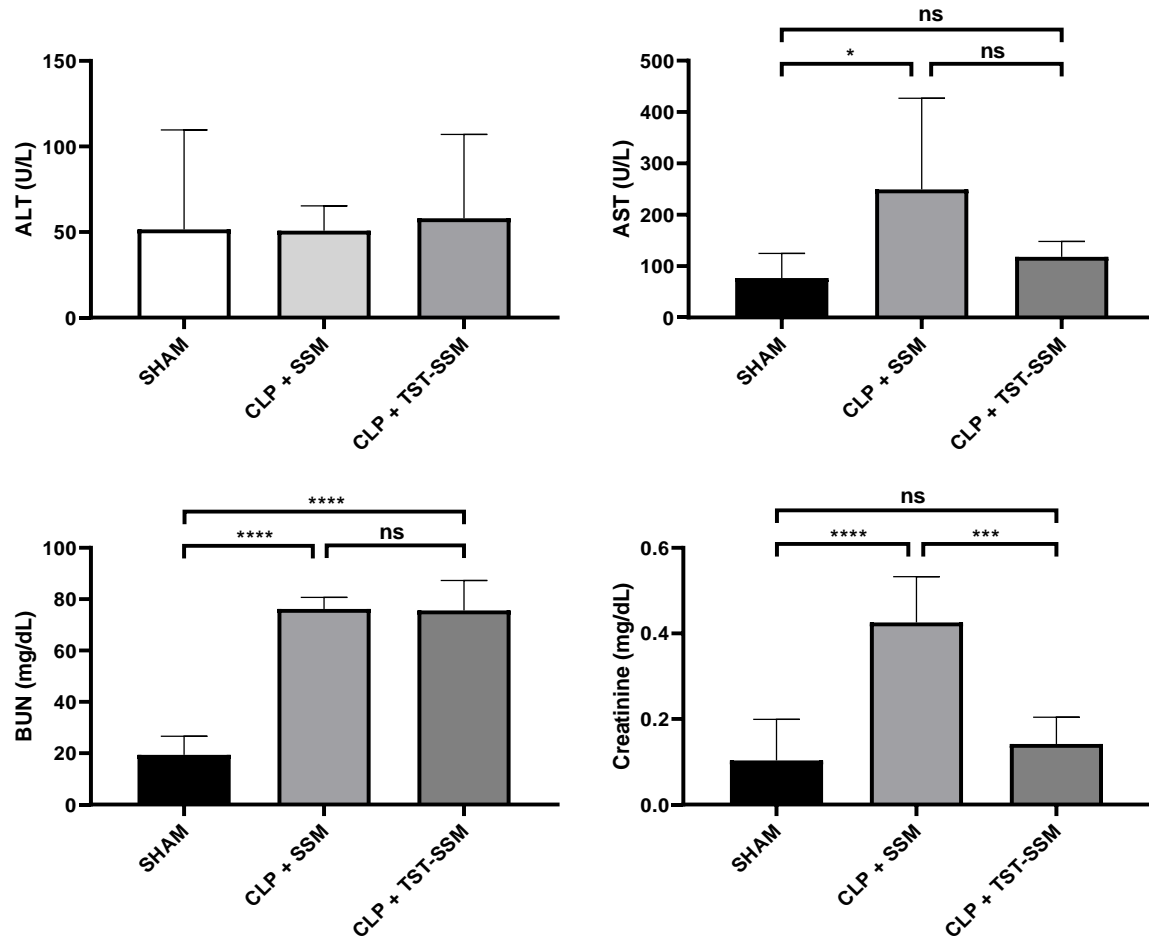


Figure 49: Biomarkers of hepatic and renal injury.

C57BL/6 mice (5-6 per group) were subjected to CLP or SHAM surgery. CLP animals received empty micelles (SSM) or TST nanomedicine (TST-SSM) IP at 6h and all animals were euthanized at 24h. Hepatic biomarkers (AST and ALT) and renal biomarkers (BUN and creatinine) were measured from heparinized plasma samples. Values are mean \pm standard deviation. Results were analyzed by one-way ANOVA with Tukey's multiple comparisons. Ns = non-significant, * $p < 0.05$, *** $p < 0.001$, **** $p < 0.0001$.

3.5. Bacterial burden

We evaluated the bacterial burden in fresh blood and peritoneal lavage of sham or treated CLP animals euthanized at 24h. Our purpose was to determine if TST-SSM treatment could reduce the microbial burden in septic mice. We observed that TST-SSM treatment significantly reduce the bacterial burden in both blood and peritoneal lavage (**Figure 50**). No bacterial growth was observed in sham-control animals.

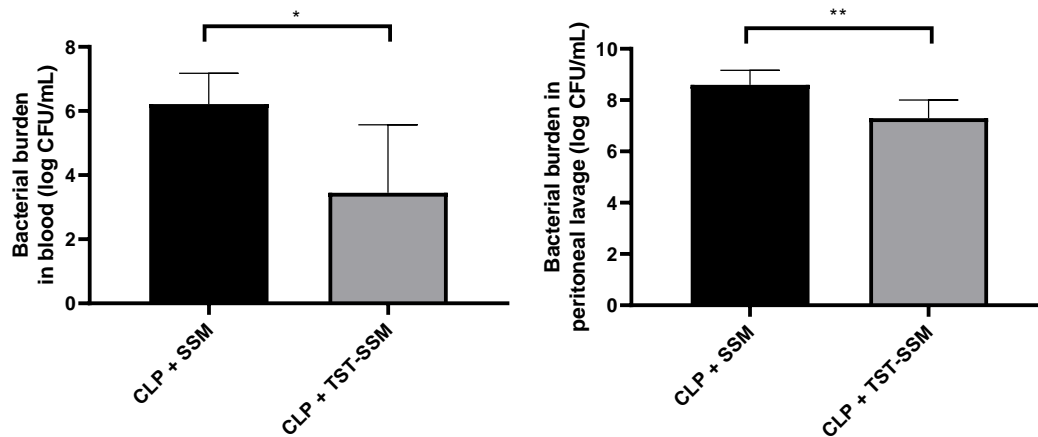


Figure 50: Bacterial burden in blood and peritoneal lavage.

C57BL/6 mice (5-6 per group) were subjected to CLP surgery and received empty micelles (SSM) or TST nanomedicine (TST-SSM) IP at 6h. All animals were euthanized at 24h and fresh blood and peritoneal lavage collected for microbiological culture. Results were log-transformed and analyzed by one-tailed Mann-Whitney test. $P < 0.05$ was considered statistically significant. * $p < 0.05$, ** $p < 0.01$.

IV. DISCUSSION

A. Development of TST-SSM nanomedicine

(Previously published as Esparza, K., Onyuksel, H. (2019) Development of co-solvent freeze-drying method for the encapsulation of water-insoluble thioestrepton in sterically stabilized micelles, *Int. J. Pharm.* 556, 21-29).

TST is a promising natural drug molecule discovered in 1955 with potent antibiotic activity against Gram-positive that never made to the clinics because of its low aqueous solubility and delivery issues. The primary purpose of this study was to formulate TST in a safe and efficient delivery system to improve the drug aqueous solubility, stability and enable its therapeutic application. We selected SSM as an ideal drug delivery system because of its safety, simple composition, efficient solubilization of hydrophobic drugs, reproducible preparation, and ability to passively target drugs to inflamed tissues (Lim, Banerjee, and Onyuksel 2012). SSM is also known to increase the biological half-life of drugs by protecting drugs from degradation and evading clearance by the reticuloendothelial system or renal filtration (Sethi et al. 2013). Given the benefits of SSM, we selected SSM as an ideal delivery system for TST.

1. Drug encapsulation by the thin-film hydration method

We determined that the solubility of TST is 3.5 μM in PBS (**TABLE VII**). This result is in close agreement with Bausch et al. (2005) who reported a TST solubility of 5 μM in a media containing 5% of DMSO in 10mM MOPS buffer (Bausch, Poliakova, and Draper 2005). The low water solubility is the main barrier to the clinical development of TST since the drug tends to aggregate upon administration. To overcome this problem,

we encapsulated the drug in SSM nanocarrier to improve the drug solubilization in aqueous media.

The thin-film hydration is a convenient method that our laboratory has been using to encapsulate hydrophobic molecules in SSM at a bench-scale (O. M. Koo, Rubinstein, and Onyuksel 2005; Gülçür et al. 2013; Krishnadas, Rubinstein, and Onyuksel 2003). Using this method, we found that a molar ratio of 17.2 (phospholipid: drug) yielded consistent drug loading of 5 TST molecules per micelle (diameter ~15 nm) without the presence of larger drug particles (**Figure 20**). Our results were not in agreement with another study which reported much higher encapsulation efficiency for TST-SSM at a molar ratio of 3:1 (phospholipid: drug) (M. Wang and Gartel 2011). However, according to our calculations, this molar ratio would result in a drug loading of 30 TST molecules per micelle. Given the large molecular size of TST (1664.89 Da) and its high hydrophobicity, it is unlikely that such a high load of TST would be dissolved in a molecular form in the interior of SSM. In fact, based on the particle size of Gartel's nanomedicine of 100 nm in diameter (M. Wang and Gartel 2011), we believe that those nanoparticles are in fact large drug aggregates coated with phospholipid monomers – also known as sterically stabilized particle (SSP) (Cesur et al. 2009; Gülçür et al. 2013). Despite the high drug loading of SSP, such delivery system is not suitable for further development because of its lack of reproducibility and the need for drug dissolution for activity. On the other hand, the TST-SSM nanomedicine reported in this thesis is very likely to contain the encapsulated drug in a molecular form based on the relatively lower drug load (5 drug molecules per micelle), which is readily available to exert activity *in vivo* upon release. Although TST-SSM has great potential for clinical use, its production

by the thin-film hydration method posed a significant barrier for the translation of this nanomedicine to the clinics.

The thin-film hydration method exhibits several limitations for the further development of micellar nanomedicines. Since this method requires a large surface area to form the thin-film, it cannot be scaled-up in its original version due to size restrictions of round bottom flasks and rotary evaporator capacity. In addition, the generation of uniform ultrasonic energy to large volume materials is technically challenging and, if not well controlled, the excessive heat can cause drug and phospholipid degradation. This technique also requires the use of volatile toxic organic solvents such as methanol or chloroform, which may pose toxicological concerns depending on the residual levels present in the final product (“Q3C - Tables and List Guidance for Industry” 2017). Lastly, the resulting product still requires further sterilization and freeze-drying for long-term storage, therefore increasing costs and production time of SSM nanomedicines. These limitations prompted us to investigate the co-solvent freeze-drying as an alternative scalable method to encapsulate TST in SSM.

2. Drug encapsulation by the co-solvent freeze-drying method

The use of organic co-solvents in freeze-drying, particularly TBA, is a known practice in the pharmaceutical industry to improve the solubility and stability of drug molecules in aqueous solutions before freeze-drying (Rey and May 2010). For example, Caverject® (alprostadil injection) is manufactured with 20% of TBA: water (v/v) to reduce drug hydrolysis in solution before freeze-drying (Teagarden and Baker 2002). However, in 2004, Fournier and colleagues reported for the first time the use of TBA to

specifically aid the drug encapsulation in polymeric micelles. According to the proposed method, TBA infiltrated in the core of micelles and facilitated the drug incorporation due to micelle swelling. The freeze-drying process was then used to purify the preparation from TBA and allow reconstitution with a biocompatible diluent (dextrose 5% or 0.9% saline) (E. Fournier et al. 2004). We applied this co-solvent method to encapsulate TST in SSM with the same maximum loading ratio as obtained by the thin-film hydration, but additional particles besides micelles were observed in the formulation (**Figure 21**). This result prompted us to investigate the behavior of DSPE-PEG₂₀₀₀ micelles in TBA: water co-solvent and identify possible ways to adapt this method to our needs.

We observed that contrary to the swelling observed with PVP-b-PDLLA micelles (**Figure 8**) (E. Fournier et al. 2004), DSPE-PEG₂₀₀₀ micelles were disrupted in the presence of increasing amounts of TBA (**Figure 22** and **Figure 23**). Reasons for such behavior are unclear, but differences in monomer structures (single hydrophobic tail in PVP-b-PDLLA versus double acyl chains in DSPE-PEG₂₀₀₀) or hydrophobic and hydrophilic balances could explain the varying susceptibility to micellar assembly and disruption with TBA. We observed particles measuring 7.6 nm in diameter at 90% of TBA (v/v), which could represent inversed micelles with PEG moieties facing the center and hydrophobic acyl chains pointing towards the TBA-rich media. The use of such a solvent system for freeze-drying could pose technical challenges for the drying phases due to the lower accessibility of water molecules trapped in the core. Based on this result, we developed a new model for TST encapsulation in DSPE-PEG₂₀₀₀ micelles that follows similar basic principles as the thin-film method.

In our co-solvent freeze-drying encapsulation method (**Figure 9**), we proposed that the main role of TBA: water co-solvent system was to solubilize all ingredients prior to freeze-drying without the formation of micelles. The freeze-drying process would remove the solvent from the system and generate a lyophilized cake with large surface area and ingredients evenly dispersed throughout the cake similar to the thin-film. The reconstitution of the cake with aqueous media should promote micelle self-assembly with concurrent drug encapsulation driven by hydrophobic forces. We optimized this co-solvent freeze-drying method to achieve similar maximum drug loading as the thin-film hydration.

The increase of TBA proportion in the co-solvent freeze-drying from 50% to 75% did not affect the loading efficiency (**Figure 24**) or reconstitution time (**Figure 30**) of TST-SSM but prevented cake collapse and slightly increased cake porosity (**Figure 30**). These results confirmed that the presence of drug particles in the solution prior to freeze-drying was not responsible for the poor drug loading, otherwise, the increase in hydrophobicity of the solution would have improved drug dissolution and loading. The improvement of cake porosity can be attributed to the formation of larger solvent crystals during freezing (Kasraian and DeLuca 1995). TBA: water mixtures form larger solvent crystal sizes at 70% w/w (Kasraian and DeLuca 1995). When large solvent crystals are removed during freeze-drying, they leave large spaces behind, facilitating the removal of solvent from deeper levels of the cake and improving the cake porosity (Rey and May 2010). Samples with higher proportions of TBA are also expected to sublime at faster rates due to its high vapor pressure. Rapid sublimation improves cake stability because the solvent can be removed before samples reach collapse

temperature (Ni et al. 2001). The increase in TBA proportion also increases the system's viscosity and reduces solute mobility during cake formation (Ni et al. 2001). Since the proportion of TBA did not improve drug loading, we decided to explore the role of reconstitution.

A noticed difference between the thin-film hydration and the co-solvent freeze-drying employed in this study was the method of cake reconstitution. In the first case, the thin film was reconstituted with vortexing and sonication (**Figure 5**), while in the second method, the lyophilized cake was reconstituted by hand swirling (**Figure 9**), which is the appropriate method in the clinical setting. Although all reconstitution techniques can be used for both encapsulation methods, the additional energy provided by sonication and vortexing accelerates the release of solutes from the exposed surface of the dried matrix into the solvent. The faster dissolution of thin-film or lyophilized cake promotes an efficient drug loading because hydrophobic molecules are rapidly incorporated in the micelle core before they have the change to find each other and aggregate. However, we found that regardless of the reconstitution method for the co-solvent freeze-drying technique, only one TST molecule could be encapsulated in each SSM without forming larger particles. Samples reconstituted by sonication were considerably less turbid than other methods (**Figure 25**). However, this phenomenon was likely due to the size reduction of drug precipitates rather than avoidance of drug aggregation. Although the input of mechanical energy accelerates the dissolution of solute molecules into the solvent, in the case of co-solvent freeze-drying method, the additional energy was not enough to promote improvement of the drug loading in SSM. This observation led us to investigate other ways to improve the cake reconstitution.

Another critical difference between the thin-film hydration and co-solvent freeze-drying methods is the accessibility of the solvent to the solutes during reconstitution. Although both thin-film and lyophilized cakes exhibit large surface areas, lyophilized cakes require an additional step of solvent penetration to allow contact between the solvent and the cake's internal surface area. This penetration is not required in the thin-film as the most surface area is exposed to the outer environment and readily available to interact with the solvent. The penetration of solvents into the cake can be affected by the cake porosity and surface polarity. Larger interconnected channels allow faster permeation of fluids through lyophilized cakes, particularly products prone to rapid increase of viscosity (Beech et al. 2015). Since the viscosity of DSPE-PEG₂₀₀₀ solutions increases proportionally with the phospholipid concentration (Vukovic et al. 2011), it is possible that the increase in porosity could improve the water penetration and cake reconstitution. In addition, the surface polarity might interfere with the penetration of water into the cake pores. A predominantly hydrophobic surface might repel water molecules and hinder the wetting of the cake during reconstitution. Since most of the cake's components in our case are hydrophobic and fully exposed to the surface, it is not surprising that those cakes were difficult to reconstitute and resulted in poor drug loading. To overcome the water penetration problem, we incorporated PBS salts before freeze-drying to improve the cake's structure and affinity to water. Traditionally, our laboratory has used PBS (pKa 2.1, 7.2, and 12.3) as an SSM vehicle because it is a common buffer system used in several FDA-approved injectable pharmaceuticals with documented safety and ability to maintain solution pH at physiological levels (Akers 2016). However, for freeze-dried products, PBS can induce drastic pH shifts during

freezing due to selective crystallization of the dibasic salt, which can be problematic for pH-sensitive molecules such as proteins, but not TST (Thorat and Suryanarayanan 2019; Pikal-Cleland and Carpenter 2001). The addition of PBS salts before freeze-drying notably improved the reconstitution time (**Figure 30**), cake porosity (**Figure 30**), and drug loading (**Figure 27**), allowing us to produce TST-SSM with the maximum loading of 5 TST molecules per SSM. This result could be attributed to the improvement of overall cake hydrophilicity and the cake affinity with the reconstituting vehicle (water) which serves as driving force for the water penetration into the porous cake. In addition, colligative properties of PBS likely contributed to the increase the size of solvent crystals during the freezing process, resulting in favorable changes in the cake morphology (**Figure 30**). When salts are placed in aqueous media, they dissociate in ions and interact very strongly with water molecules, blocking water molecules from coming together to form ice crystals. As a result, the freezing point of the solution is decreased compared to pure water, slowing the freezing process of the co-solvent system. A slow freezing process is known to generate larger solvent crystal sizes due to the increased mobility of water molecules compared to a faster freezing process. When those large solvent crystals are removed by sublimation, they leave behind equally large spaces which contribute to the increased porosity of the lyophilized cake (Rey and May 2010). However, in the presence of salts, the solubility of DSPE-PEG₂₀₀₀ was impaired at 75% TBA, resulting in phospholipid precipitation (**Figure 26**). This phenomenon is likely due to the sequestration of water molecules by PBS salts which lowered the availability of water molecules to solubilize DSPE-PEG₂₀₀₀, leading to phospholipid aggregation. Therefore, the co-solvent composition must be adjusted to maintain all

ingredients in solution, which in our case was 50% TBA: 2X PBS for a formulation containing 277.8 μM of TST and 5 mM of DSPE-PEG₂₀₀₀ (loading of 5 drug molecules per micelle).

Previous studies from our lab have shown that DSPE-PEG₂₀₀₀ formulations can be freeze-dried at phospholipid concentrations above 5 mM without any lyo- or cryoprotectants (Lim, Rubinstein, and Önyüksel 2008). However, DSPE-PEG₂₀₀₀ concentrations between 10-15 mM are preferred as they exhibit a more elegant cake appearance without significant intermicellar interactions (Lim, Rubinstein, and Önyüksel 2008). Therefore, we doubled and tripled ingredient amounts to produce TST-SSM with higher strength. We observed that the increase of ingredients in the cake enhanced the reconstitution time and resulted in drug aggregation (**Figure 28** and **Figure 30**). This phenomenon could be due to the increase in cake density which reduced the cake porosity and enhanced the viscosity of the solution. The change in cake porosity with increase phospholipid concentration was not noticeable by SEM (**Figure 30**), therefore more robust techniques such as mercury intrusion porosimeter would be appropriate to quantify changes in cake porosity. To improve the strength of the formulation, we produced a fluffy cake containing 5mM of DSPE-PEG₂₀₀₀ (volume 6 mL) and reconstituted it with one third of the fill volume (2 mL). As a result, we obtained our optimized TST-SSM nanomedicine devoid of any larger particles with 238-fold total increase of aqueous solubility (**Figure 29**). Interestingly, as we increased the fill volume to 12 mL in the same vial size (20 mL), the formulation became harder to reconstitute with one third of the fill volume and drug aggregation was observed (**Figure 29**). This

phenomenon was likely caused by the limited space inside the vial which interfered with the sample agitation required for uniform cake reconstitution.

The optimized TST-SSM formulation designed to be reconstituted in one third of the fill volume for a final concentration 833.4 μM TST and 15 mM DSPE-PEG₂₀₀₀ exhibited less than 0.05% (w/w) residual TBA, which is below reported by the commercially available product Caverject (1.3%) and therefore believed to be safe (Teagarden and Baker 2002). Also, the osmolality of our optimized formulation was 312 mOsm/kg which is close to isotonic levels desired for safe intravenous administration (W. Wang 2015).

3. Stability of TST-SSM nanomedicine

Formulation stability is an important parameter to ensure that medicines maintain their physical, chemical, and therapeutic properties during the time of processing, transport, storage, and usage by the patient. Optimized TST-SSM formulation was prepared by the co-solvent freeze-drying with 277.8 μM TST and 5 mM DSPE-PEG₂₀₀₀ (fill volume 6 mL). After storage at different temperature and humidity conditions, samples were reconstituted in deionized water with one-third of the fill volume (2 mL) to obtain a final concentrated product with 833.4 μM TST and 15 mM DSPE-PEG₂₀₀₀. We assessed the short-term stability of reconstituted nanomedicine and the long-term stability of the freeze-dried TST-SSM nanomedicine product.

The short-term stability of the reconstituted TST-SSM nanomedicine was evaluated at different temperature conditions to establish the period that the formulation remains stable for use after reconstitution. We determined that TST-SSM remains biologically active for a day after reconstitution when stored at 25°C, and at least 7 days

at 4°C. The loss of antimicrobial activity (**TABLE XI**) was not accompanied by changes in particle size (**Figure 31** and **Figure 32**) or drug concentration (**Figure 33**). In contrast, previous studies in our laboratory have shown that camptothecin encapsulated in SSM was stable for 7 days when stored at 25°C (O. M. Koo, Rubinstein, and Onyuksel 2005). The difference in stability between TST-SSM and Camptothecin-SSM could be attributed to the antimicrobial testing used for TST-SSM. The microdilution assay requires sample incubation at 37°C for 24 hours to allow bacterial growth. This additional thermal stress likely affected the drug stability of TST-SSM during the assay resulting in loss of activity after sample characterization. Storage at 25°C made TST-SSM more susceptible to destabilization than samples stored at 4°C due to the higher molecular mobility prior to the assay.

The long-term shelf stability of TST-SSM lyophilized cakes was studied to establish the maximum period that the nanomedicine can be stored without significant loss of their physicochemical and biological properties. This evaluation was based on storage conditions established on the Q1A(R2), a guideline developed by the International Council for Harmonization of Technical Requirements for Pharmaceuticals for Human Use (ICH) ("Stability Testing of New Drug Substances and Products Q1A(R2)" 2003). We observed that freeze-dried TST-SSM remained stable for up to 7 months when stored at 5°C or 30°C/ 65% RH. Freeze-dried formulations kept at 40°C/ 75% RH started showing signs of degradation at 1 month with the presence of large particles (**Figure 35** and **Figure 36**), decreased the concentration of the drug (**Figure 37**), and appearance of degradation products in the HPLC chromatogram (**Figure 38**). However, the drug loss in the formulation was not enough to change the MIC result, and

therefore, the product was still considered biologically active (**TABLE XIII**). MIC values are discrete data because antibiotic drugs are tested at prefixed concentrations rather than continuous values. In our case, TST-SSM was plated at 2-fold dilutions, but the drug degradation observed at 40°C/ 75% RH was only 16%, which was not enough to alter the MIC to the next concentration level. Finally, we observed that although vial samples were flushed with Argon gas and sealed with a rubber stopper, all freeze-dried cakes gained humidity during storage (final humidity <1.2%) (**TABLE XII**). The rise in moisture on the lyophilized cake during storage can lead to formulation destabilization and degradation (Rey and May 2010). There are two ways that moisture could have entered the vial: (1) leaks on the interface between glass vial and stopper or (2) external moisture permeation through the stopper (Donovan et al. 2007). Therefore, to address these issues, we could improve closure integrity by identifying a combination of glass vial, rubber stopper, and aluminum crimp cap with tighter seal or selecting a stopper with lower moisture vapor transmission rate (Donovan et al. 2007).

B. In vitro activity of TST-SSM nanomedicine

TST possesses potent antimicrobial activity against Gram-positive bacteria, but low water insolubility prevents its clinical application (Just-Baringo, Albericio, and Álvarez 2014). To overcome this challenge, we encapsulated TST in SSM and tested the antimicrobial activity *in vitro* by the microdilution assay. We observed 2 to 8-fold improvement of bacterial activity compared to the free drug dissolved in 4% DMSO among various organisms, including MRSA USA 300 (**TABLE XIV**). This was the first time that SSM has been successfully applied for antibiotic molecules without losing activity *in vitro*. Previous studies in our laboratory have reported the loss of *in vitro*

activity of amphiphilic antimicrobials after encapsulation in SSM possibility due to the hindrance of essential drug charges (Brandenburg et al. 2012; Williams et al. 2012). Amphiphilic cationic peptides usually exert their antimicrobial effect by interacting electrostatically with the negative bacterial cell components (LPS in Gram-negative and teichoic acids in Gram-positive bacteria) and disrupting the cell membrane (Malmsten 2014). Since DSPE-PEG₂₀₀₀ phospholipid contains a positively charged phosphate head, cationic peptides might strongly bind to SSM and prevent drug activity on bacterial cells.

We investigated possible reasons for the improved drug activity of TST-SSM nanomedicine compared to the free drug. We found that SSM does not enhance the drug accumulation in bacterial cells (**Figure 40**), but instead it protects the drug from degradation at the conditions of the antimicrobial testing (37°C for 24h) (**Figure 41**). In this drug stability test (**Figure 41**), cell lysate appeared to protect drug degradation better than bacteria supernatant or fresh media. This behavior could be attributed to the reduced concentration of proteins and other components in the cell lysate compared to the other two media. The presence of proteins and other components in the media can predispose the drug to degradation as reactive species originated from their own degradation initiate a chain of degradation reactions. The absence of water in the core of micelles can prevent the hydrolysis of loaded drugs, thus prolonging its chemical stability (O. M. Koo, Rubinstein, and Onyuksel 2005).

C. *In vivo* efficacy of TST-SSM nanomedicine

1. Filtration of reconstituted TST-SSM nanomedicine for animal studies

Parenteral preparations must be sterile to prevent the introduction of microbes in the body upon drug administration. Heat-sensitive liquid formulations such as TST-SSM nanomedicine require a combination of aseptic filtration and aseptic processing to ensure the sterility of the final product (Parag Kolhe, Shah, and Rathore 2013). In the case of the co-solvent freeze-drying encapsulation method, sterilizing filtration could take place after all ingredients are homogenously combined in the co-solvent system in a mixing tank. A stream of this bulk solution can be forced through a 0.22 μm bacteria-retentive membrane filter in-line before being directed for filling into glass vials. The entire process after filtration must be under aseptic conditions to prevent microbial contamination, including the filling of vials, freeze-drying, and vial closure steps. The type of filter to be used for filtration needs to be decided according to the affinity between solvent, solutes, and filter material. This type of sterilization process has already been applied for some marketed products that employ TBA: water co-solvent such as alprostadil (Caverject[®]), bendamustine (Treanda[®]), and bortezomib (Velcade[®]) (Teagarden, Petre, and Gold 1998; Brittain and Franklin 2013; Puppala et al. 2016). Since our manifold-style freeze-dryer is not suitable for aseptic processing, we were unable to implement this sterilization process in the laboratory. Instead, we filtered the reconstituted TST-SSM formulation through a 0.22 μm PES membrane to sterilize the formulation intended for animal studies. We observed no changes in particle size (**Figure 42** and **Figure 43**), drug concentration (**Figure 44**), or drug antimicrobial activity (**TABLE XV**) before or after sterilizing filtration. Previous studies from our laboratory had

shown that filtration through a 0.22 μm tortuous pores polyvinylidene fluoride membranes (PVDF) (Durapore®) or straight pores polycarbonate membrane (Nucleopore®) did not affect the properties of another SSM nanomedicine (GLP1-SSM) (Lim et al. 2011). According to the manufacturer, PES filters exhibit faster flow, while PVDF presents the lowest protein binding. Nevertheless, our results indicated that 0.22 μm PES membrane is also an effective sterilizing filter for SSM nanomedicines.

2. Staphylococcal pneumonia

We evaluated the antibiotic activity of TST-SSM in a mouse model of staphylococcal pneumonia in 5 independent experiments. Lung infection was induced by intratracheal inoculation of approximately 1×10^8 CFU of MRSA USA300 and treatment was administered by retro-orbital injection at 6h (single dose) or repeated at 16h (multiple doses) before euthanasia at 24h. In all cases, we were unable to observe a significant reduction of bacterial burden in the lungs after treatment with TST-SSM (**Figure 45**). In addition, TST levels were undetectable in lungs of animals treated with a single nanomedicine dose but were quantifiable in animals treated with a second dose of TST-SSM (**TABLE XVI**). This indicated that although TST was present in lungs, drug levels were not sufficiently high to exert antimicrobial effect (**Figure 45**). In addition, in experiment 4 (**Figure 45**) we administered particles of TST in 10% DMSO and detected drug levels in lungs about 18-fold higher than mice treated with TST-SSM (**TABLE XVI**). This enhanced lung accumulation was likely due to the entrapment of large particles in fine pulmonary capillaries. Despite that, TST did not exhibit antibiotic activity *in vivo* because drug molecules were in an aggregated form. The drug is only available to interact with the molecular target and exert biological activity once it dissolves in the

surrounding aqueous environment, which in the case of highly hydrophobic compounds, it can be a very slow process. However, we made an interesting observation from an experimental error that changed our perspective on the role of TST-SSM. In experiment 3, we accidentally prepared an inoculum with bacterial concentration 2-fold higher than expected. As a result, animals became excessive ill and started dying before the end of the experiment (24h). Curiously, 1 out of 3 animals who received TST-SSM died compared to 2 out of 3 animals who received empty micelles. Although the number of animals in the experiment was too low to reach any valid conclusion, the results indicated that TST-SSM could prevent mortality in severe infections, which is often associated with sepsis.

TST is reported to inhibit TLR-9 activation *in vitro* and reduce signs of psoriasis-like inflammation *in vivo* (Lai et al. 2015). On the other hand, a study using *tlr9^{-/-}* knockout animals with MRSA USA300 pneumonia demonstrated reduced bacterial clearance and increased pulmonary inflammation and injury as a result of TLR9 deficiency (van der Meer and Achouiti 2016). Therefore, it is possible that TST-SSM nanomedicine inhibits TLR9 activation *in vivo* and reduces the ability of infected animals in clearing the bacteria using their immune system. Moreover, to the best of our knowledge, the only study testing the antibiotic activity of TST *in vivo* used mortality as an outcome of treatment instead of bacterial burden in animals with peritoneal infection (Steinberg, Jambor, and Suydam 1955). We believed that TST had prevented mortality by suppressing the excessive inflammatory response caused by sepsis, rather than just directly targeting the bacteria.

3. Polymicrobial sepsis

TST is a potent TLR9 inhibitor able to reduce excessive skin inflammation in a psoriasis mouse model (Lai et al. 2015). On the other hand, TLR9 inhibition by gene deletion (Hu et al. 2015; Yasuda et al. 2008), small interfering RNA (L. Liu et al. 2012), and chemical inhibitor (chloroquine) (Yasuda et al. 2008) has shown to reduce the excessive, inflammation and mortality of CLP-induced sepsis, a clinically relevant model of polymicrobial sepsis. Despite this connection, to the best of our knowledge, the anti-sepsis property of TST has never been reported in the literature until now. We found that a single IP dose of TST-SSM nanomedicine (20 mg/kg) administered 6h after CLP surgery significantly improved the median survival of septic mice from 31h to 44h, but all septic animals were deceased by the end of the experiment (**Figure 46**). Other studies have demonstrated more pronounced effects of TLR-9 inhibition on sepsis survival. Hu and colleagues observed survival rate after CLP surgery of 70% of TLR9 knockout Balb/c mice compared to 20% in wild type mice (Hu et al. 2015). However, in this case the gene knockout was associated with a complete loss of TLR9 receptor and a more prominent protective response. Also, the authors performed CLP surgery with 2 punctures instead of 3, which likely caused a less severe septic condition. Liu and colleagues reported similar results as Hu et al. after silencing TLR-9 expression in C57Bl/6 mice with TLR9 siRNA plasmid obtaining ~80% survival in treatment group versus ~20% in control (L. Liu et al. 2012). In this study, however, authors punctured the cecum twice and administered broad-spectrum antibiotics as a supportive measure, which likely reduced the severity of the disease and enhanced the recovery. Yasuda and colleagues observed survival of 24% versus 55% of elderly C57Bl/6 mice (32-40

weeks old, which are more susceptible to sepsis) treated with vehicle-only or chloroquine 6h after the CLP surgery (Yasuda et al. 2008). In this case, CLP surgery was performed with 2 punctures and animals received broad-spectrum antibiotics as supportive measure which likely contributed to the outcome. A knockout TLR9 study performed by the same group revealed similar results as Hu et al., with 23% survival in wild-type mice after CLP surgery versus 70% in knockout mice (Hu et al. 2015). It is possible that if we increase the dose of TST-SSM in our study or the frequency of injection, we can promote the complete survival of treated animals. Also, the combination of TST-SSM nanomedicine with conventional broad-antibiotics can provide a synergistic therapeutic approach to improve the overall survival and recovery from sepsis.

The improvement of median survival time after treatment with TST-SSM nanomedicine in CLP-induced sepsis was accompanied by reduced systemic pro-inflammatory markers IL-6 and TNF- α (**Figure 47**), reduced vasodilatory nitric oxide derivatives in plasma (**Figure 48**), improved biomarkers for renal and hepatic functions (**Figure 49**), and reduction of bacterial load in the blood and peritoneal lavage (**Figure 50**). This is a significant benefit of TST-SSM nanomedicine which if translated to the clinical setting that can prevent rapid death from septic shock and improve the chances of recovery from sepsis. It is unclear the contribution of the direct antibiotic activity of TST-SSM in ameliorating sepsis, but future experiments using alternative models of sepsis (LPS or *Escherichia coli* infection) can help us to understand the exact role of TST-SSM in sepsis in the absence of Gram-positive infection.

4. Other activities

Incidentally, during the development of this project, we collaborated with Dr. Joanna Burdette to evaluate the role of TST in the treatment of high grade serous ovarian cancer *in vivo* (Hardy et al. 2019). TST is reported to reduce the expression of transcription factor FOXM1 which plays a role in cell proliferation and tumorigenesis (Kwok et al. 2008; M. Wang and Gartel 2011). Dr. Burdette's group identified that TST also destabilized the oncogenic transcription factor PAX8 and could potentially attenuate cancer progression and aggressiveness (Hardy et al. 2019). However, when TST was dissolved in 30% DMSO and administered intraperitoneally (IP) to tumor-bearing mice, animals suffered severe weight loss and had to be euthanized for humane reasons (Hardy et al. 2019). Postmortem examination revealed intense drug precipitation in the peritoneal cavity of TST-treated mice, which likely caused severe toxicity. To overcome these delivery and toxicity issues, we provided the optimized TST-SSM nanomedicine to Burdette's group. After IP administration of TST-SSM nanomedicine, we observed a significant amelioration in tumor burden compared to empty micelle treatment and reduced tissue levels of FOXM1 and PAX8 proteins **(Figure 51)** (Hardy et al. 2019). This study further illustrated the practicality of SSM as a safe and effective delivery system for hydrophobic drugs like TST.

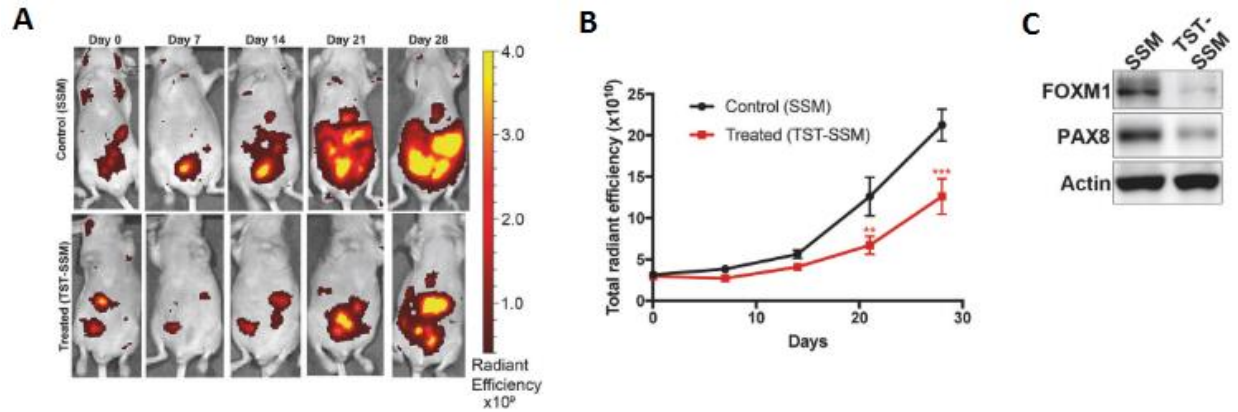


Figure 51: Activity of TST-SSM nanomedicine against high grade serous ovarian cancer mouse model.

(A) *In vivo* imaging system and (B) quantification of total radiant efficiency of athymic nude mice with OVCAR8^{RFP} tumor and treated three times per week for 4 weeks with SSM (control) or TST-SSM (20 mg/kg/dose). (C) Immunoblot for FOXM1 and PAX8 protein levels in tumor cells retrieved from SSM or TST-SSM treated animals.

Adapted by permission from the Copyright Clearance Center: Springer Nature, Oncogene (Hardy et al. 2019), Copyright 2019.

V. CONCLUSIONS

1. We successfully developed TST-SSM injectable nanomedicine to overcome TST delivery issues and enabled its therapeutic use *in vivo*. The apparent aqueous solubility of TST in our final optimized formulation was improved 238-fold with a drug loading of 5 drug molecules per micelle (833.4 μM of TST and 15mM of DSPE-PEG₂₀₀₀). The nanomedicine preparation was reproducible with a particle size of approximately 13 nm. Drug encapsulation in SSM provides various benefits over other delivery systems that make it ideal for further clinical development. SSM is a simple, reproducible nanocarrier composed of a single phospholipid ingredient (DSPE-PEG₂₀₀₀) with documented safety since it is present in the FDA-approved drug Doxil®. In addition, SSM enhances solubility and stability of drugs by accommodating them in a hydrophobic core environment with a water-compatible PEGylated surface. This protective outer layer is known to prevent particle opsonization and elimination by the reticuloendothelial system, thus enhancing the drug's biological half-life. Finally, due to its ideal nanosize, SSM targets loaded drugs to tissues with enhanced vascular permeability which is characteristic of cancer and inflamed sites. This so-called passive targeting increases drug availability at the site of action for better drug efficacy while reducing toxic effects in healthy tissues.
2. We developed a novel scalable method to encapsulate TST in DSPE-PEG₂₀₀₀ micelles using the co-solvent freeze-drying technique. In this method, both hydrophobic drug and phospholipid are combined in TBA: PBS co-solvent and freeze-dried to form a porous lyophilized cake with evenly dispersed ingredients.

The cake is reconstituted in water to promote micelle self-assembly and concomitant drug encapsulation. We found that the presence of PBS salts in the lyophilized cake remarkably improved the cake porosity and reconstitution time, resulting in optimum drug loading of 5 drug molecules per micelle. Furthermore, we increased the strength of the formulation by preparing lyophilized cakes with 5mM of DSPE-PEG₂₀₀₀ and reconstituting it in one-third of the fill volume. Based on the ease of preparation, reproducibility, and feasible scaling-up, we believe that this formulation and drug encapsulation process has great potential for clinical translation.

3. The optimized TST-SSM formulation exhibited satisfactory storage stability in both reconstituted and freeze-dried form. The freeze-dried formulation was stable for at least 7 months when stored at 5°C and 30°C/ 60% RH without significant changes in particle size, drug concentration, and antimicrobial activity. Samples stored at 40°C/ 75% RH were active for at least 7 months, but due to the generation of degradation products and large particles, this storage condition should be avoided. After reconstitution in water, the liquid formulation was stable for 7 days when refrigerated at 4°C, but only one day when stored at 25°C. Sterilizing filtration through 0.22 µm PES membrane did not affect nanomedicine properties.
4. We were able to encapsulate an antibiotic molecule in SSM without losing the activity *in vitro*. Previous attempts from our laboratory to encapsulate amphiphilic antibiotics have failed due to the hindering of essential drug charges by SSM. However, encapsulation of TST in SSM did not impair the drug activity *in vitro* or *in vivo* because this molecule is hydrophobic and it does not require activity charge

for activity. In fact, TST-SSM nanomedicine was 2 to 8-fold more potent than free drug dissolved in 4% DMSO against several Gram-positive bacteria, including MRSA USA300. The improvement of the *in vitro* activity of TST-SSM was due to the protective effects of SSM in preventing chemical degradation of encapsulated TST in the experimental conditions of the antimicrobial test. Besides improvements in drug solubility and stability, encapsulation of antibiotics in SSM can enhance the safety and efficacy of antibiotic therapies by passively targeting the drug to infected sites with increased vascular permeability and spare healthy tissues from toxic effects.

5. We could not demonstrate *in vivo* antimicrobial activity of TST-SSM against staphylococcal pneumonia. Low dose (2.4 mg/kg/dose) or higher doses (7.2 mg/kg/dose) of TST-SSM via retroorbital injection did not significantly reduce the bacterial burden in the lungs in a total of 5 independent experiments. Since Although TST-SSM exhibited direct *in vitro* antimicrobial activity against MRSA USA 300, we believe that, under *in vivo* conditions, the anti-inflammatory properties of TST (TLR-9 inhibitor) interferes with the host's ability in clearing the infection.
6. A single-dose of TST-SSM nanomedicine (20 mg/kg) via IP improved the median survival of mice with CLP-induced polymicrobial sepsis from 31h to 44h compared to empty micelles. Treated animals presented reduced bacterial burden in blood and peritoneal lavage, improved renal (creatinine) and hepatic (AST) function biomarker levels, reduced vasodilator nitric oxide derivatives, and reduced plasma levels of pro-inflammatory cytokines IL-6 and TNF- α . This was the first time that

TST was shown to improve the mice's survival and disease markers in a polymicrobial sepsis model.

VI. FUTURE DIRECTIONS

1. The co-solvent freeze-drying method described in this thesis was developed in a manifold-style freeze-dryer without temperature control in the drying chamber. For this reason, samples had to be frozen externally and drying cycle details could not be controlled or recorded. Therefore, it would be beneficial to test the method in a shelf-style freeze-dryer with cooling shelves to optimize the freeze-drying cycle parameters and obtain satisfactory lyophilized products in a shorter time. This could reduce the costs associated with the freeze-drying process and make the product more cost-effective.
2. We learned that TST can be encapsulated in SSM without losing its antimicrobial activity *in vitro* due to the lack of electrostatic interaction with the nanocarrier. Given global crisis of bacterial resistance and the need of new therapeutic options to target resistant microorganisms, we can enable the use of other hydrophobic antibiotics by encapsulating them in SSM for safe and effective delivery to localized infections. Examples for these antibiotics include other members of the thiopeptide drug class such as micrococcin P or nosiheptide.
3. The scalable co-solvent freeze-drying method can be applied to encapsulate other hydrophobic drugs in SSM and facilitate their clinical translation. The proportion of TBA might have to be adjusted on a case-to-case basis to maintain both drug and phospholipid in solution. The freeze-drying cycle parameters can also be optimized for improved manufacturing efficiency.

4. In this study, we used phosphate salts as the buffering agent of the TST-SSM optimized formulation due to its known safety and ability to maintain solution pH at physiological ranges. However, other buffer salts besides phosphate can be explored in the co-solvent freeze-drying method to control the pH of SSM nanomedicine at desired levels. Commonly used buffer salts in freeze-dried injectables are citrate (pka 3.1, 4.8, 6.4), acetate (pka 4.8) and histidine (pka 1.8, 6.1, 9.2) (Akers 2016).
5. The *in vivo* antibiotic activity of TST-SSM could not be verified in the staphylococcal pneumonia possibility due to the anti-inflammatory effect of TST on the host immune system. It remains to be investigated if this is a tissue-specific phenomenon or if the antibiotic and anti-inflammatory properties of TST-SSM can be modulated with different drug doses. The dose of TST-SSM was limited by the maximum volume of administration via retro-orbital injection, but higher doses via IP injection could be tested in the future. Also, it would also be interesting to evaluate the antibiotic effect of TST-SSM in the treatment of staphylococcal pneumonia in TLR-9 knockout mice to confirm the interfering pathway.
6. We demonstrated that TST-SSM significantly improved the survival of mice with polymicrobial sepsis, supposedly through TLR-9 inhibition. However, it is unclear if the antimicrobial activity of TST also contributed to the positive outcome. Since TST only targets Gram-positive bacteria, it would be useful to compare the bacterial Gram profile in the blood and peritoneal lavage of septic animals with or without TST-SSM treatment. In addition, one could study the effect of TST-SSM

in sepsis induced by LPS or *Escherichia coli* to confirm the anti-sepsis mechanism of TST-SSM in the absence of Gram-positive infection.

7. Encapsulation of TST in SSM nanocarrier enabled the safe administration of the drug *in vivo* and the study of its antimicrobial, anti-sepsis, and anticancer properties. TST-SSM nanomedicine can be further tested for other indicated disease states such as tuberculosis, malaria, and different cancer types.

REFERENCES

- Abbas, Abul K., Andrew H. Lichtman, and Shiv Pillai. 2015. *Cellular and Molecular Immunology*. 8th ed. Philadelphia: Elsevier Saunders.
- Abdelwahed, Wassim, Ghania Degobert, Serge Stainmesse, and Hatem Fessi. 2006. "Freeze-Drying of Nanoparticles: Formulation, Process and Storage Considerations." *Advanced Drug Delivery Reviews* 58 (15): 1688–1713. <https://doi.org/10.1016/j.addr.2006.09.017>.
- Akers, Michael J. 2016. *Sterile Drug Products: Formulation, Packaging, Manufacturing and Quality*. London: Informa Healthcare.
- Aminake, Makoah N., Sebastian Schoof, Ludmilla Sologub, Monika Leubner, Marc Kirschner, Hans Dieter Arndt, and Gabriele Pradel. 2011. "Thiostrepton and Derivatives Exhibit Antimalarial and Gametocytocidal Activity by Dually Targeting Parasite Proteasome and Apicoplast." *Antimicrobial Agents and Chemotherapy* 55 (4): 1338–48. <https://doi.org/10.1128/AAC.01096-10>.
- Anbazhagan, Arivarasu N., Mentor Thaqi, Shubha Priyamvada, Dulari Jayawardena, Anoop Kumar, Tarunmeet Gujral, Ishita Chatterjee, et al. 2017. "GLP-1 Nanomedicine Alleviates Gut Inflammation." *Nanomedicine: Nanotechnology, Biology and Medicine* 13: 659–65. <https://doi.org/10.1016/j.nano.2016.08.004>.
- Ashok, Beena, Lise Arleth, Rex P. Hjelm, Israel Rubinstein, and Hayat Önyüksel. 2004. "In Vitro Characterization of PEGylated Phospholipid Micelles for Improved Drug Solubilization: Effects of PEG Chain Length and PC Incorporation." *Journal of Pharmaceutical Sciences* 93 (10): 2476–87. <https://doi.org/10.1002/jps.20150>.
- Azzopardi, E. A., E. L. Ferguson, and D. W. Thomas. 2013. "The Enhanced Permeability Retention Effect: A New Paradigm for Drug Targeting in Infection." *Journal of Antimicrobial Chemotherapy* 68 (2): 257–74. <https://doi.org/10.1093/jac/dks379>.
- Bagley, Mark C., James W. Dale, Eleanor A. Merritt, and Xin Xiong. 2005. "Thiopeptide Antibiotics." *Chemical Reviews* 105 (2): 685–714. <https://doi.org/10.1021/cr0300441>.
- Baka, Edit, John E A Comer, and Krisztina Takács-Novák. 2008. "Study of Equilibrium Solubility Measurement by Saturation Shake-Flask Method Using Hydrochlorothiazide as Model Compound." *Journal of Pharmaceutical and Biomedical Analysis* 46 (2): 335–41. <https://doi.org/10.1016/j.jpba.2007.10.030>.
- Banerjee, Amrita, and Hayat Onyüksel. 2012. "Peptide Delivery Using Phospholipid Micelles." *WIREs Nanomedicine and Nanobiotechnology* 4 (5): 562–74. <https://doi.org/10.1002/wnan.1185>.

- . 2013. “A Novel Peptide Nanomedicine for Treatment of Pancreatogenic Diabetes.” *Nanomedicine: Nanotechnology, Biology, and Medicine* 9 (6): 722–28. <https://doi.org/10.1016/j.nano.2012.12.005>.
- Bausch, Sarae L., Ekaterina Poliakova, and David E. Draper. 2005. “Interactions of the N-Terminal Domain of Ribosomal Protein L11 with Thiostrepton and rRNA.” *Journal of Biological Chemistry* 280 (33): 29956–63. <https://doi.org/10.1074/jbc.M504182200>.
- Beech, Karen E., James G. Biddlecombe, Christopher F. Van Der Walle, Lee A. Stevens, Sean P. Rigby, Jonathan C. Burley, and Stephanie Allen. 2015. “Insights into the Influence of the Cooling Profile on the Reconstitution Times of Amorphous Lyophilized Protein Formulations.” *European Journal of Pharmaceutics and Biopharmaceutics* 96: 247–54. <https://doi.org/10.1016/j.ejpb.2015.07.029>.
- Bien, Justyna, Olga Sokolova, and Przemyslaw Bozko. 2011. “Characterization of Virulence Factors of Staphylococcus Aureus : Novel Function of Known Virulence Factors That Are Implicated in Activation of Airway Epithelial Proinflammatory Response.” *Journal of Pathogens*, 1–13. <https://doi.org/10.4061/2011/601905>.
- Bone, R. C., R. A. Balk, F. B. Cerra, R. P. Dellinger, A. M. Fein, W. A. Knaus, R. M.H. Schein, and W. J. Sibbald. 1992. “Definitions for Sepsis and Organ Failure and Guidelines for the Use of Innovative Therapies in Sepsis.” *Chest* 101 (6): 1644–55. <https://doi.org/10.1378/chest.101.6.1644>.
- Brandenburg, KS, I Rubinstein, RT Sadikot, and Hayat Önyüksel. 2012. “Polymyxin B Self-Associated with Phospholipid Nanomicelles.” *Pharmaceutical Development and Technology* 17 (6): 654–60. <https://doi.org/10.3109/10837450.2011.572893>.
- Brisson-noel, Anne, Pascal Delrieull, Daniel Samainli, and Patrice Courvalins. 1988. “Inactivation of Lincosaminide Antibiotics in Staphylococcus.” *The Journal of Biological Chemistry* 263 (31): 15880–87.
- Brittain, Jason Edward, and Joe Craig Franklin. 2013. Bendamustine pharmaceutical compositions. US 8.436,190 B2, issued 2013.
- Bruniera, R, FM Ferreira, LRM Saviolli, MR Bacci, D Feder, M da Luz Goncalves Pedreira, MA Sorgini Peterlini, LA Azzalis, VB Campos Junqueira, and FLA Fonseca. 2015. “The Use of Vancomycin with Its Therapeutic and Adverse Effects : A Review.” *European Review for Medical and Pharmacological Sciences* 19: 694–700.
- CDC. 2013. “Antibiotic Resistance Threats in the United States, 2013.” <https://doi.org/CS239559-B>.
- Cesur, Hacer, Israel Rubinstein, Ashwini Pai, and Hayat Onyüksel. 2009. “Self-Associated Indisulam in Phospholipid-Based Nanomicelles: A Potential Nanomedicine for Cancer.” *Nanomedicine* 5 (2): 178–83.

<https://doi.org/10.1038/jid.2014.371>.

- Chambers, Henry F, and Frank R Deleo. 2009. "Waves of Resistance: Staphylococcus Aureus in the Antibiotic Era." *Nature Reviews Microbiology* 7 (9): 629–41. <https://doi.org/10.1038/nrmicro2200.Waves>.
- Chary, C., Rambhav, S., Venkateswerlu, G. 1990. "Inactivation of Thiostrepton by Copper (II)." *Biology of Metals* 3: 48–53.
- Chaudhry, Hina, Juhua Zhou, Yin Zhong, Mir Mustafa Ali, Franklin McGuire, Prakash S. Nagarkatti, and Mitzi Nagarkatti. 2013. "Role of Cytokines as a Double-Edged Sword in Sepsis." *In Vivo* 27 (6): 669–84.
- Chiu, M. L., M. Folcher, T. Katoh, A. M. Puglia, J. Vohradsky, B.-S. Yun, H. Seto, and C. J. Thompson. 1999. "Broad Spectrum Thiopeptide Recognition Specificity of The Streptomyces Lividans TipAL Protein and Its Role in Regulating Gene Expression." *Journal of Biological Chemistry* 274 (29): 20578–86. <https://doi.org/10.1074/jbc.274.29.20578>.
- Courvalin, Patrice. 2006. "Vancomycin Resistance in Gram-Positive Cocci." *Clinical Infectious Diseases* 42: S25-34.
- Cron, MJ, DG Whitehead, IR Hooper, B Heinemann, and J Lein. 1956. "Bryamycin, a New Antibiotic." *Antibiotic Chemotherapy* 6 (1): 63–67.
- Cundliffe, E. 1978. "Mechanism of Resistance to Thiostrepton in the Producing-Organism Streptomyces Azureus." *Nature* 272 (5656): 792–95. <https://doi.org/10.1038/272792a0>.
- Dagar, Aparna, Antonina Kuzmis, Israel Rubinstein, Marin Sekosan, and Hayat Onyuksel. 2012. "VIP-Targeted Cytotoxic Nanomedicine for Breast Cancer." *Drug Delivery Translational Research* 2 (6): 454–62. <https://doi.org/10.1038/jid.2014.371>.
- David, Michael Z, and Robert S Daum. 2017. "Treatment of Staphylococcus Aureus Infections." *Current Topics in Microbiology and Immunology* 409: 325–83. <https://doi.org/10.1007/82>.
- Dejager, Lien, Iris Pinheiro, Eline Dejonckheere, and Claude Libert. 2011. "Cecal Ligation and Puncture: The Gold Standard Model for Polymicrobial Sepsis?" *Trends in Microbiology* 19 (4): 198–208. <https://doi.org/10.1016/j.tim.2011.01.001>.
- Delcour, A. 2009. "Outer Membrane Permeability and Antibiotic Resistance." *Biochimica et Biophysica Acta* 1794 (5): 808–16. <https://doi.org/10.1016/j.bbapap.2008.11.005>.
- DeLeo, Frank R., Michael Otto, Barry N. Kreiswirth, and Henry F. Chambers. 2010. "Community-Associated Meticillin-Resistant Staphylococcus Aureus." *The Lancet* 375 (9725): 1557–68. [https://doi.org/10.1016/S0140-6736\(09\)61999-1](https://doi.org/10.1016/S0140-6736(09)61999-1).

- Dellinger, R. Phillip, Mitchell M. Levy, Jean M. Carlet, Julian Bion, Margaret M. Parker, Roman Jaeschke, Konrad Reinhart, et al. 2008. "Surviving Sepsis Campaign: International Guidelines for Management of Severe Sepsis and Septic Shock: 2008." *Intensive Care Medicine* 34 (1): 17–60. <https://doi.org/10.1007/s00134-007-0934-2>.
- Diep, Binh An, Amy M Palazzolo-ballance, Pierre Tattevin, Li Basuino, Kevin R Braughton, R Adeline, Liang Chen, et al. 2008. "Contribution of Pantone-Valentine Leukocidin in Staphylococcus Aureus Pathogenesis." *PloS One* 3 (9): e3198. <https://doi.org/10.1371/journal.pone.0003198>.
- Doak, Bradley Croy, Björn Over, Fabrizio Giordanetto, and Jan Kihlberg. 2014. "Oral Druggable Space beyond the Rule of 5: Insights from Drugs and Clinical Candidates." *Chemistry and Biology* 21 (9): 1115–42. <https://doi.org/10.1016/j.chembiol.2014.08.013>.
- Docobo-Pérez, Fernando, Rafael López-Rojas, Juan Domínguez-Herrera, Manuel E. Jiménez-Mejías, Cristina Pichardo, José Ibáñez-Martínez, and Jerónimo Pachón. 2012. "Efficacy of Linezolid versus a Pharmacodynamically Optimized Vancomycin Therapy in an Experimental Pneumonia Model Caused by Methicillin-Resistant Staphylococcus Aureus." *Journal of Antimicrobial Chemotherapy* 67 (8): 1961–67. <https://doi.org/10.1093/jac/dks142>.
- Donovan, P. D., V. Corvari, M. D. Burton, and N. Rajagopalan. 2007. "Effect of Stopper Processing Conditions on Moisture Content and Ramifications for Lyophilized Products: Comparison of 'Low' and 'High' Moisture Uptake Stoppers." *PDA Journal of Pharmaceutical Science and Technology* 61 (1): 51–58.
- Donovick, Richard, Pagano Joseph F, and John Vandeputte. 1961. Thiostrepton, its salts, and production. US2982689 A, issued 1961. <https://docs.google.com/viewer?url=patentimages.storage.googleapis.com/pdfs/US2982689.pdf>.
- Esparza, Karina, and Hayat Onyuksel. 2019. "Development of Co-Solvent Freeze-Drying Method for the Encapsulation of Water-Insoluble Thiostrepton in Sterically Stabilized Micelles." *International Journal of Pharmaceutics* 556: 21–29. <https://doi.org/10.1016/j.ijpharm.2018.12.001>.
- Farver, Carol F. 2019. "Bacterial Diseases." In *Pulmonary Pathology*, edited by Dani S. Zander and Carol F. Farver, Second Edi, 163–200. Elsevier Inc. <https://doi.org/10.1016/B978-0-323-39308-9.00010-8>.
- Fink, Susan L, and Sheldon Campbell. 2018. *Chapter 3 - Infection and Host Response*. Edited by William B. Coleman and Gregory J. Tsongalis. *Molecular Pathology*. Second Edi. Elsevier Inc. <https://doi.org/10.1016/B978-0-12-802761-5.00003-1>.
- Fournier, Benedicte, and Dana J Philpott. 2005. "Recognition of Staphylococcus Aureus by the Innate Immune System." *Clinical Microbiology Reviews* 18 (3): 521–40.

<https://doi.org/10.1128/CMR.18.3.521>.

- Fournier, Elvire, Marie-Hélène Dufresne, Damon C. Smith, Maxime Ranger, and Jean-Christophe Leroux. 2004. "A Novel One-Step Drug-Loading Procedure for Water-Soluble Amphiphilic Nanocarriers." *Pharmaceutical Research* 21 (6): 962–68. <https://doi.org/10.1023/B:PHAM.0000029284.40637.69>.
- Furneri, P. M., M. Fresta, G. Puglisi, and G. Tempera. 2000. "Ofloxacin-Loaded Liposomes: In Vitro Activity and Drug Accumulation in Bacteria." *Antimicrobial Agents and Chemotherapy* 44 (9): 2458–64. <https://doi.org/10.1128/AAC.44.9.2458-2464.2000>.
- Gandhi, Salil, Takaya Tsueshita, Hayat Önyüksel, Rinku Chandiwalla, and Israel Rubinstein. 2002. "Interactions of Human Secretin with Sterically Stabilized Phospholipid Micelles Amplify Peptide-Induced Vasodilation in Vivo." *Peptides* 23 (8): 1433–39. [https://doi.org/10.1016/S0196-9781\(02\)00092-X](https://doi.org/10.1016/S0196-9781(02)00092-X).
- Gordon, Rachel J, and Franklin D Lowy. 2008. "Pathogenesis of Methicillin-Resistant Staphylococcus Aureus Infection." *Clinical Infectious Diseases* 46 (Suppl 5): S350-359. <https://doi.org/10.1086/533591>.
- Gould, Ian M., Michael Z. David, Silvano Esposito, Javier Garau, Gerard Lina, Teresita Mazzei, and Georg Peters. 2012. "New Insights into Meticillin-Resistant Staphylococcus Aureus (MRSA) Pathogenesis, Treatment and Resistance." *International Journal of Antimicrobial Agents* 39 (2): 96–104. <https://doi.org/10.1016/j.ijantimicag.2011.09.028>.
- Gualerzi, Claudio O., Letizia Brandi, Attilio Fabbretti, and Cynthia L. Pon, eds. 2014. *Antibiotics: Targets, Mechanisms and Resistance*. Weinheim: Wiley VCH.
- Gülçür, Ece, Mentor Thaqi, Fatima Khaja, Antonina Kuzmis, and Hayat Onyüksel. 2013. "Curcumin in VIP-Targeted Sterically Stabilized Phospholipid Nanomicelles: A Novel Therapeutic Approach for Breast Cancer and Breast Cancer Stem Cells." *Drug Delivery and Translational Research* 3 (6): 1–25. <https://doi.org/10.1007/s13346-013-0167-6>.
- Habazettl, Judith, Martin Allan, Pernille Rose Jensen, Hans-Jürgen Sass, Charles J. Thompson, and Stephan Grzesiek. 2014. "Structural Basis and Dynamics of Multidrug Recognition in a Minimal Bacterial Multidrug Resistance System." *Proceedings of the National Academy of Sciences* 111 (51): E5498–5507. <https://doi.org/10.1073/pnas.1412070111>.
- Hal, Sebastian J Van, Slade O Jensen, Vikram L Vaska, Björn A Espedido, David L Paterson, and Iain B Gosbell. 2012. "Predictors of Mortality in Staphylococcus Aureus Bacteremia." *Clinical Microbiology Reviews* 25 (2): 362–86. <https://doi.org/10.1128/CMR.05022-11>.
- Hardy, Laura R, Melissa R Pergande, Karina Esparza, Kimberly N Heath, Hayat

- Onyuksel, Stephanie M Cologna, and Joanna E Burdette. 2019. "Proteomic Analysis Reveals a Role for PAX8 in Peritoneal Colonization of High Grade Serous Ovarian Cancer That Can Be Targeted with Micelle Encapsulated Thiostrepton." *Oncogene* 38 (32): 6003–16. <https://doi.org/https://doi.org/10.1038/s41388-019-0842-2>.
- Herrmann, Inge K., Maricela Castellon, David E. Schwartz, Melanie Hasler, Martin Urner, Guochang Hu, Richard D. Minshall, and Beatrice Beck-Schimmer. 2013. "Volatile Anesthetics Improve Survival after Cecal Ligation and Puncture." *Anesthesiology* 119: 901–6.
- Hidron, Alicia I., Cari E. Low, Eric G. Honig, and Henry M. Blumberg. 2009. "Emergence of Community-Acquired Methicillin-Resistant *Staphylococcus aureus* Strain USA300 as a Cause of Necrotising Community-Onset Pneumonia." *The Lancet Infectious Diseases* 9 (6): 384–92. [https://doi.org/10.1016/S1473-3099\(09\)70133-1](https://doi.org/10.1016/S1473-3099(09)70133-1).
- Hirai, Makiko, Norimitsu Kadowaki, Toshio Kitawaki, Haruyuki Fujita, Akifumi Takaori-Kondo, Ryutaro Fukui, Kensuke Miyake, et al. 2011. "Bortezomib Suppresses Function and Survival of Plasmacytoid Dendritic Cells by Targeting Intracellular Trafficking of Toll-like Receptors and Endoplasmic Reticulum Homeostasis." *Blood* 117 (2): 500–509. <https://doi.org/10.1182/blood-2010-05-284737>.
- Hotchkiss, Richard S., Guillaume Monneret, and Didier Payen. 2013. "Sepsis-Induced Immunosuppression: From Cellular Dysfunctions to Immunotherapy." *Nature Reviews Immunology* 13 (12): 862–74. <https://doi.org/10.1038/nri3552>.
- Hottot, Aurélie, Séverine Vessot, and Julien Andrieu. 2007. "Freeze Drying of Pharmaceuticals in Vials: Influence of Freezing Protocol and Sample Configuration on Ice Morphology and Freeze-Dried Cake Texture." *Chemical Engineering and Processing: Process Intensification* 46 (7): 666–74. <https://doi.org/10.1016/j.cep.2006.09.003>.
- Hu, Dan, Xiaohua Yang, Yianxiao Xiang, Hui Li, Hui Yan, Jun Zhou, Yi Caudle, Xiumei Zhang, and Deling Yin. 2015. "Inhibition of Toll-like Receptor 9 Attenuates Sepsis-Induced Mortality through Suppressing Excessive Inflammatory Response." *Cell Immunology* 295 (2): 92–98. <https://doi.org/10.1016/j.cellimm.2015.03.009>.Inhibition.
- Jayawardena, Dulari, Arivarasu N. Anbazhagan, Grace Guzman, Pradeep K. Dudeja, and Hayat Onyuksel. 2017. "Vasoactive Intestinal Peptide Nanomedicine for the Management of Inflammatory Bowel Disease." *Molecular Pharmaceutics* 14 (11): 3698–3708. <https://doi.org/10.1021/acs.molpharmaceut.7b00452>.
- Jevons, M. P. 1961. "'Celbenin' - Resistant Staphylococci." *British Medical Journal* 1: 124–25. <https://doi.org/10.1136/bmj.1.5219.124-a>.
- Johnson, Elizabeth R, and Michael A Matthay. 2010. "Acute Lung Injury: Epidemiology, Pathogenesis, and Treatment." *Journal of Aerosol Medicine and Pulmonary Drug*

- Delivery* 23 (4): 243–52. <https://doi.org/10.1089/jamp.2009.0775>.
- Just-Baringo, Xavier, Fernando Albericio, and Mercedes Álvarez. 2014. “Thiopeptide Antibiotics: Retrospective and Recent Advances.” *Marine Drugs* 12 (1): 317–51. <https://doi.org/10.3390/md12010317>.
- Kahlenberg, J Michelle, and Mariana J Kaplan. 2013. “Little Peptide, Big Effects: The Role of LL-37 in Inflammation and Autoimmune Disease.” *Journal of Immunology* 191 (10): 4895–4901. <https://doi.org/10.4049/jimmunol.1302005>.
- Kasraian, Kasra, and Patrick P. DeLuca. 1995. “Thermal Analysis of the Tertiary Butyl Alcohol-Water System and Its Implications on Freeze-Drying.” *Pharmaceutical Research* 12 (4): 484–90. <https://doi.org/10.1023/A:1016233408831>.
- Kawai, Taro, and Shizuo Akira. 2010. “The Role of Pattern-Recognition Receptors in Innate Immunity : Update on Toll-like Receptors.” *Nature Immunology* 11 (5): 373–84. <https://doi.org/10.1038/ni.1863>.
- Kidd, James M., Kamilia Abdelraouf, and David P. Nicolau. 2019. “Comparative Efficacy of Human-Simulated Epithelial Lining Fluid Exposures of Tedizolid, Linezolid and Vancomycin in Neutropenic and Immunocompetent Murine Models of Staphylococcal Pneumonia.” *Journal of Antimicrobial Chemotherapy* 74 (4): 970–77. <https://doi.org/10.1093/jac/dky513>.
- Kiedrowski, Megan R, Jordan R Gaston, Brian R Kocak, Stefanie L Coburn, Stella Lee, Joseph M Pilewski, Michael M Myerburg, and M Bomberger. 2018. “Staphylococcus Aureus Biofilm Growth on Cystic Fibrosis Airway Epithelial Cells Is Enhanced during Respiratory Syncytial Virus Coinfection.” *MSphere* 3 (4): 1–17.
- Koo, Otilia M., Israel Rubinstein, and Hayat Onyuksel. 2005. “Camptothecin in Sterically Stabilized Phospholipid Micelles: A Novel Nanomedicine.” *Nanomedicine: Nanotechnology, Biology, and Medicine* 1 (1): 77–84. <https://doi.org/10.1016/j.nano.2004.11.002>.
- Koo, Otilia May Yue, Israel Rubinstein, and Hayat Onyuksel. 2011. “Actively Targeted Low-Dose Camptothecin as a Safe, Long-Acting, Disease-Modifying Nanomedicine for Rheumatoid Arthritis.” *Pharmaceutical Research* 28 (4): 776–87. <https://doi.org/10.1007/s11095-010-0330-4>.
- Kourtis, Athena P., Kelly Hatfield, James Baggs, Yi Mu, Isaac See, Erin Epton, Joelle Nadle, et al. 2019. “Vital Signs: Epidemiology and Recent Trends in Methicillin-Resistant and in Methicillin-Susceptible Staphylococcus Aureus Bloodstream Infections — United States.” <https://www.medscape.org/viewarticle/912570>.
- Krishnadas, Aparna, Israel Rubinstein, and Hayat Onyuksel. 2003. “Sterically Stabilized Phospholipid Mixed Micelles: In Vitro Evaluation as a Novel Carrier for Water-Insoluble Drugs.” *Pharmaceutical Research* 20 (2): 297–302.

- Krismer, Bernhard, Christopher Weidenmaier, Alexander Zipperer, and Andreas Peschel. 2017. "The Commensal Lifestyle of *Staphylococcus Aureus* and Its Interactions with the Nasal Microbiota." *Nature Reviews Microbiology* 15 (11): 675–87. <https://doi.org/10.1038/nrmicro.2017.104>.
- Kumar, Anand, Daniel Roberts, Kenneth E. Wood, Bruce Light, Joseph E. Parrillo, Satendra Sharma, Robert Suppes, et al. 2006. "Duration of Hypotension before Initiation of Effective Antimicrobial Therapy Is the Critical Determinant of Survival in Human Septic Shock." *Critical Care Medicine* 34 (6): 1589–96. <https://doi.org/10.1097/01.CCM.0000217961.75225.E9>.
- Kutscher, Austin H, Edward V Zegarelli, Robin M Rankow, James Mercadante, and John D Piro. 1959. "Clinical Laboratory Studies on a New Topical Antibiotic: Thiostrepton." *Pharmacology and Therapeutics* 12 (8): 967–74.
- Kuzmis, Antonina, Sok Bee Lim, Esha Desai, Eunjung Jeon, Bao-Shiang Lee, Israel Rubinstein, and Hayat Onyüksel. 2011. "Micellar Nanomedicine of Human Neuropeptide Y." *Nanomedicine : Nanotechnology, Biology, and Medicine* 7 (4): 464–71. <https://doi.org/10.1016/j.nano.2011.01.004>.
- Kwok, Jimmy M-M, Stephen S Myatt, Charles M Marson, R Charles Coombes, Demetra Constantinidou, and Eric W-F Lam. 2008. "Thiostrepton Selectively Targets Breast Cancer Cells through Inhibition of Forkhead Box M1 Expression." *Molecular Cancer Therapeutics* 7 (7): 2022–32. <https://doi.org/10.1158/1535-7163.MCT-08-0188>.
- Labandeira-Rey, Maria, Florence Couzon, Sandrine Boisset, Eric L. Brown, Michele Bes, Yvonne Benito, Elena M. Barbu, et al. 2007. "Staphylococcus Aureus Panton-Valentine Leukocidin Causes Necrotizing Pneumonia." *Science* 315 (February): 1130–33.
- Lai, Chao-Yang, Da-Wei Yeh, Chih-Hao Lu, Yi-Ling Liu, Li-Rung Huang, Cheng-Yuan Kao, Huan-Yuan Chen, et al. 2015. "Identification of Thiostrepton as a Novel Inhibitor for Psoriasis-like Inflammation Induced by TLR7-9." *Journal of Immunology (Baltimore, Md. : 1950)* 195 (8): 3912–21. <https://doi.org/10.4049/jimmunol.1500194>.
- Letourneau, Alyssa R. 2017. "Beta-Lactam Antibiotics: Mechanisms of Action and Resistance and Adverse Effects." UptoDate. 2017. <https://www.uptodate-com.proxy.cc.uic.edu/contents/beta-lactam-antibiotics-mechanisms-of-action-and-resistance-and-adverse-effects?search=Penicillins> •Cephalosporins
•Cephameycins
•Carbapenems&source=search_result&selectedTitle=1~150&usage_type=default&
- Levin, Todd P, Byungse Suh, Peter Axelrod, Allan L Truant, and Thomas Fekete. 2005. "Potential Clindamycin Resistance in Clindamycin-Susceptible , Erythromycin-Resistant *Staphylococcus Aureus*: Report of a Clinical Failure." *Antimicrobial Agents and Chemotherapy* 49 (3): 1222–24.

<https://doi.org/10.1128/AAC.49.3.1222>.

- Levy, Mitchell M., Laura E. Evans, and Andrew Rhodes. 2018. "The Surviving Sepsis Campaign Bundle: 2018 Update." *Critical Care Medicine* 46 (6): 997–1000. <https://doi.org/10.1097/CCM.0000000000003119>.
- Levy, Stuart B, and Bonnie Marshall. 2004. "Antibacterial Resistance Worldwide: Causes, Challenges and Responses." *Nat.Med.* 10 (1078-8956 (Print)): S122–29. <https://doi.org/10.1038/nm1145>.
- Lewis, Kim. 2013. "Platforms for Antibiotic Discovery." *Nature Reviews. Drug Discovery* 12 (5): 371–87. <https://doi.org/10.1038/nrd3975>.
- Li, Chaoxuan, Feifei Zhang, and Wendy L Kelly. 2011. "Heterologous Production of Thiostrepton A and Biosynthetic Engineering of Thiostrepton Analogs." *Molecular BioSystems* 7 (1): 82–90. <https://doi.org/10.1039/c0mb00129e>.
- Liao, Rijng, and Wen Liu. 2011. "Thiostrepton Maturation Involving a Deesterification-Amidation Way to Process the C-Terminally Methylated Peptide Backbone." *Journal of the American Chemical Society* 133 (9): 2852–55. <https://doi.org/10.1021/ja1111173>.
- Lim, Sok Bee, Amrita Banerjee, and Hayat Onyüksel. 2012. "Improvement of Drug Safety by the Use of Lipid-Based Nanocarriers." *Journal of Controlled Release* 163 (1): 34–45. <https://doi.org/10.1016/j.jconrel.2012.06.002>.
- Lim, Sok Bee, Israel Rubinstein, and Hayat Önyüksel. 2008. "Freeze Drying of Peptide Drugs Self-Associated with Long-Circulating, Biocompatible and Biodegradable Sterically Stabilized Phospholipid Nanomicelles." *International Journal of Pharmaceutics* 356 (1–2): 345–50. <https://doi.org/10.1016/j.ijpharm.2008.01.014>.
- Lim, Sok Bee, Israel Rubinstein, Ruxana T Sadikot, James E Artwohl, and Hayat Önyüksel. 2011. "A Novel Peptide Nanomedicine against Acute Lung Injury: GLP-1 in Phospholipid Micelles." *Pharmaceutical Research* 28 (3): 662–72. <https://doi.org/10.1007/s11095-010-0322-4>.
- Lima Procópio, Rudi Emerson de, Ingrid Reis da Silva, Mayra Kassawara Martins, João Lúcio de Azevedo, and Janete Magali de Araújo. 2012. "Antibiotics Produced by Streptomyces." *Brazilian Journal of Infectious Diseases* 16 (5): 466–71. <https://doi.org/10.1016/j.bjid.2012.08.014>.
- Liu, Catherine, Arnold Bayer, Sara E. Cosgrove, Robert S. Daum, Scott K. Fridkin, Rachel J. Gorwitz, Sheldon L. Kaplan, et al. 2011. "Clinical Practice Guidelines by the Infectious Diseases Society of America for the Treatment of Methicillin-Resistant Staphylococcus Aureus Infections in Adults and Children." *Clinical Infectious Diseases* 52 (3). <https://doi.org/10.1093/cid/ciq146>.
- Liu, Lixia, Yong Li, Zhenjie Hu, Jie Su, Yan Huo, Bibo Tan, Xiaoling Wang, and Yueping

- Liu. 2012. "Small Interfering RNA Targeting Toll-Like Receptor 9 Protects Mice against Polymicrobial Septic Acute Kidney Injury." *Nephron Experimental Nephrology* 122 (1–2): 51–61. <https://doi.org/10.1159/000346953>.
- Locke, Jeffrey B., Douglas E. Zuill, Caitlyn R. Scharn, Jennifer Deane, Daniel F. Sahm, Richard V. Goering, Stephen G. Jenkins, and Karen J. Shaw. 2014. "Identification and Characterization of Linezolid-Resistant Cfr-Positive *Staphylococcus Aureus* USA300 Isolates from a New York City Medical Center." *Antimicrobial Agents and Chemotherapy* 58 (11): 6949–52. <https://doi.org/10.1128/AAC.03380-14>.
- Maeda, Hiroshi. 2012. "Vascular Permeability in Cancer and Infection as Related to Macromolecular Drug Delivery, with Emphasis on the EPR Effect for Tumor-Selective Drug Targeting." *Proceedings of the Japan Academy. Series B, Physical and Biological Sciences* 88 (3): 53–71. <https://doi.org/10.2183/pjab.88.53>.
- Malmsten, Martin. 2014. "Antimicrobial Peptides." *Upsala Journal of Medical Sciences* 119 (2): 199–204. <https://doi.org/10.3109/03009734.2014.899278>.
- Mcconkey, Glenn A, M John Rogers, and Thomas F Mccutchan. 1997. "Inhibition of *Plasmodium Falciparum* Protein Synthesis." *The Journal of Biological Chemistry* 272 (4): 2046–49.
- Mcguinness, Will A, Natalia Malachowa, and Frank R Deleo. 2017. "Vancomycin Resistance in *Staphylococcus Aureus*." *Yale Journal of Biology and Medicine* 90: 269–81.
- Meer, Anne Jan van der, and Achmed Achouiti. 2016. "Toll-Like Receptor 9 Enhances Bacterial Clearance and Limits Lung Consolidation in Murine Pneumonia Caused by Methicillin-Resistant *Staphylococcus Aureus*." *Molecular Medicine* 22 (1): 1. <https://doi.org/10.2119/molmed.2015.00242>.
- Mizgerd, Joseph P., and Shawn J. Skerrett. 2008. "Animal Models of Human Pneumonia." *American Journal of Physiology-Lung Cellular and Molecular Physiology* 294: L387–98. <https://doi.org/10.1152/ajplung.00330.2007>.
- Mombeshora, Molly, and Stanley Mukanganyama. 2017. "Development of an Accumulation Assay and Evaluation of the Effects of Efflux Pump Inhibitors on the Retention of Chlorhexidine Digluconate in *Pseudomonas Aeruginosa* and *Staphylococcus Aureus*." *BMC Research Notes* 10 (1): 1–9. <https://doi.org/10.1186/s13104-017-2637-2>.
- Naguib, Youssef W, Hannah L O'Mary, Zhengrong Cui, and Alan B Watts. 2016. "Injectable Formulations of Poorly Water-Soluble Drugs." In *Formulating Poorly Water Soluble Drugs*, edited by Robert O Williams III, Alan B Watts, and Dave A Miller, 257–93. Cham: Springer International Publishing. https://doi.org/10.1007/978-3-319-42609-9_6.
- Naraqi, Sirus, and Geoff McDonnell. 1981. "Hematogenous Staphylococcal Pneumonia

- Secondary to Soft Tissue Infection.” *CHEST* 79 (2): 173–75.
<https://doi.org/10.1378/chest.79.2.173>.
- Nema, S, R J Washkuhn, and R J Brendel. 1997. “Excipients and Their Use in Injectable Products.” *PDA Journal of Pharmaceutical Science and Technology* 51 (4): 166–71. <http://www.ncbi.nlm.nih.gov/pubmed/9277127>.
- Nguyen, Hien M, and Christopher J Graber. 2010. “Limitations of Antibiotic Options for Invasive Infections Caused by Methicillin-Resistant Staphylococcus Aureus: Is Combination Therapy the Answer?” *Journal of Antimicrobial Chemotherapy* 65: 24–36. <https://doi.org/10.1093/jac/dkp377>.
- Ni, Nina, Marc Tesconi, S. Esmail Tabibi, Shanker Gupta, and Samuel H. Yalkowsky. 2001. “Use of Pure T-Butanol as a Solvent for Freeze-Drying: A Case Study.” *International Journal of Pharmaceutics* 226 (1–2): 39–46.
[https://doi.org/10.1016/S0378-5173\(01\)00757-8](https://doi.org/10.1016/S0378-5173(01)00757-8).
- Nicolaou, K. C. 2012. “How Thiostrepton Was Made in the Laboratory.” *Angewandte Chemie (International Ed. in English)* 51 (50): 12414–36.
<https://doi.org/10.1038/jid.2014.371>.
- Nicolaou, K. C., Mark Zak, Shai Rahimipour, Anthony A. Estrada, Sang Hyup Lee, Aurora O’Brate, Paraskevi Giannakakou, and M. Reza Ghadiri. 2005. “Discovery of a Biologically Active Thiostrepton Fragment.” *Journal of the American Chemical Society* 127 (43): 15042–44. <https://doi.org/10.1021/ja0552803>.
- Nireesha, G R, L Divya, C Sowmya, N Venkateshan, M Niranjana Babu, and V Lavakumar. 2013. “Lyophilization / Freeze Drying - An Review.” *International Journal of Novel Trends in Pharmaceutical Sciences* 3 (4): 87–98.
- Niu, Hongxia, Rebecca Yee, Peng Cui, Lili Tian, Shuo Zhang, Wanliang Shi, David Sullivan, Bingdong Zhu, Wenhong Zhang, and Ying Zhang. 2017. “Identification of Agents Active against Methicillin-Resistant Staphylococcus Aureus USA300 from a Clinical Compound Library.” *Pathogens* 6 (3): 44.
<https://doi.org/10.3390/pathogens6030044>.
- Norrby, Ragnar, Mair Powell, Bo Aronsson, Dominique L Monnet, Irja Lutsar, Ioan Stelian Bocsan, Otto Cars, Helen Giamarellou, and Inge C. Gyssens. 2009. “The Bacterial Challenge: Time to React.” Stockholm. <https://doi.org/10.2900/2518>.
- Olsen, Randall J, Scott D Kobayashi, Ara A Ayeras, Madiha Ashraf, Shawna F Graves, Willie Ragasa, Tammy Humbird, et al. 2010. “Lack of a Major Role of Staphylococcus Aureus Pantone-Valentine Leukocidin in Lower Respiratory Tract Infection in Nonhuman Primates.” *The American Journal of Pathology* 176 (3): 1346–54. <https://doi.org/10.2353/ajpath.2010.090960>.
- Onyuksel, Hayat, Eunjung Jeon, and Israel Rubinstein. 2009. “Nanomicellar Paclitaxel Increases Cytotoxicity of Multidrug Resistant Breast Cancer Cells.” *Cancer Letters*

- 274 (2): 327–30. <https://doi.org/10.1016/j.canlet.2008.09.041>.
- Pagano, J.F., M;J. Weinstein, H.A. Stout, and R. Donovick. 1955. “Thiostrepton, a New Antibiotic. I. In Vitro Studies.” *Antibiotics Annual: Proceedings of the Symposium on Antibiotics* 3: 554–59.
- Parag Kolhe, Mrinal Shah, and Nitin Rathore. 2013. *Sterile Product Development. Formulation, Process, Quality and Regulatory Considerations*. New York: Springer. <https://doi.org/https://doi-org.proxy.cc.uic.edu/10.1007/978-1-4614-7978-9>.
- Parker, Dane. 2017. “Humanized Mouse Models of Staphylococcus Aureus Infection.” *Frontiers in Immunology* 8 (MAY): 1–6. <https://doi.org/10.3389/fimmu.2017.00512>.
- Payne, David J., Michael N. Gwynn, David J. Holmes, and David L. Pompliano. 2007. “Drugs for Bad Bugs: Confronting the Challenges of Antibacterial Discovery.” *Nature Reviews Drug Discovery* 6 (1): 29–40. <https://doi.org/10.1038/nrd2201>.
- Peacock, Sharon J, and Gavin K Paterson. 2015. “Mechanisms of Methicillin Resistance in Staphylococcus Aureus.” *Annual Review of Biochemistry* 84: 577–601. <https://doi.org/10.1146/annurev-biochem-060614-034516>.
- Perichon, Bruno, and Patrice Courvalin. 2009. “VanA-Type Vancomycin-Resistant Staphylococcus Aureus.” *Antimicrobial Agents and Chemotherapy* 53 (11): 4580–87. <https://doi.org/10.1128/AAC.00346-09>.
- Peyrani, Paula, Marty Allen, Timothy L Wiemken, Nadia Z Haque, Marcus J Zervos, Kimbal D Ford, Ernesto G Scerpella, et al. 2011. “Severity of Disease and Clinical Outcomes in Patients With Hospital-Acquired Pneumonia Due to Methicillin-Resistant Staphylococcus Aureus Strains Not Influenced by the Presence of the Panton-Valentine Leukocidin Gene.” *Clinical Infectious Diseases* 53 (8): 766–71. <https://doi.org/10.1093/cid/cir541>.
- Peyrani, Paula, Timothy L Wiemken, Robert Kelley, Marcus J Zervos, Daniel H Kett, Thomas M File Jr, Gary E Stein, et al. 2014. “Higher Clinical Success in Patients with Ventilator-Associated Pneumonia Due to Methicillin-Resistant Staphylococcus Aureus Treated with Linezolid Compared with Vancomycin : Results from the IMPACT-HAP Study.” *Critical Care* 18 (R118): 1–9.
- Pikal-Cleland, Katherine A., and John F. Carpenter. 2001. “Lyophilization-Induced Protein Denaturation in Phosphate Buffer Systems: Monomeric and Tetrameric β -Galactosidase.” *Journal of Pharmaceutical Sciences* 90 (9): 1255–68. <https://doi.org/10.1002/jps.1078>.
- Porse, Bo T., Ilia Leviev, Alexander S. Mankin, and Roger A. Garrett. 1998. “The Antibiotic Thiostrepton Inhibits a Functional Transition within Protein L11 at the Ribosomal GTPase Centre.” *Journal of Molecular Biology* 276 (2): 391–404. <https://doi.org/10.1006/jmbi.1997.1541>.

- Prince, Alice, Hui Wang, Kipyegon Kitur, and Dane Parker. 2017. "Humanized Mice Exhibit Increased Susceptibility to Staphylococcus Aureus Pneumonia." *Journal of Infectious Diseases* 215 (9): 1386–95. <https://doi.org/10.1093/infdis/jiw425>.
- Puppala, Ravikumar, Srinivas Laxminarayan Pathi, Dharmaraj Ramachandra Rao, and Rajendra Narayanrao Kankan. 2016. Process for the Preparation of Bortezomib Mannitol Ester. US 2016/0075736A1, issued 2016.
- "Q3C - Tables and List Guidance for Industry." 2017. Food and Drug Administration. 2017. <https://www.fda.gov/media/71737/download>.
- Ranieri, Michael R.M., Derek C. K. Chan, Luke N. Yaeger, Madeleine Rudolph, Sawyer Karabelas-Pittman, Hamdi Abdo, Jessica Chee, Hanjeong Harvey, Uyen Nguyen, and Lori L. Burrows. 2019. "Thiostrepton Hijacks Pyoverdine Receptors to Inhibit Growth of Pseudomonas Aeruginosa." *Antimicrobial Agents and Chemotherapy*, 1–23. <https://doi.org/10.1128/aac.00472-19>.
- Ranieri, V. Marco, B. Taylor Thompson, Philip S. Barie, Jean-François Dhainaut, Ivor S. Douglas, Simon Finfer, Bengt Gårdlund, et al. 2012. "Drotrecogin Alfa (Activated) in Adults with Septic Shock." *The New England Journal of Medicine* 366 (22): 2055–64.
- Rello, Jordi, Francisco Valenzuela-Sánchez, Maria Ruiz-Rodriguez, and Silvia Moyano. 2017. "Sepsis: A Review of Advances in Management." *Advances in Therapy*. <https://doi.org/10.1007/s12325-017-0622-8>.
- Rello, Jordi, Francisco Velenzuela-Sanchez, Maria Ruiz-Rodriguez, and Silvia Moyano. 2017. "Sepsis : A Review of Advances in Management." *Advances in Therapy* 34: 2393–2411. <https://doi.org/10.1007/s12325-017-0622-8>.
- Rey, Louis, and Joan May, eds. 2010. *Freeze Drying/ Lyophilization of Pharmaceutical and Biological Products*. Third. London: Informa Healthcare.
- Rhodes, Andrew, Laura E. Evans, Waleed Alhazzani, Mitchell M. Levy, Massimo Antonelli, Ricard Ferrer, Anand Kumar, et al. 2017. *Surviving Sepsis Campaign: International Guidelines for Management of Sepsis and Septic Shock: 2016*. *Critical Care Medicine*. Vol. 45. <https://doi.org/10.1097/CCM.0000000000002255>.
- Riedemann, Niels C, Ren-feng Guo, and Peter A Ward. 2003. "The Enigma of Sepsis." *The Journal of Clinical Investigation* 112 (4): 460–67. <https://doi.org/10.1172/JCI200319523.Historical>.
- Sause, William E., Peter T. Buckley, William R. Strohl, A. Simon Lynch, and Victor J. Torres. 2016. "Antibody-Based Biologics and Their Promise to Combat Staphylococcus Aureus Infections." *Trends in Pharmacological Sciences* 37 (3): 231–41. <https://doi.org/10.1016/j.tips.2015.11.008>.
- Sawai, Toyomitsu, Kazunori Tomono, Katsunori Yanagihara, Yoshihiro Yamamoto,

- Mitsuo Kaku, Youichi Hirakata, Hironobu Koga, Takayoshi Tashiro, and Shigeru Kohno. 1997. "Role of Coagulase in a Murine Model of Hematogenous Pulmonary Infection Induced by Intravenous Injection of Staphylococcus Aureus Enmeshed in Agar Beads." *Infection and Immunity* 65 (2): 466–71.
- Schäberle, Till F., and Ingrid M. Hack. 2014. "Overcoming the Current Deadlock in Antibiotic Research." *Trends in Microbiology* 22 (4): 165–67. <https://doi.org/10.1016/j.tim.2013.12.007>.
- Schoof, Sebastian, Gabriele Pradel, Makoah N. Aminake, Bernhard Ellinger, Sascha Baumann, Marco Potowski, Yousef Najajreh, Marc Kirschner, and Hans Dieter Arndt. 2010. "Antiplasmodial Thioestrepton Derivatives: Proteasome Inhibitors with a Dual Mode of Action." *Angewandte Chemie - International Edition* 49 (19): 3317–21. <https://doi.org/10.1002/anie.200906988>.
- "Sepsis: Data and Reports." 2016. 2016. <https://www.cdc.gov/sepsis/datareports/index.html>.
- Sethi, Varun, Israel Rubinstein, Antonina Kuzmis, Helen Kastrissios, James Artwohl, and Hayat Onyuksel. 2013. "Novel, Biocompatible, Disease Modifying Nanomedicine of VIP for Rheumatoid Arthritis." *Molecular Pharmaceutics* 10 (2): 728–38. <https://doi.org/10.1021/mp300539f.Novel>.
- Shlaes, David M., Dan Sahm, Carol Opiela, and Brad Spellberg. 2013. "The FDA Reboot of Antibiotic Development." *Antimicrobial Agents and Chemotherapy* 57 (10): 4605–7. <https://doi.org/10.1128/AAC.01277-13>.
- Siberry, George K, Tsigereda Tekle, Karen Carroll, and James Dick. 2003. "Failure of Clindamycin Treatment of Methicillin-Resistant Staphylococcus Aureus Expressing Inducible Clindamycin Resistance In Vitro." *Clinical Infectious Diseases* 37: 1257–60.
- Simmons, Jeff, and Jean-Francois Pittet. 2015. "The Coagulopathy of Acute Sepsis." *Current Opinion in Anesthesiology* 28 (2): 227–36. <https://doi.org/10.1097/ACO.000000000000163.The>.
- Singer, Mervyn, Clifford S. Deutschman, Christopher Warren Seymour, Manu Shankar-Hari, Djillali Annane, Michael Bauer, Rinaldo Bellomo, et al. 2016. "The Third International Consensus Definitions for Sepsis and Septic Shock (Sepsis-3)." *JAMA - Journal of the American Medical Association* 315 (8): 801–10. <https://doi.org/10.1001/jama.2016.0287>.
- Sinko, Patrick J. 2011. *Martin's Physical Pharmacy and Pharmaceutical Sciences*. Edited by David B. Troy. Sixth. Baltimore: Lippincott Williams & Wilkins, a Wolters Kluwer business.
- Sivagnanam, Soupramanien, and Dirk Deleu. 2003. "Red Man Syndrome." *Critical Care* 7: 119–21. <https://doi.org/10.1186/cc1871>.

- Sousa, Marta Aires De, and Herminia de Lencastre. 2004. "Bridges from Hospitals to the Laboratory: Genetic Portraits of Methicillin-Resistant *Staphylococcus Aureus* Clones." *FEMS Immunology and Medical Microbiology* 40: 101–11. [https://doi.org/10.1016/S0928-8244\(03\)00370-5](https://doi.org/10.1016/S0928-8244(03)00370-5).
- Spaan, András N., Thomas Henry, Willemien J.M. Van Rooijen, Magali Perret, Cédric Badiou, Piet C. Aerts, Johan Kemmink, et al. 2013. "The Staphylococcal Toxin Panton-Valentine Leukocidin Targets Human C5a Receptors." *Cell Host and Microbe* 13 (5): 584–94. <https://doi.org/10.1016/j.chom.2013.04.006>.
- Spizek, J., and T. Rezanka. 2004. "Lincomycin, Clindamycin and Their Applications." *Applied Microbiology and Biotechnology* 64: 455–64. <https://doi.org/10.1007/s00253-003-1545-7>.
- "Stability Testing of New Drug Substances and Products Q1A(R2)." 2003. International Council for Harmonization of Technical Requirements for Pharmaceuticals for Human Use. 2003. https://www.ich.org/fileadmin/Public_Web_Site/ICH_Products/Guidelines/Quality/Q1A_R2/Step4/Q1A_R2__Guideline.pdf.
- Steinberg, Bernard A., William P. Jambor, and Lyda O. Suydam. 1955. "Thiostrepton, a New Antibiotic. III In Vivo Studies." *Antibiotics Annual : Proceedings of the Symposium on Antibiotics* 3: 562–65.
- Teagarden, Dirk L., William J. Petre, and Paul M. Gold. 1998. Stabilized Prostaglandin E1. 5,741,523, issued 1998.
- Teagarden, Dirk L, and David S Baker. 2002. "Practical Aspects of Lyophilization Using Non-Aqueous Co-Solvent Systems." *European Journal of Pharmaceutical Sciences* 15: 115–33. [https://doi.org/https://doi.org/10.1016/S0928-0987\(01\)00221-4](https://doi.org/https://doi.org/10.1016/S0928-0987(01)00221-4).
- Tenover, Fred C., and Richard V. Goering. 2009. "Methicillin-Resistant *Staphylococcus Aureus* Strain USA300: Origin and Epidemiology." *Journal of Antimicrobial Chemotherapy* 64 (3): 441–46. <https://doi.org/10.1093/jac/dkp241>.
- Thomas, Michael C, Todd W Mitchell, and Stephen J Blanksby. 2006. "Thiostrepton Biosynthesis: Prototype for a New Family of Bacteriocins." *Journal of the American Chemical Society* 128 (1): 4327–34. <http://www.ncbi.nlm.nih.gov/pubmed/19265401>.
- Thorat, Alpana A., and Raj Suryanarayanan. 2019. "Characterization of Phosphate Buffered Saline (PBS) in Frozen State and after Freeze-Drying." *Pharmaceutical Research* 36 (7). <https://doi.org/10.1007/s11095-019-2619-2>.
- Tong, Steven Y C, Joshua S Davis, Emily Eichenberger, Thomas L Holland, and Vance G Fowler. 2015. "Staphylococcus Aureus Infections : Epidemiology , Pathophysiology , Clinical Manifestations , and Management." *Clinical Microbiology Reviews* 28 (3): 603–61. <https://doi.org/10.1128/CMR.00134-14>.

- "Toxnet - Thiostrepton USP." n.d. <https://chem.nlm.nih.gov/chemidplus/rn/1393-48-2>.
- Traeger, Tobias, Pia Koerner, Wolfram Kessler, Katharina Cziupka, Stephan Diedrich, Alexandra Busemann, Claus-Dieter Heidecke, and Stefan Maier. 2010. "Colon Ascendens Stent Peritonitis (CASP) - a Standardized Model for Polymicrobial Abdominal Sepsis." *Journal of Visualized Experiments*, no. 46: 1–5. <https://doi.org/10.3791/2299>.
- Trejo, William H., Loretta D. Dean, Josip Pluscec, Edward Meyers, and William E. Brown. 1977. "Streptomyces Laurentii, a New Species Producing Thiostrepton." *The Journal of Antibiotics* 30 (8): 639–43. <https://doi.org/10.7164/antibiotics.30.639>.
- Trimble, Michael J., Patrik Mlynárčik, Milan Kolář, and Robert E.W. Hancock. 2016. "Polymyxin: Alternative Mechanisms of Action and Resistance." *Cold Spring Harbor Perspectives in Medicine* 6 (10): 1–22. <https://doi.org/10.1101/cshperspect.a025288>.
- Tsiodras, Sotirios, Howard S Gold, George Sakoulas, George M Eliopoulos, Christine Wennersten, Lata Venkataraman, Robert C Moellering Jr, and Mary Jane Ferraro. 2001. "Linezolid Resistance in a Clinical Isolate of Staphylococcus Aureus." *The Lancet* 358: 207–8.
- Ventura, Christy L., Roger Higdon, Laura Hohmann, Daniel Martin, Eugene Kolker, H. Denny Liggitt, Shawn J. Skerrett, and Craig E. Rubens. 2008. "Staphylococcus Aureus Elicits Marked Alterations in the Airway Proteome during Early Pneumonia." *Infection and Immunity* 76 (12): 5862–72. <https://doi.org/10.1128/IAI.00865-08>.
- Vincent, Jean-louis, Jordi Rello, John Marshall, Eliezer Silva, Antonio Anzueto, Claude D Martin, Rui Moreno, et al. 2009. "International Study of the Prevalence and Outcomes of Infection in Intensive Care Units." *The Journal of the American Medical Association* 302 (21): 2323–29.
- Vukovic, Lela, Fatima A Khatib, Stephanie P Drake, Antonett Madriaga, Kenneth S Brandenburg, Petr Kral, and Hayat Onyuksel. 2011. "Structure and Dynamics of Highly PEG-Ylated Sterically Stabilized Micelles in Aqueous Media." *Journal of the American Chemical Society* 133 (34): 13481–88. <https://doi.org/10.1021/ja204043b>.
- Vuković, Lela, Antonett Madriaga, Antonina Kuzmis, Amrita Banerjee, Alan Tang, Kevin Tao, Neil Shah, Petr Král, and Hayat Onyuksel. 2013. "Solubilization of Therapeutic Agents in Micellar Nanomedicines." *Langmuir* 29 (51): 15747–54. <https://doi.org/10.1021/la403264w>.
- Wang, Ming, and Andrei L. Gartel. 2011. "Micelle-Encapsulated Thiostrepton as an Effective Nanomedicine for Inhibiting Tumor Growth and for Suppressing FOXM1 in Human Xenografts." *Molecular Cancer Therapeutics* 10 (12): 2287–97. <https://doi.org/10.1016/j.immuni.2010.12.017>.Two-stage.
- Wang, Wei. 2015. "Tolerability of Hypertonic Injectables." *International Journal of*

- Pharmaceutics* 490 (1–2): 308–15. <https://doi.org/10.1016/j.ijpharm.2015.05.069>.
- Ward, Nicholas S., and Mitchell M. Levy, eds. 2017. *Sepsis. Definitions, Pathophysiology and the Challenge of Bedside Management*. Cham: Humana Press, Cham. <https://doi.org/https://doi-org.proxy.cc.uic.edu/10.1007/978-3-319-48470-9>.
- Weisblum, B., and V. Demohn. 1970. "Inhibition by Thiostrepton of the Formation of a Ribosome-Bound Guanine Nucleotide Complex." *FEBS Letters* 11 (3): 149–52.
- Wen, Haitao. 2013. "Sepsis Induced by Cecal Ligation and Puncture Haitao." *Methods Mol Biol* 1031: 117–24. <https://doi.org/10.1007/978-1-62703-481-4>.
- Williams, Richard L., Sok Bee Lim, Hayat Onyuksel, and Phillip T. Marucha. 2012. "Sterically Stabilized Phospholipid Micelles Reduce Activity of a Candidate Antimicrobial Wound Healing Adjunct." *International Journal of Peptide Research and Therapeutics* 18 (3): 195–203. <https://doi.org/10.1007/s10989-012-9292-1>.
- Wunderink, Richard G, Michael S Niederman, Marin H Kollef, Andrew F Shorr, Mark J Kunkel, Alice Baruch, William T Mcgee, Arlene Reisman, and Jean Chastre. 2012. "Linezolid in Methicillin-Resistant Staphylococcus Aureus Nosocomial Pneumonia: A Randomized, Controlled Study." *Clinical Infectious Diseases* 54: 621–29. <https://doi.org/10.1093/cid/cir895>.
- Yalkowsky, S.H., J.F. Krzyzaniak, and G.H. Ward. 1998. "Formulation-Related Problems Associated with Intravenous Drug Delivery." *Journal of Pharmaceutical Sciences* 87 (7): 787–96. <https://doi.org/10.1021/js980051i>.
- Yasuda, Hideo, Asada Leelahavanichkul, Shinichiro Tsunoda, James W. Dear, Yoshiyuki Takahashi, Shuichi Ito, Xuzhen Hu, et al. 2008. "Chloroquine and Inhibition of Toll-like Receptor 9 Protect from Sepsis-Induced Acute Kidney Injury." *American Journal of Physiology - Renal Physiology* 294 (5): F1050–58. <https://doi.org/10.1152/ajprenal.00461.2007>.Chloroquine.
- Zhang, Feifei, and Wendy L. Kelly. 2015. "Saturation Mutagenesis of TsrA Ala4 Unveils a Highly Mutable Residue of Thiostrepton A." *ACS Chem Biol* 10 (4): 998–1009. <https://doi.org/10.1126/scisignal.274pe36>.Insulin.
- Zheng, Qingfei, Qinglan Wang, Shoufeng Wang, Jiequn Wu, Qian Gao, and Wen Liu. 2015. "Thiopeptide Antibiotics Exhibit a Dual Mode of Action against Intracellular Pathogens by Affecting Both Host and Microbe." *Chemistry and Biology* 22 (8): 1002–7. <https://doi.org/10.1016/j.chembiol.2015.06.019>.
- Zuluaga, Andres F., Beatriz E. Salazar, Carlos A. Rodriguez, Anna X. Zapata, Maria Agudelo, and Omar Vesga. 2006. "Neutropenia Induced in Outbred Mice by a Simplified Low-Dose Cyclophosphamide Regimen: Characterization and Applicability to Diverse Experimental Models of Infectious Diseases." *BMC Infectious Diseases* 6: 1–10. <https://doi.org/10.1186/1471-2334-6-55>.

APPENDICES

APPENDIX A: Animal protocols approval letters.



Office of Animal Care and Institutional
Biosafety Committee (M/C 672)
Office of the Vice Chancellor for Research
206 Administrative Office Building
1737 West Polk Street
Chicago, Illinois 60612

July 20, 2017

Steve Dudek
Medicine/Pulmonary, Critical Care & Sleep Medicine
M/C 719

Dear Dr. Dudek:

The modifications requested in modification indicated below pertaining to your approved protocol indicated below have been reviewed and approved in accordance with the Animal Care Policies of the University of Illinois at Chicago on 7/20/17.

Title of Application: Acute Lung Injury and Pneumonitis Studies, Mechanisms and Intervention Strategies

ACC Number: 15-244

Modification Number: 16

Nature of Modification:

- 1) *Addition of 110 C57 mice to test the efficacy of treatment with thiostrepton in DMSO or nanoparticles following WT active MRSA infection. Vancomycin will be used as a positive control. All work and euthanasia will be in ABSL2 BRL 175.*
- 2) *Addition of personnel: Karina Esparza and Nikolas Polite*

Condition of Approval: *Karina Esparza must have a general orientation to animal facilities and in personnel orientation to ABSL2 facility prior to initiation. Nikolas Polite must have general orientation to animal facilities prior to initiation. He is not approved for ABSL2.*

Protocol Approved: 1/14/2016

Current Approval Period: 12/15/2016 to 12/15/2017. *Protocol is eligible for 1 additional year of renewal prior to expiration and resubmission.*

Current Funding: *Portions of this protocol are supported by the funding sources indicated in the table below.*
Number of funding sources: 10

Funding Agency	Funding Title			Portion of Funding Matched
NIH	Role of Sphingolipids in Pathobiology of Lung Injury			Protocol is linked to form G G protocol #13-216
Funding Number	Current Status	UIC PAF NO.	Performance Site	Funding PI
PO1 HL098050	Funded	201007207	UIC	Viswanathan Natarajan; mProject 2 and

APPENDIX A (continued)



October 12, 2017

Steven M. Dudek
Medicine/Pulmonary, Critical Care & Sleep Medicine
M/C 719

Office of Animal Care and
Institutional Biosafety Committees (MC 672)
Office of the Vice Chancellor for Research
206 Administrative Office Building
1737 West Polk Street
Chicago, Illinois 60612-7227

Dear Dr. Dudek:

The modifications requested in modification indicated below pertaining to your approved protocol indicated below have been reviewed in accordance with the Institutional Biosafety Committee Policies of the University of Illinois at Chicago and approved on **October 12, 2017**.

Title of Application: Vascular Endothelial Aspects of Lung Injury and Lung Inflammatory Diseases

IBC Number: 16-006

Modification Number: 05

Nature of Modification: *Addition of new sterically stabilized micelles for administration of drugs to mice in approved MRSA model.*

The records of the Institutional Biosafety Committee will be revised to reflect these changes. Thank you for complying with the Institutional Biosafety Committee Policies and Procedures of UIC.

Sincerely,

A handwritten signature in black ink, appearing to read "Randal C. Jaffe", is written over a light blue horizontal line.

Randal C. Jaffe, Ph.D.
Chair, Institutional Biosafety Committee
RCJ/ mbb

cc: IBC File, Jeffrey Jacobson, Lichun Wang, Lucille Meliton

APPENDIX A (continued)



Office of Animal Care and Institutional
Biosafety Committee (M/C 672)
Office of the Vice Chancellor for Research
206 Administrative Office Building
1737 West Polk Street
Chicago, Illinois 60612

August 5, 2019

Richard Minshall
Pharmacology
M/C 868

Dear Dr. Minshall:

The modifications requested in modification indicated below pertaining to your approved protocol indicated below have been reviewed and approved in accordance with the Animal Care Policies of the University of Illinois at Chicago on 08/01/2019.

Title of Application: New Strategies for Treating Septic Vasculopathy, Inflammation, and Thrombosis

ACC Number: 17-138

Modification Number: 2

Nature of Modification:

- 1) Request for additional 57 C57 mice to test the therapeutic value of thiostrepton-SSM for treatment of sepsis using the cecum ligation and puncture (CLP) model.
- 2) Personnel Addition: Karina Esparza

Protocol Approved: 10/6/2017

Current Approval Period: 8/15/2018 to 8/15/2019. Protocol is eligible for 1 additional year of renewal prior to expiration and resubmission.

Current Funding: Portions of this protocol are supported by the funding sources indicated in the table below.

Number of funding sources: 2

Funding Agency	Funding Title			Portion of Funding Matched
NIH	New strategies for treating septic vasculopathy, inflammation and thrombosis (Institutional #00003528)			Portion of Grant is matched Other portion is covered under 16-208
Funding Number	Current Status	UIC PAF NO.	Performance Site	Funding PI
R01 HL 125356 (years 1-5)	Funded	201404177	UIC	Xiaoping Du (contract PI)/Richard Minshall MPI
Funding Agency	Funding Title			Portion of Funding Matched

APPENDIX A (continued)

<i>AHA-American Heart Association</i>	<i>Inhibition of endothelial cell von WillebrandFactor secretion reduces thrombotic complications in sickle cell disease (Institutional # 00436138)</i>			<i>All matched</i>
Funding Number	Current Status	UIC PAF NO.	Performance Site	Funding PI
<i>19POST344200-12</i>	<i>Funded</i>		<i>UIC</i>	<i>Mit Suk Bae</i>

This institution has Animal Welfare Assurance Number A3460.01 on file with the Office of Laboratory Animal Welfare, NIH. This letter may only be provided as proof of IACUC approval for those specific funding sources listed above in which all portions of the grant are matched to this ACC protocol.

Thank you for complying with the Animal Care Policies and Procedures of UIC.

Sincerely yours,



Amy Lasek, PhD
Chair, Animal Care Committee
AL/s
cc: BRL, ACC File, Maricela Castellon

APPENDIX B: Copyright clearance proofs



RightsLink®

[Home](#)
[Create Account](#)
[Help](#)




Title: Development of co-solvent freeze-drying method for the encapsulation of water-insoluble thiotrepton in sterically stabilized micelles

Author: Karina Esparza, Hayat Onyuksel

Publication: International Journal of Pharmaceutics

Publisher: Elsevier

Date: 10 February 2019

© 2018 Elsevier B.V. All rights reserved.

LOGIN

If you're a [copyright.com](#) user, you can login to RightsLink using your copyright.com credentials. Already a [RightsLink](#) user or want to [learn more?](#)

Please note that, as the author of this Elsevier article, you retain the right to include it in a thesis or dissertation, provided it is not published commercially. Permission is not required, but please ensure that you reference the journal as the original source. For more information on this and on your other retained rights, please visit: <https://www.elsevier.com/about/our-business/policies/copyright#Author-rights>

[BACK](#)
[CLOSE WINDOW](#)

Copyright © 2019 [Copyright Clearance Center, Inc.](#) All Rights Reserved. [Privacy statement](#). [Terms and Conditions](#).
Comments? We would like to hear from you. E-mail us at customer@copyright.com

APPENDIX B (continued)



RightsLink®

[My Orders](#)
[My Library](#)
[My Profile](#)

Welcome kdeoli2@uic.edu [Log out](#) | [Help](#)

[My Orders](#) > [Orders](#) > [All Orders](#)

License Details

This Agreement between University of Illinois at Chicago -- Karina Esparza ("You") and Springer Nature ("Springer Nature") consists of your license details and the terms and conditions provided by Springer Nature and Copyright Clearance Center.

[Print](#)
[Copy](#)

License Number	4637170412571
License date	Jul 27, 2019
Licensed Content Publisher	Springer Nature
Licensed Content Publication	Nature Immunology
Licensed Content Title	The role of pattern-recognition receptors in innate immunity: update on Toll-like receptors
Licensed Content Author	Taro Kawai, Shizuo Akira
Licensed Content Date	Apr 20, 2010
Licensed Content Volume	11
Licensed Content Issue	5
Type of Use	Thesis/Dissertation
Requestor type	academic/university or research institute
Format	print and electronic
Portion	figures/tables/illustrations
Number of figures/tables/illustrations	2
High-res required	no
Will you be translating?	no
Circulation/distribution	>50,000
Author of this Springer Nature content	no
Title	Thiostrepton Encapsulated in Sterically Stabilized Micelles for the Treatment of Staphylococcal Pneumonia and Sepsis
Institution name	University of Illinois at Chicago
Expected presentation date	Sep 2019
Portions	Figures 1 and 2.
Requestor Location	University of Illinois at Chicago 833 S Wood St CHICAGO, IL 60612 United States Attn: University of Illinois at Chicago
Total	0.00 USD

APPENDIX B (continued)



RightsLink®

My Orders

My Library

My Profile

Welcome kdeoli2@uic.edu [Log out](#) | [Help](#)[My Orders](#) > [Orders](#) > [All Orders](#)

License Details

This Agreement between University of Illinois at Chicago -- Karina Esparza ("You") and Springer Nature ("Springer Nature") consists of your license details and the terms and conditions provided by Springer Nature and Copyright Clearance Center.

Print

Copy

License Number	4638190316507
License date	Jul 29, 2019
Licensed Content Publisher	Springer Nature
Licensed Content Publication	Nature Reviews Immunology
Licensed Content Title	Sepsis-induced immunosuppression: from cellular dysfunctions to immunotherapy
Licensed Content Author	Richard S. Hotchkiss, Guillaume Monneret, Didier Payen
Licensed Content Date	Nov 15, 2013
Licensed Content Volume	13
Licensed Content Issue	12
Type of Use	Thesis/Dissertation
Requestor type	academic/university or research institute
Format	print and electronic
Portion	figures/tables/illustrations
Number of figures/tables/illustrations	1
High-res required	no
Will you be translating?	no
Circulation/distribution	>50,000
Author of this Springer Nature content	no
Title	Thiostrepton Encapsulated in Sterically Stabilized Micelles for the Treatment of Staphylococcal Pneumonia and Sepsis
Institution name	University of Illinois at Chicago
Expected presentation date	Sep 2019
Portions	Figure 1 theory 1
Requestor Location	University of Illinois at Chicago 833 S Wood St CHICAGO, IL 60612 United States Attn: University of Illinois at Chicago
Total	0.00 USD

APPENDIX B (continued)

7/29/2019

PubMed Central, Figure 1: Yale J Biol Med. 2017 Jun; 90(2): 269–281. Published online 2017 Jun 23.

PMC full text: [Yale J Biol Med. 2017 Jun; 90\(2\): 269–281.](#)

<< Prev Figure 1 Next >>

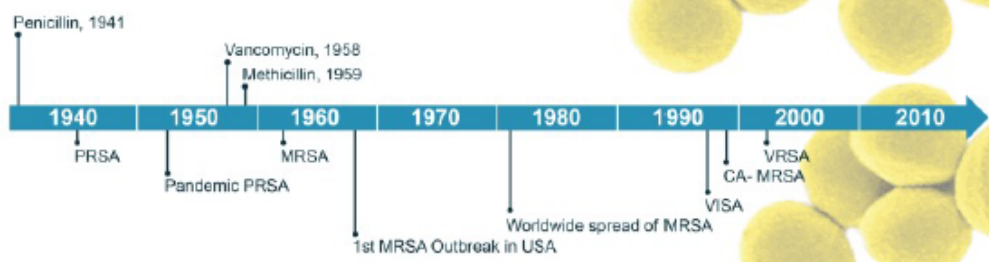
Published online 2017 Jun 23.

[Copyright/License](#) [Request permission to reuse](#)

Copyright Published by Yale Journal of Biology and Medicine 2017.
This work is written by US Government employees and is in the public domain in the US.

This is an open access article, free of all copyright, and may be freely reproduced, distributed, transmitted, modified, built upon, or otherwise used by anyone for any lawful purpose. The work is made available under the Creative Commons CC0 public domain dedication.

Figure 1

***Staphylococcus aureus* Drug Resistance and Epidemics**

Timeline delineating the advent of antibiotic therapies and subsequent emergence of antibiotic-resistant *S. aureus*.

Images in this article

Click on the image to see a larger version.

APPENDIX B (continued)



RightsLink®

My Orders My Library My Profile Welcome kdeoli2@uic.edu Log out Help

My Orders > Orders > All Orders

License Details

This Agreement between University of Illinois at Chicago -- Karina Esparza ("You") and Springer Nature ("Springer Nature") consists of your license details and the terms and conditions provided by Springer Nature and Copyright Clearance Center.

Print Copy

License Number	4638260595195
License date	Jul 29, 2019
Licensed Content Publisher	Springer Nature
Licensed Content Publication	Cellular and Molecular Life Sciences
Licensed Content Title	Host defense peptides as new weapons in cancer treatment
Licensed Content Author	N. Papo, Y. Shai
Licensed Content Date	Jan 1, 2005
Licensed Content Volume	62
Licensed Content Issue	7
Type of Use	Thesis/Dissertation
Requestor type	academic/university or research institute
Format	print and electronic
Portion	figures/tables/illustrations
Number of figures/tables/illustrations	1
Will you be translating?	no
Circulation/distribution	>50,000
Author of this Springer Nature content	no
Title	Thiostrepton Encapsulated in Sterically Stabilized Micelles for the Treatment of Staphylococcal Pneumonia and Sepsis
Institution name	University of Illinois at Chicago
Expected presentation date	Sep 2019
Portions	Figure 1
Requestor Location	University of Illinois at Chicago 833 S Wood St CHICAGO, IL 60612 United States Attn: University of Illinois at Chicago
Total	0.00 USD

APPENDIX B (continued)



RightsLink®

My Orders

My Library

My Profile

Welcome kdeoli2@uic.edu [Log out](#) | [Help](#)[My Orders](#) > [Orders](#) > [All Orders](#)

License Details

This Agreement between University of Illinois at Chicago -- Karina Esparza ("You") and Elsevier ("Elsevier") consists of your license details and the terms and conditions provided by Elsevier and Copyright Clearance Center.

[Print](#)[Copy](#)

License Number	4640220582151
License date	Aug 01, 2019
Licensed Content Publisher	Elsevier
Licensed Content Publication	Trends in Pharmacological Sciences
Licensed Content Title	Antibody-Based Biologics and Their Promise to Combat Staphylococcus aureus Infections
Licensed Content Author	William E. Sause, Peter T. Buckley, William R. Strohl, A. Simon Lynch, Victor J. Torres
Licensed Content Date	Mar 1, 2016
Licensed Content Volume	37
Licensed Content Issue	3
Licensed Content Pages	11
Type of Use	reuse in a thesis/dissertation
Portion	figures/tables/illustrations
Number of figures/tables/illustrations	1
Format	both print and electronic
Are you the author of this Elsevier article?	No
Will you be translating?	No
Original figure numbers	Figure 1
Title of your thesis/dissertation	Thiostrepton Encapsulated in Sterically Stabilized Micelles for the Treatment of Staphylococcal Pneumonia and Sepsis
Publisher of new work	University of Illinois at Chicago
Expected completion date	Sep 2019
Estimated size (number of pages)	1
Requestor Location	University of Illinois at Chicago 833 S Wood St CHICAGO, IL 60612 United States Attn: University of Illinois at Chicago 98-0397604
Publisher Tax ID	
Total	0.00 USD

APPENDIX B (continued)



RightsLink®

Home

Account
Info

Help


informa
healthcare

Title: Polymyxin B self-associated with phospholipid nanomicelles

Author: Kenneth S. Brandenburg, , Israel Rubinstein, et al

Publication: Pharmaceutical Development and Technology

Publisher: Taylor & Francis

Date: Dec 1, 2012

Rights managed by Taylor & Francis

Logged in as:
Karina Esparza
University of Illinois at Chicago

Account #:
3001492655

[LOGOUT](#)

Thesis/Dissertation Reuse Request

Taylor & Francis is pleased to offer reuses of its content for a thesis or dissertation free of charge contingent on resubmission of permission request if work is published.

[BACK](#)
[CLOSE WINDOW](#)

Copyright © 2019 [Copyright Clearance Center, Inc.](#) All Rights Reserved. [Privacy statement](#). [Terms and Conditions](#).
Comments? We would like to hear from you. E-mail us at customercare@copyright.com

APPENDIX B (continued)

8/13/2019

University of Illinois at Chicago Mail - FW: CSHL Press Reprint Permission Request Form



Karina Esparza <ksdeol2@uic.edu>

FW: CSHL Press Reprint Permission Request Form

2 messages

Brown, Carol <brown@cshl.edu>
 To: 'ksdeol2@uic.edu' <ksdeol2@uic.edu>

Tue, Aug 13, 2019 at 2:21 PM

Permission is granted for the use of Fig 1, p.2 in the article detailed below in your PhD thesis only. Please include complete reference and copyright to Cold Spring Harbor Laboratory Press.

Best wishes for success with your thesis,

Carol C. Brown
 Books Development, Marketing and Sales
 Cold Spring Harbor Laboratory Press
 500 Sunnyside Blvd
 Woodbury, New York 11797
 516 422 4038 ph.
 516 422 4095 fx.
brown@cshl.edu

-----Original Message-----


From: reprint@cshl.edu (mailto:reprint@cshl.edu)
 Sent: Monday, July 29, 2019 3:17 PM
 To: Reprint
 Subject: CSHL Press Reprint Permission Request Form

Default Info
 Default Info - line2

Name: Karina Esparza
 Company/Institution: University of Illinois at Chicago
 Library Address: 833 S. Wood St, MC 865, Room 335
 Library Address (line 2):
 City: Chicago
 State (US and Canada): IL
 Country: United States
 Zip: 60612
 Title: PhD Candidate
 Lab/Department: 3601 Pharmaceutical Sciences
 Phone: 3124783106
 Fax:
 Email: ksdeol2@uic.edu
 Title of Publication: Thioestrepton Encapsulated in Sterically Stabilized Micelles for the Treatment of Staphylococcal Pneumonia and Sepsis
 Authors/Editors: Karina Esparza
 Date of Publication:
 Publisher: PhD Thesis
 Title of CSHLP Journal/Book: Cold Spring Harb Perspect Med
 Title of Article/Chapter: Polymyxin: Alternative Mechanisms of Action and Resistance
 CSHL Authors/Editors: Michael J. Trimble, Patrick Myndorik, Milan Kraljic, and Robert E.W. Hancock
 Page Numbers: 2
 Figure Numbers: 1
 Figure Page Numbers:
 Copyright Date:
 Language:
 Territory:
 Format: Print and electronic
 Additional comments: I would like to include figure 1B on my PhD thesis dissertation.

Ipaddress: 128.248.143.042
 Default Footer
 Default Footer - line2

APPENDIX B (continued)



[My Orders](#)
[My Library](#)
[My Profile](#)
Welcome kdeoifi2@uic.edu [Log out](#) | [Help](#)

[My Orders](#) > [Orders](#) > [All Orders](#)

License Details

This Agreement between University of Illinois at Chicago -- Karina Esparza ("You") and Springer Nature ("Springer Nature") consists of your license details and the terms and conditions provided by Springer Nature and Copyright Clearance Center.

[Print](#)
[Copy](#)

License Number	4675560785551
License date	Sep 24, 2019
Licensed Content Publisher	Springer Nature
Licensed Content Publication	Pharmaceutical Research
Licensed Content Title	A Novel One-Step Drug-Loading Procedure for Water-Soluble Amphiphilic Nanocarriers
Licensed Content Author	Elvire Fournier, Marie-Hélène Dufresne, Damon C. Smith et al
Licensed Content Date	Jan 1, 2004
Licensed Content Volume	21
Licensed Content Issue	6
Type of Use	Thesis/Dissertation
Requestor type	academic/university or research institute
Format	print and electronic
Portion	figures/tables/illustrations
Number of figures/tables/illustrations	1
Will you be translating?	no
Circulation/distribution	50000 or greater
Author of this Springer Nature content	no
Title	Thiostrepton Encapsulated in Sterically Stabilized Micelles for the Treatment of Staphylococcal Pneumonia and Sepsis
Institution name	University of Illinois at Chicago
Expected presentation date	Sep 2019
Portions	Figure 2, top graph.
Requestor Location	University of Illinois at Chicago 833 S Wood St
	CHICAGO, IL 60612 United States Attn: University of Illinois at Chicago
Total	0.00 USD

APPENDIX B (continued)

9/25/2019

Creative Commons — Attribution 4.0 International — CC BY 4.0

This page is available in the following languages:



Creative Commons License De
Attribution 4.0 International (CC BY 4.0)



This is a human-readable summary of (and not a substitute for) the [license](#).

You are free to:

Share — copy and redistribute the material in any medium or format

Adapt — remix, transform, and build upon the material

for any purpose, even commercially.

The licensor cannot revoke these freedoms as long as you follow the license terms.

Under the following terms:

Attribution — You must give appropriate credit, provide a link to the license, and indicate if changes were made. You may do so in any reasonable manner, but not in any way that suggests the licensor endorses you or your use.

No additional restrictions — You may not apply legal terms or technological measures that legally restrict others from doing anything the license permits.

Notices:

You do not have to comply with the license for elements of the material in the public domain or where your use is permitted by an applicable exception or limitation.

No warranties are given. The license may not give you all of the permissions necessary for your intended use. For example, other rights such as publicity, privacy, or moral rights may limit how you use the material.

APPENDIX B (continued)



RightsLink®

Home

Account
Info

Help

SPRINGER NATURE

Title: Proteomic analysis reveals a role for PAX8 in peritoneal colonization of high grade serous ovarian cancer that can be targeted with micelle encapsulated thiostrepton

Author: Laura R. Hardy et al

Publication: Oncogene

Publisher: Springer Nature

Date: Jul 11, 2019

Copyright © 2019, Springer Nature

Logged in as:
Karina Esperza
University of Illinois at Chicago
Account #:
3001492655

LOGOUT

Author Request

If you are the author of this content (or his/her designated agent) please read the following. If you are not the author of this content, please click the Back button and select no to the question "Are you the Author of this Springer Nature content?".

Ownership of copyright in original research articles remains with the Author, and provided that, when reproducing the contribution or extracts from it or from the Supplementary Information, the Author acknowledges first and reference publication in the Journal, the Author retains the following non-exclusive rights:

To reproduce the contribution in whole or in part in any printed volume (book or thesis) of which they are the author(s).

The author and any academic institution, where they work, at the time may reproduce the contribution for the purpose of course teaching.

To reuse figures or tables created by the Author and contained in the Contribution in oral presentations and other works created by them.

To post a copy of the contribution as accepted for publication after peer review (in locked Word processing file, or a PDF version thereof) on the Author's own web site, or the Author's institutional repository, or the Author's funding body's archive, six months after publication of the printed or online edition of the Journal, provided that they also link to the contribution on the publisher's website.

Authors wishing to use the published version of their article for promotional use or on a web site must request in the normal way.

If you require further assistance please read Springer Nature's online [author reuse guidelines](#).

For full paper portion: Authors of original research papers published by Springer Nature are encouraged to submit the author's version of the accepted, peer-reviewed manuscript to their relevant funding body's archive, for release six months after publication. In addition, authors are encouraged to archive their version of the manuscript in their institution's repositories (as well as their personal Web sites), also six months after original publication.

v1.0

BACK

CLOSE WINDOW

Copyright © 2019 [Copyright Clearance Center, Inc.](#) All Rights Reserved. [Privacy statement](#). [Terms and Conditions](#).
Comments? We would like to hear from you. E-mail us at customer@copyright.com

VITA

NAME: Karina Esparza

EDUCATION:

Aug 2014 – Dec 2019 Ph.D., Biopharmaceutical Sciences, University of Illinois at Chicago, Chicago, Illinois

Advisor: Hayat Onyuksel

Thesis Title: Thiostrepton in Phospholipid Micelles:

Development of Scalable Production Method and *In Vivo* Evaluation

Jan 2007 – Sep 2013 B.PHARM., Pharmacy and Biochemistry, The University of São Paulo, São Paulo, Brazil

Jun 2012 – May 2013 Exchange undergraduate program, The university of Montana, Missoula, Montana

Brazil Science without Borders Exchange Program

PROFESSIONAL EXPERIENCE:

Ago 2015 – Dec 2019 University of Illinois at Chicago, Chicago, Illinois
Teaching Assistant

Assisted instructors and facilitated classes in the disciplines of pharmaceutics, pharmacokinetics, and pharmacotherapy.

Nov 2013 – Apr 2014 Alcon Laboratories, São Paulo, Brazil
Drug Stability Analyst

Assessed physical-chemical stability of ophthalmic products; implemented in-use stability program to assess continued

integrity of multi-dose ophthalmic products; managed stability chambers for shelf-life testing, packaging stability, and accelerated aging.

May 2013 – Aug 2013 AbbVie, North Chicago, Illinois

Science Intern at Global Pharmaceutical Research and Development

Determined the range of applicability of a dual-pH dilution robotic system that simulated rat gastrointestinal tract; formulated poorly-water soluble compounds into amorphous solid dispersions or suspensions for evaluation of bio-relevant solubility and dissolution properties.

Feb. 2013 – May 2013 The University of Montana, Missoula, Montana

Undergraduate Researcher (Advisors: Andrea and Donald Stierle)

Contributed to isolate and characterize secondary metabolites of microbes isolated from unusual ecological niches.

Sep 2011 – May 2012 Marjan Farma, São Paulo, Brazil

Drug Stability Intern

Evaluated the physical-chemical stability of drug products, supplements, and cosmetics in a GMP environment.

- July 2011 – Aug 2011 Center for Toxicological Assistance (CEATOX), São Paulo, Brazil
Intern for Toxicological Emergencies
Assisted patients and health care professionals with timely clinical toxicology information.
- May 2011 – Aug 2011 The University of São Paulo, São Paulo, Brazil
Undergraduate researcher (Advisor: Tania Marcourakis)
Determined oxidative stress in lungs from rats pre-exposed to xenobiotics.
- Jan 2011 – Apr 2011 Samaritano Hospital of São Paulo, São Paulo, Brazil
Intern in Clinical Pharmacy and Pharmaceutical Care
Constructed a database for safe drug preparation and administration through feeding tubes using information obtained from pharmaceutical companies and scientific literature.
- Aug 2008 – Dec 2010 Butantan Institute, Sao Paulo, Brazil
Undergraduate Researcher (Advisor: Ana Olivia de Souza)
Isolated and characterized antifungal secondary metabolites produced by coffee tree endophytic fungi using bioactivity-guided fractionation with solid-phase extraction, liquid-liquid extraction, and HPLC purification.

PUBLICATIONS:

- Hardy, L., Pergande, M., Esparza, K., Heath, K., Onyuksel, H., Cologna, S., Burdette, J. Proteomic analysis reveals a role for PAX8 in high grade serous ovarian cancer metastasis that can be targeted with micelle encapsulated thiostrepton. *Oncogene*. 2019. 38 (32): 6003-6016.
<https://doi.org/10.1038/s41388-019-0842-2>.
- Esparza, K., Jayawardena, D., Onyuksel, H. Phospholipid Micelles for Peptide Drug Delivery. In: Weissig V, Elbayoumi T, eds. *Basic Protocols in Pharmaceutical Nanotechnology*. Springer; 2019.
- Esparza, K., Onyuksel, H. Development of Co-solvent Freeze-Drying Method for the Encapsulation of Water-insoluble Thiostrepton in Sterically Stabilized Micelles. *Int J Pharm*. 2019. 556: 21-29.
[doi:https://doi.org/10.1016/j.ijpharm.2018.12.001](https://doi.org/10.1016/j.ijpharm.2018.12.001).

ORAL AND POSTER PRESENTATIONS:

- Esparza, K., Woo, K.K., Lee, H. & Onyuksel, H. (2019, June). Optimization of Co-solvent Freeze-Drying Method for the Encapsulation of Thiostrepton in Sterically Stabilized Micelles. Poster presented at the 51st Annual Pharmaceutics Graduate Student Research Meeting (PGSRM) at the University of Madison, Madison, WI.
- Esparza, K., Woo, K.K., Lee, H. & Onyuksel, H. (2018, November). Optimization of Co-solvent Freeze-Drying Method for the Encapsulation of Thiostrepton in Sterically Stabilized Micelles. Poster presented at the American

Association of Pharmaceutical Scientists Annual Meeting PharmSci360
Washington DC.

- Esparza, K., Woo, K.K., Lee, H., Onyuksel, H. (2018, June). A Scalable Encapsulation Method of Thiostrepton in Sterically Stabilized Micelles. Podia session presented at the 50th Annual Pharmaceutics Graduate Student Research Meeting (PGSRM) at the University of Minnesota, Minneapolis, MN.
- Esparza, K., Woo, K.K., Lee, H. & Onyuksel, H. (2018, November). Optimization of Co-solvent Freeze-Drying Method for the Encapsulation of Thiostrepton in Sterically Stabilized Micelles. Poster presented at the American Association of Pharmaceutical Scientists Annual Meeting PharmSci360 Washington DC.
- Esparza, K., Woo, K.K., Lee, H. & Onyuksel, H. (2018, February). Thiostrepton in Sterically Stabilized Phospholipid Micelles: A Promising Antibacterial Nanomedicine. Poster presented at the 9th Research Day at the College of Pharmacy at the University of Illinois at Chicago, Chicago, IL.
- Esparza, K. & Onyuksel, H. (2017, November). Encapsulation of Antimicrobial Triclosan into Sterically Stabilized Micelles. Poster presented at the Annual Meeting of American Association of Pharmaceutical Scientists, San Diego, CA.
- Lima, D.O.K., & Onyuksel, H. (2015, October). Delivery of Antimicrobial Peptides in Sterically Stabilized Micelles for Reduced Toxicity. Poster presented at the Annual Meeting of American Association of Pharmaceutical Scientists, Orlando, FL.

- Lima, D.O.K., Soares, I.S., & De Souza, A.O. (2010, May). "Antifungal Compounds Produced by Coffee Tree Endophytic Fungi". Poster presented at the XXXIX Annual Meeting of The Brazilian Biochemistry and Molecular Biology Society in Foz do Iguaçu/PR, Brazil.

PATENTS:

Onyuksel H, Thaqi M, Esparza K (2018). A novel method of preparing water-insoluble drug-containing micelles that can be scaled-up. Provisional patent DH090.

HONORS AND AWARDS:

2019	Second place Poster Presentation at the 51 st Annual Pharmaceutics Graduate Student Research Meeting (PGSRM)
2019	Edward Benes Scholarship
2019	UIC Graduate Student Council Travel Award
2019	Graduate College Student Presenters Award
2018	Travel Grant Award from the Graduate Women in Science – Chicago Chapter
2018	UIC Graduate Student Council Travel Award
2015	UIC Graduate Student Council Travel Award
2015	Chicago Consular Corps Award

- 2014 Recipient of “Brazil Science without Borders” doctoral scholarship at the University of Illinois at Chicago, Chicago, Illinois.
- 2012 Recipient of “Brazil Science without Borders” undergraduate scholarship at the University of Montana, US.
- 2010 Young Scientist Award at the XII Annual Scientific Meeting of the Butantan Institute with the project “Antifungal Secondary Metabolites Produced by Endophytic Fungi”.

LEADERSHIP ROLES:

- 2016 – 2018 American Association of Pharmaceutical Scientists (AAPS)
UIC Student Chapter
Chair and former vice-chair
- 2016 – 2019 Controlled Release Society (CRS) Illinois Student Chapter
President, former vice president, former treasurer
- 2015 – 2017 Brazilian Graduate Student Conference (BRASCON)
Director/Coordinator of recruitment

PROFESSIONAL MEMBERSHIP:

- Apr 2015 - Present American Association of Pharmaceutical Scientists
- Nov 2016 - Present Graduate Women in Science (GWIS) Chicago Chapter
- Jun 2016 – Jun 2017 American Association for the Advancement of Science (AAAS)